A FIELD CELL AND HUMIDITY CELL STUDY OF METAL ATTENUATION IN NEUTRAL ROCK DRAINAGE FROM THE ANTAMINA MINE, PERU

by

Dustin Trevor Hirsche

B.Sc. (Hon.), University of Calgary, 2006

A THESIS SUBMITTED IN PARTIAL FULFILLMENT OF

THE REQUIREMENTS FOR THE DEGREE OF

MASTER OF SCIENCE

in

THE FACULTY OF GRADUATE STUDIES

(Geological Science)

THE UNIVERSITY OF BRITISH COLUMBIA

(Vancouver)

August 2012

Abstract

This work focuses on the attenuation of Mo and Zn in neutral pH drainage from waste rock at the Antamina mine in Peru. The study was designed to test the hypothesis that Mo or Zn containing leachate from one waste rock type can be attenuated when allowed to contact a different waste rock type. Mixed material stacked field cells and humidity cells connected in series, where leachate from a Mo or Zn - releasing waste rock type flowed through a second waste rock material type, were used to test this hypothesis. Both of these were new methods, which had not before been reported in the peer reviewed scientific literature related to the study of waste rock geochemistry.

Results from both the humidity cells (laboratory conditions) and field cells (field conditions) showed the same general attenuation patterns. When drainage from Mo-releasing waste rock flowed through Pb-rich black marble waste rock, Mo was removed from solution. Mo attenuation was not observed when the order of the waste rock materials was reversed such that drainage from Pb-rich material flowed through Mo-releasing intrusive rock. As, also released from the same Mo-releasing intrusive rock, showed the same attenuation pattern as Mo. Geochemical modeling suggested that wulfenite precipitation was responsible for the observed attenuation of Mo. Zn was removed from leachate both by contact with Mo-releasing intrusive rock and by contact with calcite-rich grey hornfels material. Like Zn, Cd was removed from solution by contact with calcite-rich grey hornfels. Results from geochemical modeling in PHREEQC suggested that precipitation of Zn carbonate, or Zn hydroxide minerals could not explain the observed attenuation. Scanning Electron Microscopy (SEM) suggested that Zn may have been incorporated into the crystal structure of phyllosillicate clay minerals; however, further work is needed to confirm this mechanism.

Insufficient data were available to develop a hypothesis as to the specific attenuation mechanisms responsible for removing Cd and As from solution.

In addition to shedding light on the geochemical processes controlling Mo and Zn in neutral mine drainage, this research also demonstrated the effectiveness of stacked field cells and humidity cells connected in series for the study of metal attenuation by waste rock mixing.

Preface

A version of chapter 2 will be submitted for publication with Roger D. Beckie, K. Ulrich Mayer, Sharon R. Blackmore, Leslie Smith, Bernhard Klein, Celedonio Aranda, Luis A. Rojas Bardón, and Raúl Jamanca Castañeda as co-authors. D. Trevor Hirsche (first author) helped design the experiments and install the stacked field cells at the mine, ran the humidity cells connected in series experiment, wrote the manuscript, and prepared the figures. Roger Beckie and Uli Mayer helped design the stacked field cell and humidity cells connected in series experiments, provided feedback on the manuscript, and assisted with the literature review. Leslie Smith and Bern Klein helped design both experiments. Celedonio Aranda, Sharon Blackmore, Luis Rojas Bardón, and Raúl Jamanca Castañeda helped design, procure materials for, and construct the stacked field cell experiment.

A version of chapter 3 will be submitted for publication with Roger D. Beckie and K. Ulrich Mayer as co-authors. The contribution of D. Trevor Hirsche (first author) is the same as in chapter two, in addition to performing XRD analysis, SEM analysis, geochemical modeling. Roger D. Beckie and K. Ulrich Mayer provided advice throughout the experimental design, and data interpretation processes. They also edited the manuscript.

A portion of Appendix B was modified from an Appendix in Rajiv Joiya's 2009 honors thesis in Applied Science.

Table of contents

List of tables

List of figures

Acknowledgements

Thank you to my committee: Roger Beckie, Uli Mayer, Leslie Smith, and Bern Klein for their guidance, patience, humor, and support throughout my extended tenure at UBC. None of this work could have occurred without the financial support of NSERC, Teck, and Antamina. It also would not have been possible without the hard work and know how of Antamina employees in Peru, MECOMA, and UNASAM. My fellow students provided an excellent sounding board for testing my ideas, as well as much needed emotional support. Cindy Starzyk, Diana Luévanos, Kristina Small, Pejman Rasouli, Mehrnoush Javadi, Kun Jia, Laura Laurenzi, María Lorca, John Dockrey, Nate Fretz, Sharon Blackmore, Holly Peterson, Natasha Sihota, Steve Momeyer and Dawn Paszkowski were genuinely great people to have around the office, lab, and field. While not a part of the research group, Gabriela Gottberg provided much needed advice, support, and motivation during the final months of the thesis. No acknowledgement list would be complete without mentioning my family – especially my parents and sisters who are always there when I need them. I would not have gotten very far at all in this process without the encouragement of Janaki Jayanthan. Ten years from now, more than lab work, or the process of writing this document, what I will remember most is my time in Peru. Thank you to the Barrenechea family, Cesar, Raúl Jamanca, Bartolo Valenzuela, Farah Acuña, Ami Valdez, Gabriela Apaza, Carla Tang, Mariella Caceres, Celedonio Aranda, Pablo Urrutia and other friends who are literally too numerous to list for making me feel very welcome and showing me around your beautiful country. I hope to be back soon.

Dedication

To the people of Peru – may the development of **your** resources be inclusive, sustainable, and respectful of your rich cultures.

Chapter 1: Introduction

The contamination of natural waters by acid mine drainage has received attention in the scientific literature for many decades (Colmer and Hinkle, 1947; Carpenter et al., 1983; Sullivan et al., 1988; Webster et al., 1998; Benner et al., 1999; Johnson, 2003). A common strategy for mitigating the effects of acid mine drainage is to neutralize drainage with lime or another acid neutralizing material at or near the mine site, a process which immobilizes many of the toxic metals dissolved in drainage (Johnson and Hallberg, 2005; Robinson-Lora and Brennan, 2009). In mines that exploit ore deposits hosted in carbonate-rich country rock, acid-consuming waste rock can be strategically mixed with acid-generating waste rock to limit acid release, a strategy that has been explored extensively at the Grasberg Mine in Indonesia (e.g. Andrina et al., 2006; Rusdinar, 2006). Research at the Grasberg Mine was carried out using an instrumented waste rock pile, where distinct waste rock blending techniques were applied to different sections of the pile to determine the most effective mixing style to reach the goal of acid neutralization on site (Andrina et al., 2003).

Although neutralization of mine drainage is a common strategy for mitigating its negative effects, neutral mine drainage itself is by no means benign. Many toxic metals can contaminate neutral mine drainage, including Ni, Mo, Se, Zn, and As (Lupankwa et al., 2006; Heikkinen et al., 2009; Plante at al. 2011a). This thesis forms a part of the UBC-Antamina-Teck Antamina 'Weathering of Alkaline Waste Rock project', which is dedicated to improving scientific understanding of neutral mine drainage systems. This thesis' contribution to the research project is to explore the possibility of attenuating metals by waste rock mixing in neutral mine drainage systems.

1.1 Significance of research

Zn and Mo are essential nutrients; however, in high enough concentrations they can have adverse environmental effects. In the case of Zn, concentrations of 0.3 mg/L have been shown to be toxic to some aquatic animals (Muyssen et al., 2006). In addition to having a negative effect on aquatic life in high concentrations, Mo can be toxic to livestock (Alloway, 1973; O'Connor et al., 2001; CCME, 2007). Many residents of the rural areas around the Antamina Mine depend on ranching for their livelihoods, therefore ensuring the safety of soil and water resources in the area of the mine is of the utmost importance. By improving scientific understanding of Mo and Zn mobility in neutral mine drainage waste rock systems, this research will aid in the development of tools and methodologies to predict the concentrations of these elements in mine drainage. Results from this study on waste rock mixing may also be used to design waste rock mixing schemes at mines as a means to remove these from their drainage before they are released into the environment.

In addition to improving scientific understanding of the geochemistry of neutral mine drainage, this study also introduces new approaches for researching attenuation by waste rock mixing. Few researchers have examined metal attenuation reactions in waste rock at the sub-pile scale. The few related studies in the literature researched the effects of mixing leachate or a leachate-like solution with waste rock, rather than directly mixing leachate from two different waste rock lithologies from the same mine site (Smart et al., 2010; Plante et al., 2011b). This research employs a modified version of humidity cell and field cell leaching experiments for the purpose of studying the effect of waste rock mixing on metal release. The application of field cells and humidity cells to waste rock mixing is unprecedented in the scientific literature, as discussed in chapter 2.

1.2 Site description

The Antamina mine is located approximately 270 km northeast of Lima, at an average elevation of 4,300 m above sea level (Antamina, 2011). The mine produces copper and zinc, along with smaller quantities of molybdenum and lead, from a skarn deposit formed by a series of quartz monzonite intrusions into carbonate country rock (Redwood, 1999; Love et al., 2004). Antamina mills on average 104,000 tonnes of ore and about 340,000 tonnes of waste rock daily, and is expected to close in 2029 (Klohn Crippen Berger Ltd, 2010). The mine's waste rock dumps´ location at the top of the watershed and proximity to permeable karst features makes metal leaching a concern at the site (Evans et al., 2005). Antamina receives ~1,200 mm precipitation per year, most of which falls as rain during the region´s six or seven month wet season. Very little precipitation occurs in the dry season between May and September. Antamina's mean annual temperature ranges between 5.4 and 8.5 °C (Klohn Crippen Berger Ltd, 2010). More detailed information on the study site and the other components of the research project completed up to this point can be found in Bay et al. (2009).

1.3 Study background

The portion of this study focused on Mo attenuation through waste rock mixing was motivated by observations from two distinct experiments related to Antamina's waste rock. Single material field cell experiments demonstrated that some waste rock types from the mine produced leachate with Mo concentrations of over 30 mg/L (Golder Associates, 2010). These concentrations are more than 300 times higher than the CCME Mo guideline for the protection of aquatic life of 0.073 mg/L (CCME 2007). Conlan et al.'s (2012) laboratory studies showed that the addition of lead (Pb) to neutral pH Mo-rich solutions caused

wulfenite ($PbMoO_4$) precipitation, thereby reducing aqueous Mo concentrations. Some Antamina waste rock contains significant quantities of Pb-minerals, though Pb and Mo do not occur in the same rock type. Pb and Mo-bearing rocks are co-mingled in the East Dump at Antamina, making it possible that wulfenite precipitation may lead to the reduction of Mo concentrations.

The portion of this study focused on Zn attenuation was motivated by a desire to predict the long-term quality of drainage from Antamina's Tucush waste rock dump. When this study was designed in 2009, Antamina had begun to place Zn-bearing moderately reactive waste rock in the Tucush dump, which had previously been reserved solely for low reactivity waste rock material. Mechanisms for Zn attenuation in the Tucush dump and the degree to which Zn would be attenuated by contact with non-reactive waste rock were unknown at the time. The Zn portion of the study was designed to improve understanding of Zn's fate in the Tucush dump.

1.4 Experimental approach

The full-scale waste rock dumps at Antamina are extremely heterogeneous, consisting of dozens of different lithologies, without any particular internal order (Figure 1.1 left panel). This study seeks to improve understanding of geochemical processes that may occur in the full scale dumps by focusing on attenuation reactions that occur when two distinct waste rock lithologies are mixed together. The study is designed such that leachate from one waste rock lithology (unmixed leachate) can be sampled prior to contact with the second. Leachate samples are also available after contact with both waste rock types has occurred (mixed leachate). The comparison of mixed and unmixed leachate allows for the detection of attenuation reactions that remove Zn, Mo, or other metals from solution. The parallel waste

rock mixing experiments in this study were run on two different scales: 2 m tall stacked field cells were installed at the mine site and exposed to natural precipitation (Figure 1.1, middle panel), and 30 cm tall humidity cells run in laboratory conditions at UBC (Figure 1.1, right panel). The humidity cells are connected in series such that the leachate from the first cell can be sampled, and then used to flush the second cell. The specific waste rock materials used in this study were chosen based on their previous inclusion in the associated waste rock piles, availability at the time the study was initiated, and the occurrence of elements of interest (e.g. Pb, Zn, Mo) in leachate from their single field cells at the Antamina Mine. Detailed information on the materials installed in each stacked field cell can be found in Appendix A2 of this thesis.

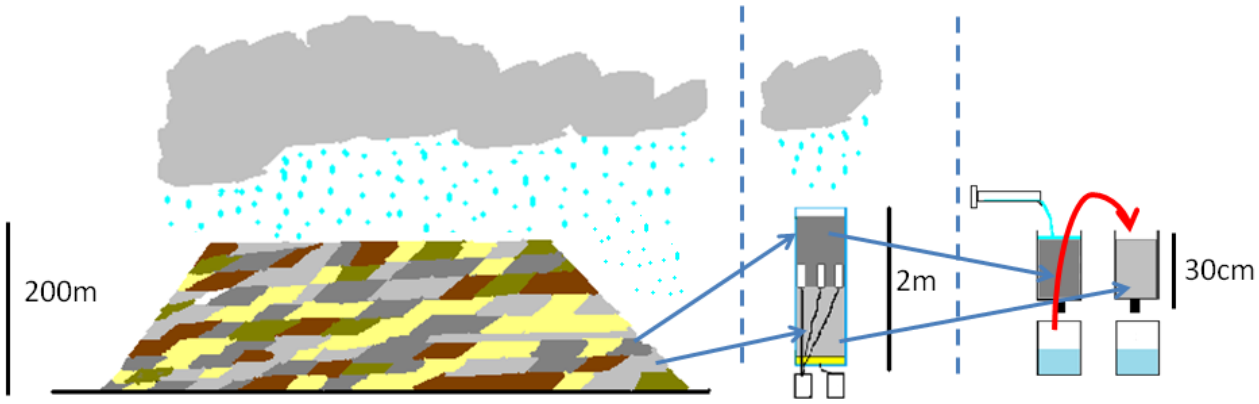

Figure 1.1 A conceptual model for the experiment, where specific material combinations from a heterogeneous waste rock pile (left) are combined in a stacked field cell experiment (middle) to react at ambient conditions. The same materials are examined in the laboratory in humidity cells connected in series, such that leachate from the top material in the stacked field cell is poured over the second field cell, as indicated by the red arrow (right).

1.5 Research objectives

The principal objectives of this thesis are to:

- Evaluate the effectiveness of stacked field cells and humidity cells connected in series for the study of metal attenuation by waste rock mixing

- Test the hypothesis that Pb could limit aqueous Mo concentrations through the precipitation of wulfenite ($PbMoO_4$) under field conditions at neutral pH
- Assess the degree to which Zn could be attenuated by contact with non-reactive hornfels or limestone material in neutral pH conditions
- Identify the mechanism(s) responsible for Zn attenuation

Secondary objectives are to:

- Determine if any other elements (aside from Zn and Mo) are attenuated in the studied waste rock mixing regimes
- Understand the hydrologic behavior of stacked field cells

1.6 Thesis structure

This thesis is written in a paper-based format. It consists of a total of five chapters: an introduction, three papers, and conclusions. The three papers are self-contained – each with an introduction, methods, and results/discussion sections. The first paper (Chapter 2) discusses in detail the methods employed in this study while describing the attenuation of As in one of the stacked field cells. The second paper (Chapter 3) describes the attenuation of Mo and Zn in two distinct stacked field cells and outlines hypotheses as to the probable mechanisms behind their attenuation. The third paper (Chapter 4) provides further background on metal attenuation observed in the study, while exploring flow in the stacked field cells. Finally, the appendices provide detailed descriptions of the materials and methods employed in this study.

Chapter 2: A novel approach to studying geochemical attenuation in mine waste rock: stacked field cells and humidity cells connected in series[1]

2.1 Introduction

Integrated waste-management strategies are becoming increasingly important to minimize liability and environmental impact of the mining industry (Kwong, 2003; Kalin, 2004). An understanding of the local environmental geochemical conditions, both in the mine itself, and the natural baseline in the surrounding area, can aid in the safe disposal of mine waste (Odor et al., 1999). One strategy that can be developed based on this understanding the mixing of different rock types to facilitate metal attenuation reactions in the waste rock dump itself. The idea of mixing different waste rock types to generate favorable geochemical conditions for metal attenuation has been studied in an acid mine drainage (AMD) context at the Grasberg mine in Indonesia (Andrina et al., 2006; Rusdinar, 2006). Andrina et al. (2006) used fully-instrumented experimental waste rock piles to assess different methods of blending carbonate-rich and acid-generating waste rock together to increase leachate pH. In this study we present the use of smaller-scale, more cost-effective field (stacked field cells) and laboratory (humidity cells connected in series) kinetic leaching tests to study the geochemical effects of waste rock mixing.

Field cell or humidity cell scale kinetic leaching tests are common tools for predicting the long-term water quality of mine drainage from waste rock dumps (e.g. Sapsford et al., 2009). Whether these tests are carried out in large-scale waste rock piles, smaller field cells, or

[1]This chapter will be submitted as a paper with the following authors list D. Trevor Hirsche, Roger D. Beckie, K. Ulrich Mayer, Sharon R. Blackmore, Leslie Smith, Bernhard Klein, Celedonio Aranda, Luis A. Rojas Bardón, Raúl Jamanca Castañeda

humidity cells in the laboratory, they tend to focus on the rates and mechanism of sulfide oxidation and metal release from single rock types (Strömberg and Banwart, 1999; Frostad et al., 2002; Benzaazoua et al., 2004; Blowes et al., 2007, Sapsford et al., 2009; Aranda et al., 2009). Attenuation reactions such as secondary mineral precipitation and adsorption onto iron hydroxides can also be very important controls on the concentrations of metals in heterogeneous waste rock dumps and the surrounding environment (Gupta et al., 1987; Odor et al., 1999; Webster et al., 1998; Trivedi and Axe, 2000; Plante et al., 2011b; Conlan et al., 2012); however, these processes are not assessed in standard kinetic leaching procedures.

To our knowledge, the only example in the scientific literature of the modification of a field cell kinetic leaching procedure to investigate attenuation reactions is the study of blending apatite with acid-generating waste rock as a means of mitigating AMD (Fyson et al., 1995; Kalin, 2004; Kalin and Harris, 2005). Kalin and Harris (2005) installed a series of 70 L barrels of acid-generating sulfidic waste rock at a mine site in northern Quebec, allowing the waste rock to react with natural precipitation under ambient conditions, and analyzing its effluent regularly over a period of several years. To demonstrate the utility of apatite blending in AMD-mitigation, they installed some barrels with pure waste rock, and others with a waste rock/apatite-bearing rock mixture, then compared the leachate pH and chemical composition between these cells.

The current study is similar to that of Kalin and Harris (2005) in that it uses barrel-sized field experiments to assess geochemical attenuation promoted by mixing different rock types together. The field cell component of this study is distinct from the work of Kalin and Harris (2005) in several respects: waste rock from the same mine site, rather than imported material, is used as the attenuating material; the attenuating and releasing materials are layered rather

than blended; the experiment is carried out at a larger scale to better account for heterogeneity; and sub-lysimeters are installed in the field cells to directly compare leachate composition before and after attenuation.

In addition to the field cell component, this paper introduces the use of humidity cells connected in series to study attenuation by waste rock mixing. Some humidity cell-like experimental designs have been previously used to study metal attenuation in waste rock in the laboratory (Smart et al., 2010; Plante et al., 2011b). These studies; however, involved application of a pre-prepared solution to waste rock material rather than mixing leachate from two different waste rock types at the humidity cell scale, which, to our knowledge, is a completely novel approach. The effectiveness of the approaches introduced in this study is demonstrated through the use of a case study involving arsenic attenuation in waste rock from the Antamina copper and zinc mine in Peru.

Antamina is located at 4,300 m above sea level in a region with approximately 1,200 mm/yr precipitation and a four to five month long annual dry season. In spite of its tropical latitude, the cooling effect of its high elevation gives Antamina an average annual temperature of between 5 and 9^{o}C (Klohn Crippen Berger Ltd, 2010). The mine produces copper and zinc, along with smaller quantities of molybdenum, bismuth, and lead, from a skarn deposit formed by a series of quartz monzonite intrusions into carbonate country rock (Redwood, 1999; Love et al., 2004). Over the first 10 years of Antamina's operations, the carbonate country rock has provided ample buffering capacity, preventing most leachate from turning acidic; however, several metals and metalloids including Mo, As, Zn, and Cu have reached high enough concentrations in neutral pH drainage to require attention (Bay et al., 2009; Aranda et al., 2009).

In this paper we demonstrate the utility of the stacked field cell and humidity cell connected in series methods to assess attenuation processes promoted by waste - rock mixing. We use these methods to investigate the use of black marble waste rock to attenuate As released from intrusive waste rock from the Antamina mine.

2.2 Methods

2.2.1 Field cells

The field cell component of this experiment was initiated in 2006 (single material field cells) and 2009 (stacked field cells) and is currently ongoing. The single material field cells consist of 205 L plastic drums filled with coned and quartered waste rock material that was passed through a 10 cm mesh sieve (Figure 2.1). The plastic drums are open at the top allowing them to collect natural precipitation, and are fitted with a sloping bottom to direct basal drainage to a leachate sample collection system (Aranda et al., 2009). The sloping bottom is protected by a 10 cm thick layer of #60 mesh silica sand covered by a piece of Geotextile. Refer to Aranda (2009) for a more detailed description of the field cell design. Leachate from these field cells is sampled regularly, whenever sufficient volume for laboratory analysis is produced over the sampling interval. Leachate samples from the field cells are analyzed for pH, conductivity, major ions, and trace metals.

2.2.2 A novel stacked field cell design for the study of waste rock mixing

Stacked field cells, where one rock type is placed above another, are used to study metal attenuation caused by waste rock mixing. The stacked field cells were constructed by placing a second barrel on top of a conventional barrel field cell used at the site to form a single, 1.8 m tall (410 L) field cell. A wooden frame was constructed to hold the field cells in place and to prevent toppling (Figure 2.1). Distinct waste rock types were placed in the bottom and top

half of each stacked field cell, such that at the midpoint of the cell the two rock types were in direct contact with each other. This arrangement mimics the type of associations between distinct rock types in typical full scale waste rock dumps.

Figure 2.1 UBC's single field cells (left) and stacked field cells (right) installed at Antamina. Each barrel is 90 cm tall with a diameter of 48 cm. The buckets placed in front of the barrels collect leachate. Each stacked field cell contains 2 to 3 different material types arranged to approximate geochemical conditions in UBC's experimental piles at Antamina, or the full-scale dumps themselves. The grey PVC tubes visible on the sides of the barrels channel drainage from the upper lysimeters.

Drainage collected from the bottom of a stacked field cell has had contact with both rock types contained in the field cell. Samples representative of leachate from the material in the top material were collected using three mini-lysimeters installed at the contact between the two material types (Figure 2.2). The mini-lysimeters were made by cutting the bottoms out of 1 L polyethylene sample bottles and covered a total of about 6.5% of the surface area of the field cells. All three mini-lysimeters drained to the same sample bucket. Holes were drilled into the sides of the plastic field cell barrels prior to the installation of the waste rock material to allow the mini-lysimeter drainage hoses to pass through the sides of the plastic barrels. These holes were sealed with silicone after the installation of the mini-lysimeters.

Figure 2.2 The upper lysimeters used to sample leachate from the top material (material 1) in the stacked field cells prior to mixing with the bottom material (material 2). The bucket "a" in the diagram indicates the bucket that collects water from the lysimeters, whereas "b" represents the bucket that collects water from the base of the field cell. The photograph to the right shows the upper lysimeters of a stacked field cell at Antamina during the installation of the second material type.

2.2.3 Humidity cells

A companion humidity cell experiment was established at the University of British Columbia in September 2010 to provide further confirmation of attenuation reactions observed in stacked field cell experiments, and to test whether the same attenuation could be replicated at a smaller scale and under laboratory conditions. To imitate the stacked field cell experiment, humidity cells were run in series, meaning that leachate from one humidity cell was collected (the leaching material), and then subsequently allowed to flow through a second humidity cell (the attenuating material).

The humidity cell procedures employed in this study were based on the standard ASTM (1996) methodology, with some important modifications. One of the principal modifications of the ASTM (1996) method was the use of a 'flood rinse', where water is added to the column by pouring it over a period of less than a minute, rather than a 'drip rinse', where water is slowly drizzled onto the waste rock surface over a period of three days. Lappako and White (2000) found that this less labour-intensive flooding procedure made little difference to leachate composition when compared to the ASTM (1996) approach. The humidity cells in

this study were also subjected to passive oxidation and humidification, being installed in an enclosed chamber with abundant standing water without air pumped through the leaching chamber. Frostad et al. (2002) found that passive oxidation better simulates field leaching conditions than active oxidation.

Waste rock material was placed into the humidity cells while still humid in an effort to maintain its original microbial community. The waste rock material installed in the humidity cells was sieved through a ¼" mesh. The sieved waste rock material was coned and quartered twice more in the laboratory prior to humidity cell installation in an effort to ensure that it was as homogeneous as possible. One kilogram of material was placed in each humidity cell. A total of 17 humidity cells were installed using 4 different material types. To demonstrate the usefulness of humidity cells for the study of attenuation, we focus on results from 8 humidity cells in particular (Table 2.1).

Table 2.1 Contents of 4 field cells installed to study metal attenuation at Antamina and 8 humidity cells installed at UBC for the same purpose. FC-black marble over intrusive and FC-intrusive over black marble are stacked field cells with two different material types, whereas UBC-1-3A and UBC-2-0A are single field cells.

Field Cell Code	Equivalent Humidity Cells	Materials Used	Purpose
UBC-1-3A	HC-13-T1	Pb-bearing black marble waste rock – one of the material types used in FC-black marble over intrusive and FC-intrusive over black marble.	Determine composition of leachate from Pb-bearing black marble
UBC-2-0A	HC-20-T1	Mo-bearing intrusive waste rock – one of the material types used in FC-black marble over intrusive and FC-intrusive over black marble.	Determine composition of leachate from Mo-bearing intrusive rock
FC-black marble over intrusive	HC-black marble over intrusive	Pb-bearing black marble on top of Mo-rich intrusive rock	Investigate possible Mo attenuation by co-precipitation with Pb
FC-intrusive over black marble	HC-intrusive over black marble	Mo-rich intrusive on top of Pb-bearing black marble	Investigate possible Mo attenuation by co-precipitation with Pb

The humidity cells themselves were constructed out of acid washed plastic Nalgene bottles with their bases removed (Figure 2.3). The smaller of the two openings in the inverted Nalgene bottles was blocked by a drainage apparatus to hold water and waste rock material in place, and allow leachate to drain out of the humidity cell when desired. A fine nylon mesh was placed at the bottom of the cell to prevent waste rock material from washing out of the humidity cell and a plastic stopcock was installed on the outside of the drainage tube so that the humidity cell could be sealed to prevent drainage, if required.

Humidity cells were housed in plastic storage bins with tight fitting lids. The lids on the bins were loose enough to allow for minor air circulation. The base of each bin was covered in a

layer of standing water (at least 1 cm deep) to ensure that the air on the inside of the bins remained at 100% relative humidity. Leachate from the humidity cells was allowed to drain into a 500 mL Nalgene bottle for posterior sampling.

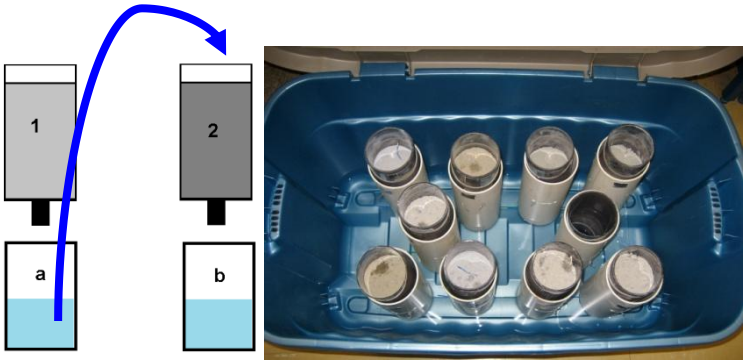

Figure 2.3 The humidity cells experiment set up at UBC to study attenuation in the laboratory. Left: a conceptual diagram showing the manner in which leachate from one material type is poured onto the attenuating material. Right: the humidity cells as they were installed at UBC. The blue bin was sealed with water at the base to keep the relative humidity high.

Humidity cells HC-32-T1, HC-32-T2, HC-20-T1, and HC-20-T2 were subjected to a modified ASTM humidity cell leaching procedure, in which 500 mL of distilled, de-ionized water was added to the cells on a weekly basis, and an hour of reaction time was allowed before the stopcocks were opened to allow water to drain from the humidity cells (ASTM, 1996).

Leachate samples were collected from humidity cells on a weekly basis throughout the first 20 weeks of the laboratory experiment, although thereafter leaching continued to occur every week, although some humidity cell leachate samples were collected every two weeks. Leachate was filtered through a 0.45 µm filter membrane into a 30 mL HDPE sample bottle, which had previously been triple-rinsed with filtered sample. Samples for cation analysis were acidified to below pH 3 with nitric acid. Immediately after the collection of the water quality sample, a separate 25 mL sample was titrated using sulfuric acid for alkalinity determination. Water quality samples were stored in a refrigerator prior to analysis for major ions, trace metals, and elemental sulfur with a Varian ES-725 ICP-OES.

2.2.4 Humidity cells connected in series

To evaluate attenuation by waste rock mixing, we developed a new protocol where leachate produced from a humidity cell containing a hypothesized releasing material was applied to a humidity cell containing a hypothesized attenuating material. This provided more representative water-to-rock ratio (compared to that in the field cells) and allowed more reaction time in the (second) humidity cell with the attenuating material, so that secondary mineral formation was not kinetically limited. A water-to-rock ratio typical of the stacked field cells was approximated by adding 230 mL of distilled water each week to the four humidity cells with metal releasing materials. The stopcock was left closed for 1 hour before the humidity cell was allowed to drain for one week. An 80 mL subsample was removed from the leachate from the first (metal releasing) humidity cell was retained for chemical analysis, and the remaining 150 mL of leachate to be passed through the second (metal attenuating) humidity cell. The stopcock at the base of the second (attenuating) humidity cell was left closed for a full 24 hours instead of just 1 hour as dictated by the standard ASTM (1996) procedure.

While maintaining water-saturated conditions at the bottom of the humidity cell for a longer period of time than proscribed in the ASTM (1996) procedure limits sulfide oxidation by restricting the supply of oxygen, it provides longer time to facilitate dissolution and re-precipitation of secondary minerals and kinetically limited adsorption reactions.

2.2.5 Illustrative example of experimental approaches: materials used

We demonstrate the stacked field cell and humidity cells connected in series protocols using waste rock from the Antamina mine site. The waste rock was selected based on three criteria: propensity to leach metals of interest, the hypothesized ability to attenuate metals of interest,

and previous use in UBC's experimental waste-rock piles (Bay et al., 2009). We focus on results from field cells containing two distinct materials: Pb-bearing black marble, UBC-1-3A; As-bearing intrusive, UBC-2-0A. A conventional single material field cell containing Pb-bearing black marble was installed in August 2006 and a different single field cell containing As-bearing intrusive rock was installed in October 2007. Additional samples of these waste rock types were stored at ambient temperatures in plastic bags under a roof or tarps until June 2009, 33 and 19 months after they were mined, when they were placed in the stacked field cells FC-black marble over intrusive and FC-intrusive over black marble (Table 2.1). Approximately 350 kg of each rock type was placed in the top and bottom half the stacked field cell.

2.2.6 Data processing procedures

Leachate chemistry data from the first two rainy seasons after installation are presented for all field cells, starting at 10 days before the first samples were collected from each cell. Data from single field cells are included on the graphs for comparison with data from the stacked field cells, given that the mini-lysimeters from the stacked field cells produced insufficient solution for chemical analysis. The time (horizontal) axis dry seasons were removed from field cell graphs to ease comparison between stacked and single field cell data, and also to remove gaps from the data series in the graphs, since water samples were not available during these times.

2.3 Performance

2.3.1 Geochemical attenuation of As

We use the example of arsenic attenuation by contact with Pb-bearing black marble to illustrate the usefulness of stacked field cells and humidity cells connected in series. Arsenic

leached from the base of FC-black marble over intrusive, reaching 0.18 mg/L seventeen weeks after initial flow from the field cells, and fluctuating between 0.15 mg/L and 0.2 mg/L for the remainder of the study period ('Stacked (base)' in top right graph, Figure 2.4). Arsenic concentrations in the black marble single field cell were consistently below 0.03 mg/L ('Single' in top right graph, Figure 2.4). The As concentration in the single sample of leachate available from the top lysimeter in FC-black marble over intrusive was 0.009 mg/L ('Stacked (Top)' in top right graph, Figure 2.4). The pH of basal leachate dipped to 6.7 shortly after installation, before stabilizing between 7.5 and 8 for most of the experimental period ('Stacked (base)' in bottom right graph, Figure 2.4). Leachate from the top lysimeter rose gradually over time from 7.5 before remaining relatively stable near 7.8 for the duration of the experiment ('Stacked (top)' in bottom right graph, Figure 2.4). Insufficient flow from the upper lysimeters in FC-black marble over intrusive led to a lack of pH data during the second year of the experiment.

Arsenic concentrations in the associated humidity cells connected in series (HC-black marble over intrusive), where leachate flowed through black marble, before making contact with intrusive material, showed similar trends to in stacked field cell FC-black marble over intrusive. As concentrations in leachate from the second humidity cell in series fluctuated between 0.1 and 0.3 mg/L in the first half of the experiment, reaching maximum of 0.39 mg/L in week 21 and exceeding 0.3 mg/L for the final 10 weeks of sampling ('Second cell' top left graph, Figure 2.4). Very little arsenic leached from the black marble waste rock, since As concentrations never exceeded the detection limit of 0.09 mg/L ('First Cell', top left graph, Figure 2.4). Leachate pH from HC-black marble over intrusive fluctuated between 7 and 8 (Bottom left graph, Figure 2.4). During the last 20 weeks of the experiment leachate

pH from the second cell in HC-black marble over intrusive tended to be 0.2-0.6 pH units higher than that of leachate pH from the first cell in HC-black marble over intrusive, suggesting that pH was increased by contact with intrusive material.

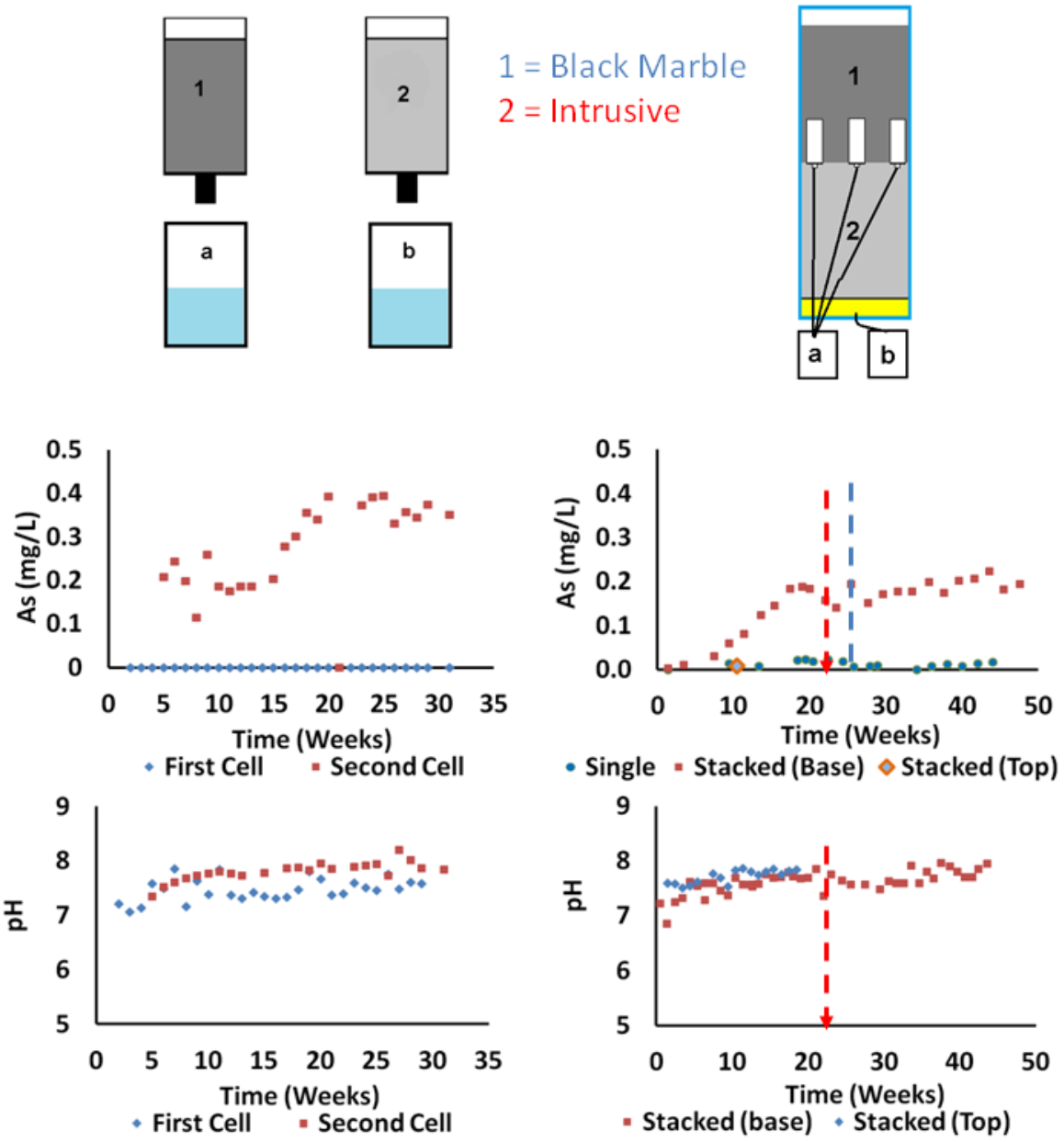

Figure 2.4 As-concentrations (middle) and leachate pH (bottom) as a function of time since the initiation of flow in stacked field cell FC-black marble over intrusive (right column) and corresponding humidity cells HC-black marble over intrusive (left column). The upper diagrams show the configuration of waste rock material in this stacked field cell and its corresponding humidity cells. The vertical red dashed line with an arrow on the field cell graphs indicates the position of the data gap at end of the first rainy season in the stacked field cell data, while the dashed blue line without the arrow indicates the end of the first rainy season on the single field cell series.

Results from the FC-intrusive over black marble revealed that contact with black marble removed As from leachate (Figure 2.5). Arsenic concentrations in the leachate from the base

of FC-intrusive over black marble were consistently below 0.01 mg/L ('Stacked (base)', top right graph, Figure 2.5). Typical As concentrations in leachate from the intrusive rock at the top of FC-intrusive over black marble ranged from 0.15 mg/L to 0.4 mg/L ('Single' top right graph, Figure 2.5). The As concentration in the sample from the upper lysimeter in FC-intrusive over black marble was 0.28 mg/L, suggesting that similar quantities of arsenic were also being released from the intrusive material at the top of the stacked field cell ('Stacked (top)', top right graph, Figure 2.5). Leachate pH from the base of FC-intrusive over black marble dipped to 6.7 before gradually increasing over several weeks to 7.5 to 7.7 ('Stacked (base)', bottom right graph, Figure 2.5). Towards the end of the study time, the pH of basal leachate from FC-intrusive over black marble exceeded 8. The pH of leachate from the upper lysimeter showed a very similar trend to that of basal leachate, although it was often 0.1 to 0.3 pH units higher ('Stacked (top)', bottom right graph, Figure 2.5).

Data from humidity cells in series HC-intrusive over black marble, where leachate from intrusive waste rock was run through black marble, demonstrated that As attenuation also occurred under laboratory conditions. Arsenic concentrations in the leachate from As-releasing intrusive material rose from around 0.17 mg/L near the beginning of the experiment to 0.4-0.5 mg/L during its final 20 weeks ('First Cell', top left graph, Figure 2.5). Arsenic concentrations in the same leachate were reduced to below detection limit after passing through the black marble in HC-intrusive over black marble ('Second Cell', top left graph, Figure 2.5). Leachate pH ranged between 7 and 8 throughout the entire duration of the experiment (Bottom left graph, Figure 2.5). Contact with the black marble appeared to increase leachate pH, making leachate from the second cell in HC-intrusive over black marble 0.2 to 0.6 pH units higher than leachate that had only passed through the first cell.

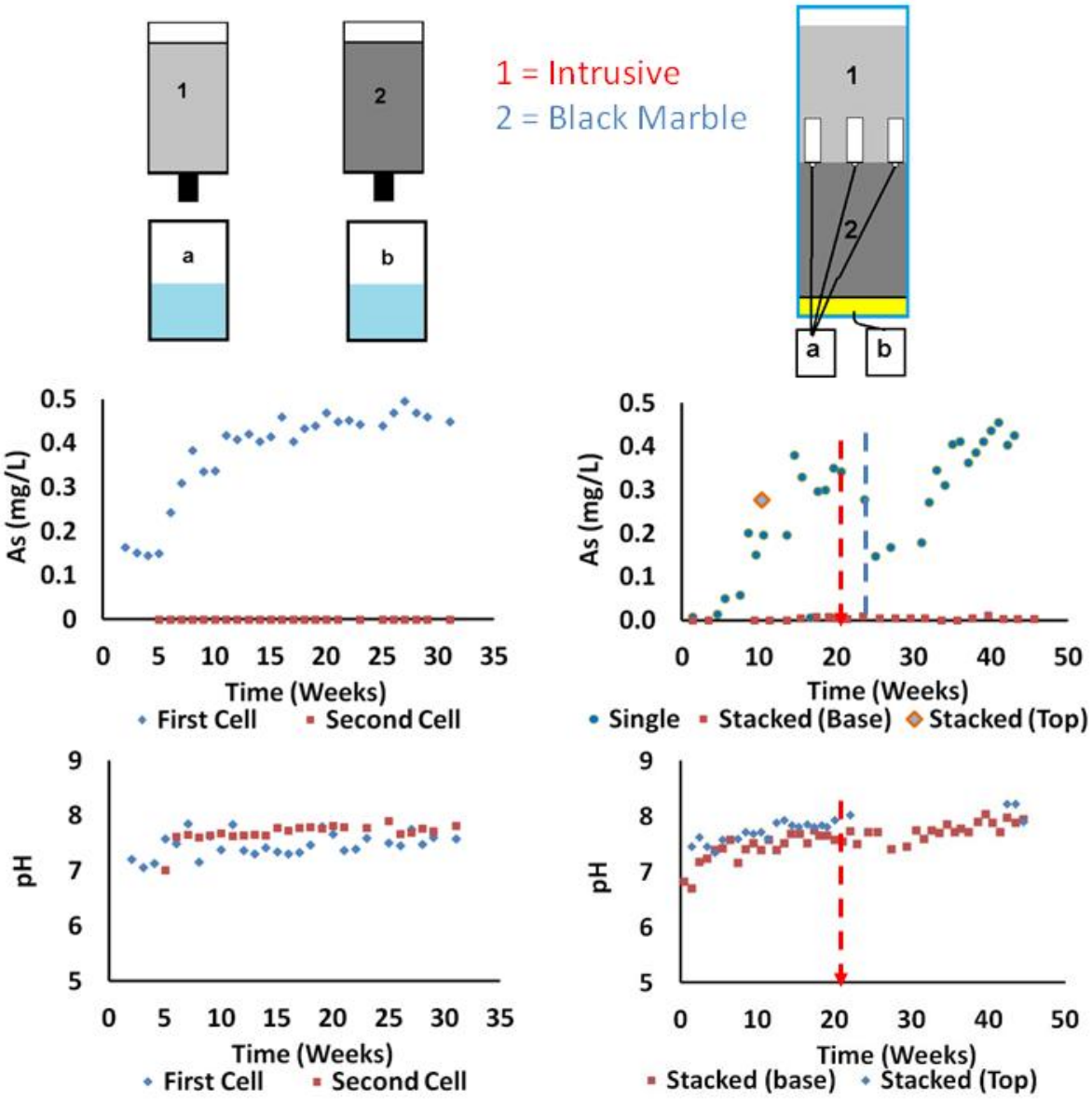

Figure 2.5 As-concentrations (middle) and leachate pH (bottom) as a function of time since the initiation of flow in stacked field cell FC-intrusive over black marble (right column) and corresponding humidity cells HC-intrusive over black marble (left column). The upper diagrams show the configuration of waste rock material in this stacked field cell and its corresponding humidity cells. The vertical red dashed line with an arrow on the field cell graphs indicates the position of the data gap at end of the first rainy season in the stacked field cell data, while the dashed blue line without the arrow indicates the end of the first rainy season on the single field cell series.

2.4 Discussion

2.4.1 Example application: arsenic attenuation

Arsenic concentrations in leachate from the intrusive rock used in this study usually ranged between 0.15 and 0.4 mg/L in field cell leachate. More than 94% of this As was removed by contact with black marble, decreasing As concentrations to below 0.01mg/L at the base of mixed material stacked field cell FC-intrusive over black marble. Arsenic concentrations in leachate from the base of FC-black marble over intrusive, where black marble was placed on top of As-releasing intrusive rock exhibited similar concentrations to those found in leachate from the unmixed single field cell of intrusive waste rock. The stacked field cells method was able to demonstrate that the order in which the waste rock was placed determined the degree of attenuation.

In spite of the differences in grain size distribution, flow regime, temperature, and experimental scale between the humidity cells and the stacked field cells, the same pattern of As attenuation was observed for both methods. As was the case in the humidity cells, arsenic was only removed from leachate when direct contact occurred between the leachate and the attenuating material (i.e. when the leachate passed through the As-releasing intrusive rock prior to making contact with the black marble). The ICP-OES method used to analyze samples from the humidity cell experiment was not as sensitive as the method employed by ALS laboratories in Lima to analyze chemistry samples from the stacked field cells, therefore a comparison of removal efficiencies at the different scales is not feasible. Arsenic concentrations were reduced to below the detection limit (0.09 mg/L) in all samples that had passed through black marble. Given that maximum As concentrations in leachate from the

first HC-intrusive over black marble cell were 0.47 mg/L, at least 80% of As was removed after contact with black marble in the humidity cell experiment.

2.4.2 Insight into attenuation mechanism

The methods presented here can provide opportunities to identify the attenuation mechanism. This has been done for Zn in a different field cell (Chapter 3), however was not possible in the case of As because if its low leachate concentration. Many researchers have identified co-precipitation with secondary iron minerals like jarrosite, or adsorption onto iron-oxide, or oxy hydroxide surfaces as important mechanisms for As attenuation in mine drainage systems (e.g. Smedley and Kinniburgh 2002; Fukushi et al., 2003 and references therein). Dixit and Hering (2003) ran batch experiments mixing As(V) containing solutions with amorphous iron oxy hydroxide solid phases and found that circum-neutral pH adsorption removed nearly all of the As from a solution that initially contained 0.7 mg/L. If such adsorption mechanisms were responsible for the attenuation of As in this study it is unclear why As was released from intrusive material in the first place, given that these secondary iron oxy hydroxide mineral phases commonly occur in waste rock and tailings due to the precipitation of iron from pyrite oxidation at circum-neutral pH (Smedley and Kinniburgh, 2002).

An alternative explanation for the pattern of As attenuation observed in this study is the co-precipitation of As and Pb in a secondary minerals such as schultenite ($PbHAsO_4$), mimetite $Pb_5(AsO_4)_3Cl$, or hydroxymimetite ($Pb_5(AsO_4)_3OH$) (Villalobos et al., 2010). Co-precipitation with Pb would explain the observation that mixing the As-bearing leachate with Pb-bearing led to a marked decline in dissolved As concentrations. In this geochemical system Pb is likely released into solution by galena (PbS) oxidation, and immobilized by the

precipitation of cerrusite ($PbCO_3$) (Chapter 3). Lead's low mobility in this system is potentially responsible for this study's observation that As is only removed from solution when As-bearing leachate comes in direct contact with Pb-bearing black marble. We hypothesize that as arsenic-bearing leachate enters the zone of active galena oxidation in this experiment, As reacts with the newly released Pb to form schultenite, mimetite or hydroxymimetite before cerrusite precipitation can occur. Further research, such as the identification of As secondary minerals in the attenuating material, is needed to identify the mechanism behind As attenuation in this study.

2.4.3 Stacked field cell performance

The results of this study provided an opportunity to evaluate the performance of the stacked field cells as means of collecting data on the geochemical attenuation potential due to waste rock mixing. One important issues was the performance of the upper lysimeters, since they provided a direct means of comparison between pre-mixing leachate chemistry and the mixed leachate that flows out of the base of the field cell. The stacked field cells were designed such that just over 6% of the total flow would be intercepted by the upper lysimeters. During the first two rainy seasons after their installation, 1.3% of the total flow was captured by the upper lysimeters in FC-intrusive over black marble, whereas only 0.3 % of the total flow was captured by FC-black marble over intrusive's upper lysimeters. The low number of data points from the upper lysimeters was not just a result of the low water volume that the upper lysimeters captured. A second factor limiting the amount of chemistry data that could be collected from the upper lysimeters was that the commercial laboratory where the samples were analyzed required at least 1L of sample for their analysis to comply with QA/QC procedures. In the third year of this experiment, a different laboratory was chosen for

leachate chemical analysis, allowing the sampling procedure to be modified to require less leachate. This change in sampling procedures has allowed for the collection of more leachate samples from the upper lysimeters in FC-intrusive over black marble, but as of the time of publication, data from these samples were not yet available.

The scarcity of leachate samples from the upper lysimeters meant that data from the single field cells was essential for interpreting the results of this study. We believe that the single field cell leachate results are valid surrogates for the upper lysimeters of the stacked field cell, since they were composed of the same homogenized waste rock. Data from this study indicate that the use of single field cell data as surrogates for data from the top of the stacked field cell has some limitations, especially when working with highly heterogeneous waste rock, it is generally satisfactory.

2.5 Conclusions and recommendations

This study leads to four important conclusions that have implications for waste rock management in neutral drainage systems: 1) Stacked field cells and humidity cells installed in series can both be used to study attenuation reactions 2) results between the methods are comparable, despite the differences in scale, 3) in addition to obtaining quantitative information on metal attenuation, the experiments are useful to develop hypothesis and guide follow-up research on metal attenuation mechanisms, and 4) Simply putting the two rock types in contact is not enough to ensure attenuation; the metal-rich leachate must have physical contact with an attenuating material to sequester as the metal.

Single field cells also allow for a better understanding of the pre-mixing leachate composition from the material in the bottom of the stacked field cell. While it is important to have separate single material field cells installed in conjunction with the stacked field cells, it

is also important to have functioning upper lysimeters in the stacked field cells to help account for waste rock heterogeneity.

This investigation has demonstrated that both stacked field cells and humidity cells connected in series can be used to study attenuation in waste rock. Some advantages of the stacked field cells are that their larger volume and larger grain size allows them to better account for sample heterogeneity and waste rock texture, and that they operate under ambient field conditions, and therefore give more representative reaction rates. Disadvantages of the stacked field cell technique include the risk of malfunctioning upper lysimeters, the extra cost associated with the implementation of their more complex design. The major advantages of the humidity cell approach are the ease of installation and sampling, the ability to control leaching conditions, the ease with which unmixed leachate from the releasing material can be sampled, and the fact that they accelerate the reactions involved with leaching and attenuation, and therefore could be used to help predict the long-term behavior of the system. Disadvantages of using humidity cells to study attenuation are that they are too small to adequately account for geochemical heterogeneity in waste rock, and do not leach under ambient field conditions. Both methods yielded similar results in this study, and further comparison between the two methods in this in Antamina waste rock suggest that running humidity cells in series can be used to reliably assess attenuation reactions due to waste rock mixing (Chapters 3 and 4).

Chapter 3: A study of Zn and Mo attenuation by waste rock mixing in neutral mine drainage from the Antamina mine in Peru using stacked field cells and humidity cells[2]

3.1 Introduction

Mine managers are increasingly aware of the importance of understanding the geochemical characteristics of ore deposits and their surrounding host rock when developing waste-rock management or mine closure plans (Kwong, 2003). Mixing different waste rock materials from the same mine site may help mitigate the environmental consequences of mine drainage. Such strategic mixing is often used in conjunction with application of off-mine amendments such as ash, lime, or alkali phosphate-bearing rock (Mehling Environmental Management, 1998; Morin and Hutt, 2000; Bertocchi et al., 2006; Hakkou et al., 2009; Robinson-Lora and Brennan, 2009). An extensive research program has been conducted at the Grasberg mine in Indonesia to examine the effectiveness of different schemes for mixing limestone and acid generating material in an effort to mitigate acid mine drainage without relying on amendments from outside the mine site (Miller et al., 2003; Andrina et al., 2006; Smart et al., 2010). Like the Grasberg mine project, most research on waste rock mixing has focused upon mixing of acid producing and neutralizing materials for the purpose of maintaining a neutral pH. In contrast, we explore the attenuation of aqueous Mo and Zn that has been released into neutral pH drainage from one waste rock type when it is mixed with a second waste rock type from the same mine.

The Antamina copper and zinc mine in the Peruvian Andes, extracts material from a Cu- and Zn-rich skarn deposit in limestone-rich country rock, which provides abundant natural

[2] A version of this chapter will be submitted for publication with D. Trevor Hirsche, Roger D. Beckie, and K. Ulrich Mayer as authors

neutralization potential (Love et al., 2004). Even though drainage from Antamina's waste rock is circum-neutral, certain metals, like Cu and Zn, and metalloids, including Mo and As, may reach high enough concentrations to require treatment (Bay et al., 2009; Aranda et al., 2009). Although both of these species are mobile in neutral conditions, they exhibit distinct chemical behaviors given that Mo occurs as an oxyanion (MoO_4^{2-}), whereas Zn^{2+} is a weakly hydrolyzing cation (Langmuir, 1997, p. 98).

Molybdenite (MoS_2) oxidation in tailings and waste rock is an important source of Mo in mine drainage systems (e.g. Borden, 2003), and the abundance of molybdenite in the waste rock at Antamina suggests that it is the major source of Mo in this study. Mo's mobility is limited by adsorption onto Al and Fe oxides below pH 5; however this mechanism is much less effective in circum-neutral pH conditions (Goldberg et al., 1996; Gustafsson et al., 2003). In circum-neutral conditions, Mo concentrations are controlled by the precipitation of minerals like wulfenite ($PbMoO_4$) and powellite ($CaMoO_4$) (Vlek and Lindsey, 1977). Laboratory experiments with artificial materials demonstrated that the precipitation of both of these minerals could play an important role in reducing Mo mobility in conditions representative of mine drainage from Antamina (Conlan et al., 2012).

Sphalerite (ZnS) is a common Zn mineral in skarn deposits, such as that mined by Antamina (Love et al., 2004; Chang and Meinert, 2008). Sphalerite oxidizes when waste rock is exposed to the atmosphere, releasing Zn into solution (Borden, 2003). Once mobile in a circum-neutral solution, Zn may be: taken up by phyllosilicate minerals (Manceau et al., 2000), precipitated as a hydroxide or carbonate secondary mineral (Gupta et al., 1987), or adsorbed on to an iron or aluminum oxides or oxy hydroxides (Trivedi and Axe, 2000).

Our research examines the geochemical attenuation of Zn and Mo through the layering of different types of waste rock from the Antamina mine. Attenuation mechanisms are investigated using stacked field cells installed in ambient conditions at the mine site. The study also includes a laboratory experiment using humidity cells connected in series such that the leachate from one material type flows through a second humidity cell with a distinct material type. More specifically, the experiments in this study were designed to determine if contact with carbonate-rich hornfels waste rock can reduce Zn concentrations, or if lead from black marble waste rock can control Mo concentrations through wulfenite precipitation.

3.2 Methods

This study used field cells, 205-L plastic barrels filled with waste rock and left exposed to ambient atmospheric conditions at the Antamina mine (Figure 3.1), and humidity cells - 1 kg samples of the same waste rock material in a laboratory at the University of British Columbia (Figure 3.2). In both the laboratory and field components of this study, the experiment was designed such that water from a Zn or Mo releasing material would have contact with another material hypothesized to be capable of reducing metal concentrations through geochemical attenuation. In the field-cell experiment, this was accomplished by placing waste rock in stacked field cells (Figure 3.1), two different waste rock materials were layered such that they had direct contact with each other. In the humidity cell experiment, leachate from the metal releasing material was poured onto the top of the attenuating material at the end of each weekly leach cycle. The current study focuses on results from three stacked field cells, six humidity cells, and four single field cells (Table 3.1).

Figure 3.1 The stacked field cells referred to in this study (left) with a schematic diagram of their internal structure (right). Each field cell contained 3 upper lysimeters installed at the contact between two material types, which were designed to sample leachate from the top material before it entered the second material. Drainage from the upper lysimeters all flowed into bucket a, whereas drainage that had been in contact with both material types flowed into bucket b. The total height of the stacked cells is 1.8 m.

Field cell leachate was collected weekly by mine site staff during the October – April wet season. Leachate from field cells is sampled regularly throughout the wet season, provided sufficient volume for laboratory analysis is produced over the sampling interval. The volume of leachate produced, and the conductivity and pH of each sample is measured in the field. Water samples are collected in plastic bottles and taken to the laboratory at Antamina for filtration through 0.45 μm filter membrane. Trace metals and cation samples are acidified with nitric acid to below pH 3 for preservation. Samples are then stored below 4^{o}C and shipped to ALS laboratories in Lima for chemical analysis using ICP-MS.

Table 3.1 Contents of the 7 field cells installed to study Mo and Zn attenuation at Antamina and 6 humidity cells installed at UBC for the same purpose. FC-black marble over intrusive and FC-intrusive over black marble are stacked field cells with two different material types, whereas UBC-1-3A and UBC-2-0A are single field cells.

Field Cell Code	Equivalent Humidity Cells	Materials Used	Purpose
UBC-1-3A	N/A	Pb-bearing black marble waste rock – one of the material types used in FC-black marble over intrusive and FC-intrusive over black marble.	Determine composition of leachate from Pb-bearing black marble
UBC-2-0A	N/A	Mo-releasing intrusive waste rock – one of the material types used in FC-black marble over intrusive and FC-intrusive over black marble.	Determine composition of leachate from Mo-releasing intrusive rock
UBC-4-5-1A	N/A	Relatively inert grey hornfels waste rock – one of the material types used in FC-exoskarn over grey hornfels.	Determine composition of leachate from hornfels waste rock
UBC-3-2A	N/A	Zn-rich exoskarn – one of the materials used in FC-exoskarn over grey hornfels	Determine the composition of leachate from Zn-rich exoskarn rock
FC-exoskarn over grey hornfels	HC-exoskarn over grey hornfels	Zn-rich exoskarn on top of grey hornfels. Only 33% of the mass of the material in the stacked field cell is Zn bearing intrusive rock, whereas the proportions of each material are roughly equal in the humidity cells.	Determine if Zn is attenuated by contact with grey hornfels material.
FC-black marble over intrusive	HC-black marble over intrusive	Pb-bearing black marble on top of Mo-rich intrusive rock	Investigate possible Mo attenuation by co-precipitation with Pb
FC-intrusive over black marble	HC-intrusive over black marble	Mo-rich intrusive on top of Pb-bearing black marble	Investigate possible Mo attenuation by co-precipitation with Pb

Leachate collected at the base of the stacked field cell represents infiltration that entered in the upper cell and flowed through both materials and hence shows the post-mixing

composition. The leachate produced by the material in the upper cell of the stacked field cells was collected and sampled from three upper lysimeters located at the interface between material types. These upper lysimeters, open to about 6% of the cross-sectional area of the field cell, most often did not produce between sampling intervals the 1-L of leachate that mine-site protocols require for chemical analysis. Consequently, although upper lysimeters usually provided enough volume to allow the measurement field parameters, the chemistry of the upper-cell leachate was frequently not available. However, conventional single – material field cells, ("single field cells"), equivalent in volume to each cell of the stacked field cells, were earlier established with the same material types used in the stacked cells. In the comparisons that follow, leachate chemistry from the single field cells containing the same material as the subject stacked field cell was considered representative of the upper cell and also compared to the post-mixing composition observed at the base of the stacked cell.

The humidity cells were operated according to the ASTM (1996) procedure, except that they were subjected to a weekly "flood" irrigation (Lapakko and White, 2000; Sapsford et al., 2009), and were not exposed to active air circulation (Frostad et al., 2002). Each week, the humidity cell containing the metal releasing material (analogous to the upper cell of a stacked field cell) was irrigated with distilled water. The leachate produced was then used to irrigate the humidity cells of the material hypothesized to contain the attenuating material (analogous to the lower cell of the stacked field cells – see Figure 3.2). Cation samples from the humidity cells were syringe filtered through a 0.45 μm, acidified to below pH 3 with nitric acid, and refrigerated in 30 mL PET sample bottles until they could be analyzed. Samples from the humidity cells were analyzed at UBC using ICP-OES. A more detailed description

of the methods used in the field cell and humidity cell experiments can be found in Chapter 2.

Figure 3.2 A schematic diagram of the humidity cells connected in series (left) demonstrating the manner in which leachate from the first humidity cell is poured directly into the second humidity cell. The humidity cell used in this study are shown on the right.

Samples from both the Zn-releasing exoskarn (UBC-3-2A) and the Zn-attenuating hornfels (UBC-4-5-1A) were ground into a fine powder with a mortar and pestle for qualitative X-ray diffraction (XRD) analysis to identify the major rock forming minerals present in each sample. Weathered and un-weathered samples of the Zn-releasing exoskarn were analyzed separately to evaluate changes in mineralogy as a result leaching in the humidity cell experiment. A similar analysis was carried out with the Zn-attenuating hornfels material, except that a sample from HC-Zn-TL, which had been exposed to Zn-rich leachate through the duration of the humidity cell experiment, was also analyzed in the hopes of identifying any Zn-bearing secondary minerals that could account for the observed attenuation. These XRD analyses were carried out using a Brucker D8 Focus X-ray diffractometer at UBC. Mineral peaks were identified using the PDF-4+ 2011 RDB database in EVA 2.0.

The Zn-attenuating hornfels material in this study was also analyzed with scanning electron microscopy (SEM). Prior to analysis, samples from this material were mounted on mineral stubs and carbon-coated for analysis in a Philips XL-30 scanning electron microscope at

UBC. A crushed, un-weathered sample, a sample that had been weathered during the 30 week humidity cell experiment, but not exposed to Zn-bearing leachate, and a sample from the top surface of the attenuating material that had been in contact with Zn-bearing leachate throughout the 30 week humidity cell experiment were mounted on metal stubs and carbon coated SEM analysis. The samples from humidity cells were collected with a stainless steel spatula. Element maps revealed an apparent abundance of scattered Zn throughout the sample. Apparent Zn-rich areas that also coincided with the shape of mineral grains in the sample were selected for energy dispersion spectrometry (EDX) analysis in order to determine their elemental composition.

The MINTEQ.V4 database in the aqueous chemical modeling program PHREEQC I version 2.18.5570 was used to better understand the geochemical processes behind the observed attenuation. Saturation indices (SI) for all Zn- and Mo-containing minerals in the MINTEQ.V4 database were calculated using the leachate chemistry from the base of field cells FC-exoskarn over grey hornfels and FC-intrusive over black marble (Table 3.2). Minerals that were at or near saturation according to the initial SI calculations were allowed to precipitate in simple reactive transport models designed to simulate Mo and Zn attenuation in field cells FC-intrusive over black marble and FC-exoskarn over grey hornfels in an unsaturated system at equilibrium with atmospheric oxygen and carbon dioxide (see table 3.2 for a list of phases and key parameters used in these models).

Table 3.2 The input parameters for the PHREEQC I models that were used simulate Zn and Mo attenuation in the basal material of stacked field cells FC-exoskarn over grey hornfels and FC-intrusive over black marble (respectively). Columns 2 and 3 (from left to right) refer to phases that were initially present in the simulated field cells, whereas column 4 lists the mineral phases that were allowed to precipitate out of solution in the simulated attenuating material. Columns 5 and 6 refer to the composition of the Mo or Zn bearing solution that was attenuated by contact with the field cells' basal material.

Modeled field cell	Equilibrium phases present	Kinetic phases present	Phases allowed to precipitate	Input Mo or Zn Concentration (mg/L)	Input solution pH
FC-intrusive over black marble	Calcite, oxygen, carbon dioxide (atmospheric)	Pyrite, galena	Cerrusite ($PbCO_3$), Anglesite ($PbSO_4$), Na_2MoO_4, Hinsdalite ($PbAl_3PO_4SO_4(OH)_6$), Wulfenite ($PbMoO_4$), H_2MoO_4, $FeMoO_4$, Powellite ($CaMoO_4$), $Pb_3(AsO_4)_2$, $Fe(OH)_2$, Ferrihydrite ($Fe(OH)_3$), Goethite (FeOOH)	4 (Mo)	7
FC-exoskarn over grey hornfels	Calcite, oxygen, carbon dioxide	Pyrite	$Fe(OH)_2$, Ferrihydrite ($Fe(OH)_3$), Goethite (FeOOH), $Zn(OH)_{2(beta)}$ $Zn(OH)_{2(epsilon)}$, $Zn(OH)_{2(gamma)}$, $Zn_2(OH)_2SO_4$, $Zn(OH)_{2(am)}$, $Zn(OH)_2$, Zincosite ($ZnSO_4$), $ZnCO_3{:}1H_2O$, Smithsonite ($ZnCO_3$)	30 (Zn)	7.2

The model domain extended from the top of the attenuating material to the base of the stacked field cell for both FC-intrusive over black marble and FC-exoskarn over grey hornfels. The model was discretized into 9 cm long reaction cells. In both models a solution with a constant chemical composition representative of leachate from the Mo or Zn source material was allowed to flow through the attenuating material continuously at a rate of about 3.5×10^{-5} m/s. The water was allowed to react with abundant calcite and pyrite in this simulation. Though this flow rate and the sulfide oxidation rates used in this modeling exercise are thought to be reasonably representative of conditions in the field cells, they are

approximations and intended to improve conceptual understanding of the system rather than precisely explain or predict geochemical behavior.

3.3 Results

3.3.1 Experimental data

The climate at the Antamina mine is distinguished by a wet season, roughly October through April, and a dry season, May through September during which no flow is produced from the field cells. Accordingly, these time periods of no flow were removed from the field-cell chemistry graphs presented in this study. Time gaps in the data series are represented by vertical dashed lines. The time scale in the horizontal axis of the chemistry graphs refers to weeks since the first leachate was collected after the field cell was installed (with the dry seasons removed). In contrast, humidity cells in lab were irrigated continuously during their operation and no gaps were removed from the plots. Single field cells were installed prior to their associated stacked field cells; however, the data from the first two rainy seasons after installation are shown in all cases.

We first examine stacked field cell FC-black marble over intrusive where Pb-bearing black marble overlies Mo-releasing intrusive rock. The Mo concentration from the first leachate sampled from the base of field cell FC-black marble over intrusive was 10.2 mg/L. As the rainy season progressed, the Mo concentration leveled off at about 3.4 mg/L (‘Stacked (base)’ in Figure 3.3, top right graph). During the second rainy season, (week 22 onwards), Mo concentrations began at around 7.2 mg/L, then eventually leveled off near 2.3 mg/L as the rainy season progressed. The single data point available from the upper-lysimeters in the black marble had a Mo concentration of 0.036 mg/L, suggesting that nearly all of the Mo in drainage at the base of the stacked cell originated from the intrusive material at the bottom

('Stacked (top)' in Figure 3.3, top right graph). Data from the single field cell with the identical Pb-bearing material ("Single" in Figure 3.3, top right graph) also indicated that very little Mo leached from the Pb-bearing top material: Mo concentrations never exceeded 0.03 mg/L during the study. The pH of basal leachate fell between 7.5 and 8 for most of the experimental period ('Stacked (base)' in Figure 3.3, bottom right graph). The pH of leachate from the upper lysimeters rose gradually over time from 7.5 before remaining relatively stable near 7.8 ('Stacked (top)' in Figure 3.3, bottom right graph).

Mo concentrations in leachate from humidity cells HC-black marble over intrusive showed very similar trends to the corresponding stacked field cells. Mo concentrations in the leachate from the first cell in HC-black marble over intrusive never exceeded the detection limit (0.09 mg/L – 'First cell' in Figure 3.3, top left graph), however after passing through the Mo-rich intrusive rock in second cell they ranged from 2 mg/L to 11 mg/L ('Second Cell' in Figure 3.3, top left graph). The Mo concentration of the first sample from the second cell of HC-black marble over intrusive exceeded 10.7 mg/L and then dropped to below 4 mg/L by week ten of the experiment, before undulating between 2.5 and 4 mg/L for final 20 weeks.

Leachate pH from HC-black marble over intrusive fluctuated between 7 and 8 (Figure 3.3, bottom left graph). During the last 20 weeks of the experiment leachate pH from the second cell tended to be 0.2-0.6 pH units higher than that of leachate from the first cell, suggesting that pH increased due to contact with Mo-rich intrusive material.

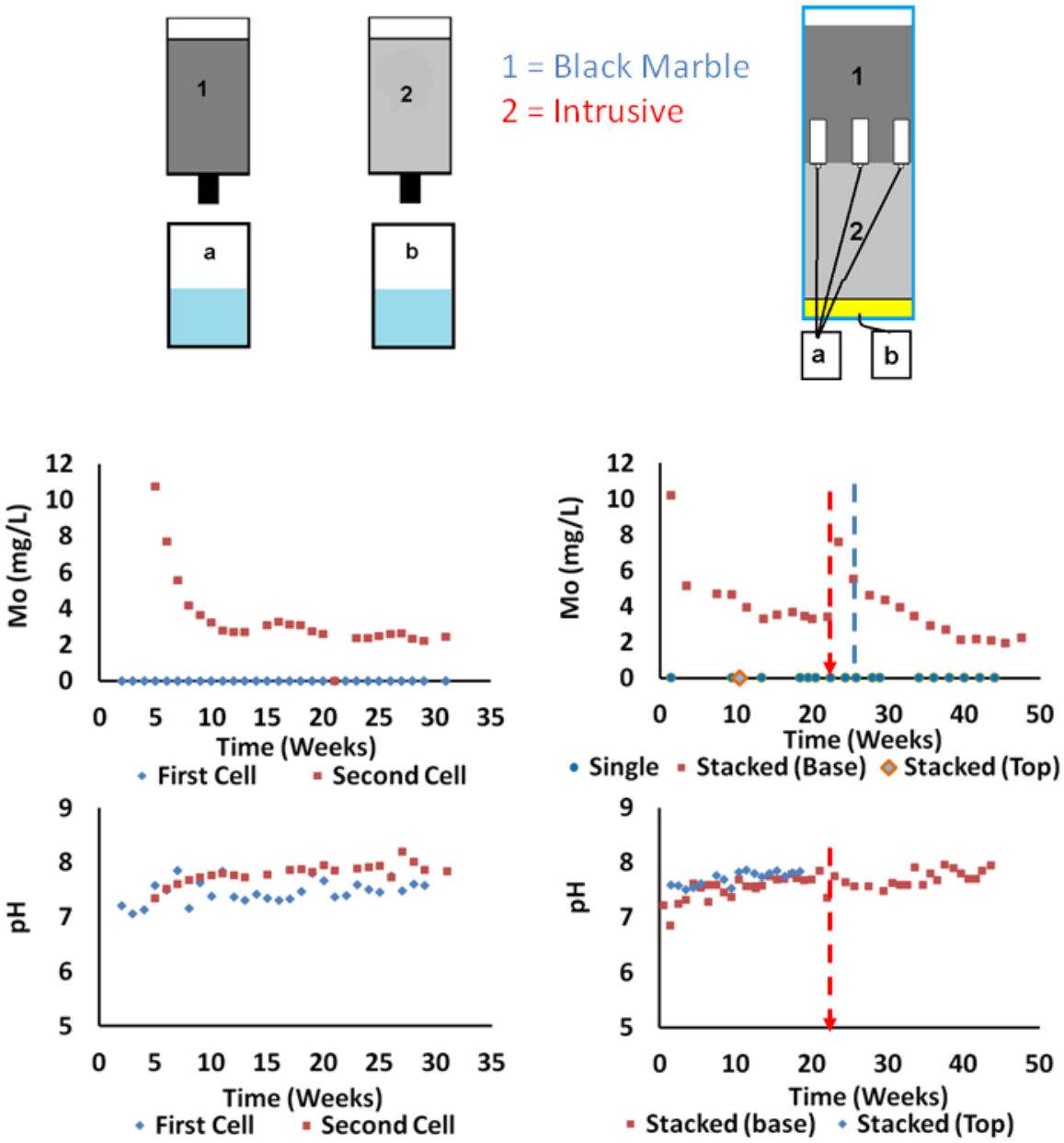

Figure 3.3 Mo-concentrations (middle) and leachate pH (bottom) as a function of time since the initiation of flow in stacked field cell FC-black marble over intrusive (right column) and corresponding humidity cells HC-black marble over intrusive (left column). The upper diagrams show the configuration of waste rock material in this stacked field cell and its corresponding humidity cells. The vertical red dashed line with an arrow on the field cell graphs indicates the position of the data gap at end of the first rainy season in the stacked field cell data, while the dashed blue line without the arrow indicates the end of the first rainy season on the single field cell series.

In FC-intrusive over black marble, the Mo-releasing intrusive rock was placed upstream of the Pb-bearing rock, so Mo-releasing leachate had direct contact with Pb-bearing material.

Indeed, compared to leachate from the base of FC-black marble over intrusive, leachate from FC-intrusive over black marble had very low Mo-concentrations, consistently less than 0.03 mg/L ('Stacked (base)' in Figure 3.4, top right graph). The single sample available from the upper lysimeters had a concentration of 6.7 mg/L, confirming that the Mo-releasing intrusive material was indeed leaching Mo in the stacked field cell ('Stacked (base)' in Figure 3.4, top right graph). Mo concentrations in leachate from a single field cell containing the identical Mo-releasing intrusive material typically showed Mo concentrations between 1 and 4 mg/L, although Mo concentrations were as low as 0.24 mg/L shortly after installation ('Single' in Figure 3.4, top right graph). Leachate pH from the base of FC-intrusive over black marble dipped to 6.7 before gradually increasing over several weeks to 7.5 to 7.7 ('Stacked (base)' in Figure 3.4, bottom right graph). Towards the end of the study time, the pH of basal leachate from FC-intrusive over black marble exceeded 8. The pH of leachate from the upper lysimeters showed a very similar trend to that of basal leachate, although it was often 0.1 to 0.3 pH units higher ('Stacked (top)' in Figure 3.4, bottom right graph).

The corresponding humidity cells also showed attenuation of Mo to below detection. Leachate from the Mo-releasing material in humidity cell HC-intrusive over black marble contained up to 6.9 mg/L Mo, although concentrations were lower for most of the experiment, generally between 1 and 1.5 mg/L ('First cell' in Figure 3.4, top left graph). Mo was removed to below detection (<0.09 mg/L) when the same leachate was passed through the Pb-rich black marble in HC-intrusive over black marble ('Second cell' in Figure 3.4, top left graph). Leachate pH ranged between 7 and 8 throughout the entire duration of the experiment. Contact with the Pb-bearing black marble appeared to increase leachate pH, making leachate from the second cell in HC-instrusive over black marble 0.2 to 0.6 pH units

higher than leachate that had only passed through the first cell (Figure 3.4, bottom left graph).

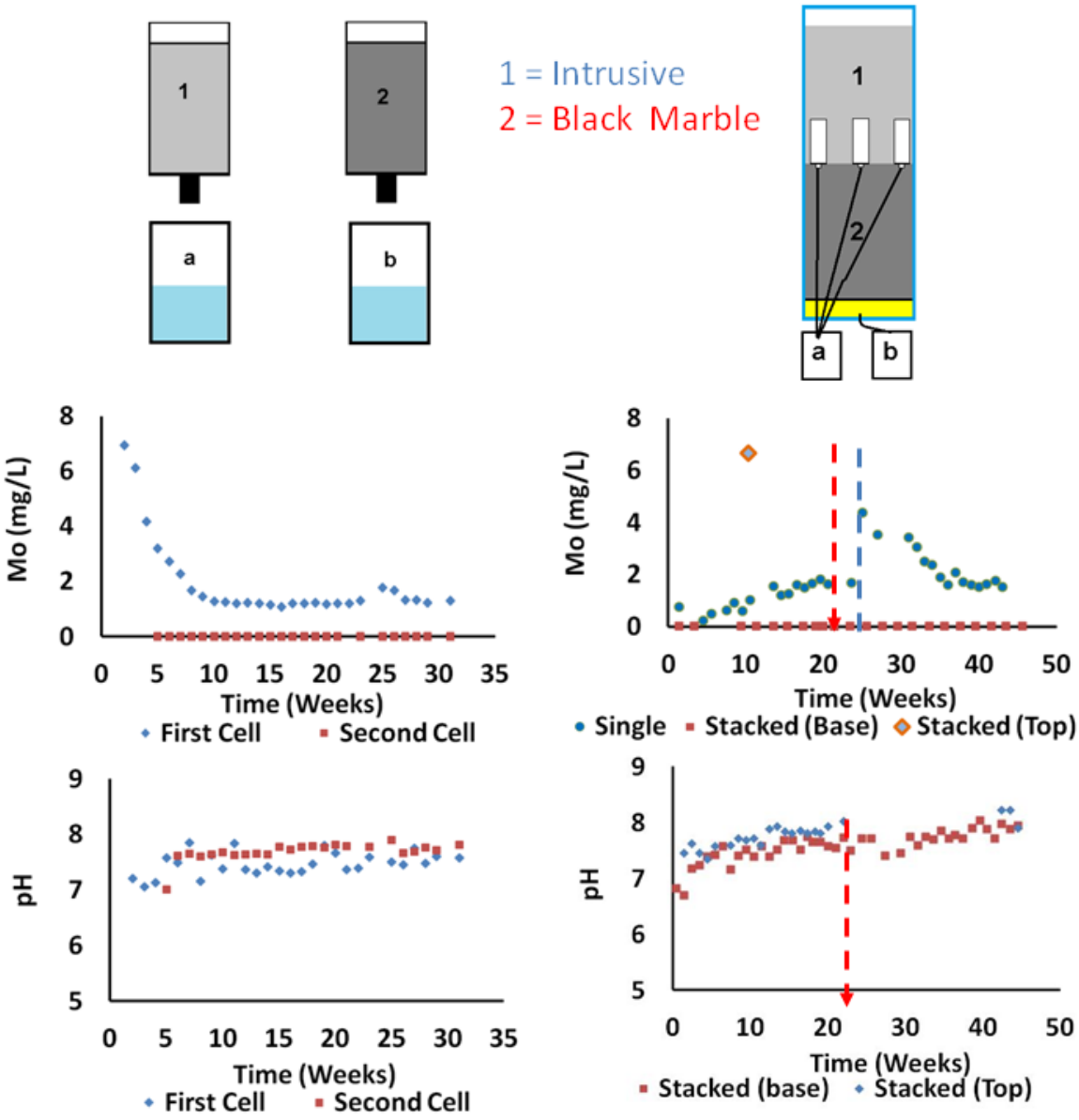

Figure 3.4 Mo-concentrations (middle) and leachate pH (bottom) as a function of time since the initiation of flow in stacked field cell FC-intrusive over black marble (right column) and corresponding humidity cells HC- intrusive over black marble (left column). The upper diagrams show the configuration of waste rock material in this stacked field cell and its corresponding humidity cells. The vertical red dashed line with an arrow on the field cell graphs indicates the position of the data gap at end of the first rainy season in the stacked field cell data, while the dashed blue line without the arrow indicates the end of the first rainy season on the single field cell series.

Field cell FC-exoskarn over grey hornfels, where Zn-bearing exoskarn is placed on top of grey hornfels waste rock, was installed specifically to study Zn attenuation. Zn concentrations from the single field cell installed with the identical Zn-releasing exoskarn waste rock produced leachate with between 22 mg/L and 42 mg/L of Zn ('Single' in Figure 3.5, top right graph). The single data point available from the upper lysimeters in the stacked field cell fell into this range with 33 mg/L Zn ('Stacked (Top)' in Figure 3.5, top right graph). Zn concentrations were much lower after contact with the hornfels waste rock at the bottom of the stacked field cell. The maximum Zn concentration of 0.5 mg/L in leachate from the base of the FC-exoskarn over grey hornfels stacked field cell was in the first available sample after the field cell was installed ('Stacked (base)' in Figure 3.5, top right graph). Subsequent Zn concentrations in basal leachate from FC-exoskarn over grey hornfels declined within two weeks to below 0.05 mg/L. Leachate pH from the upper lysimeter was constant throughout the experiment, ranging from 7.1 near the beginning of the experiment to 7.4 towards the end of the second rainy season after installation ('Stacked (top)' in Figure 3.5, bottom right graph). The pH of leachate from the base of FC-exoskarn over grey hornfels was generally higher, except the first leachate sample, which had a pH of 6.3. After the first week of leaching, the pH of basal leachate ranged from 7.1 to 8.0 ('Stacked (bottom)' in Figure 3.5, bottom right graph). For most of the experiment the pH of basal leachate was at least 0.5 pH units higher than the pH of upper lysimeter leachate. The basal leachate sample with the lowest pH also had the highest concentrations of Zn.

Data from the corresponding humidity cells also showed that contact with grey hornfels removed Zn from leachate. Zn concentrations from the first humidity cell (Zn releasing) rose from 10.5 mg/L to a maximum of 24.6 mg/L in the third week of the experiment ('First Cell'

in Figure 3.5, top left graph). After the 6th week of leaching, Zn concentrations from the first humidity cell fell gradually to below 3 mg/L. Zn concentrations in leachate from the second humidity cell never contained more than 1.8 mg/L Zn during the course of this experiment ('Second Cell' in Figure 3.5, top left graph). By the final weeks of leaching Zn in leachate from the second humidity cell had fallen below 0.16 mg/L. The pH of leachate from the Zn-releasing material in the first humidity cell varied from week to week; however, it showed a general increasing trend throughout the experiment, increasing from about 6.4 to 7.4 in 30 weeks ('First Cell' in Figure 3.5, bottom left graph). Leachate pH from the second (Zn attenuating) humidity cell was generally 0.1-0.7 pH units higher than in leachate from the first humidity cell in the series (Figure 3.5, bottom left graph). The pH of leachate from the second humidity cell was generally above 7.5, although it dipped to below 6.9 in the last week of the experiment.

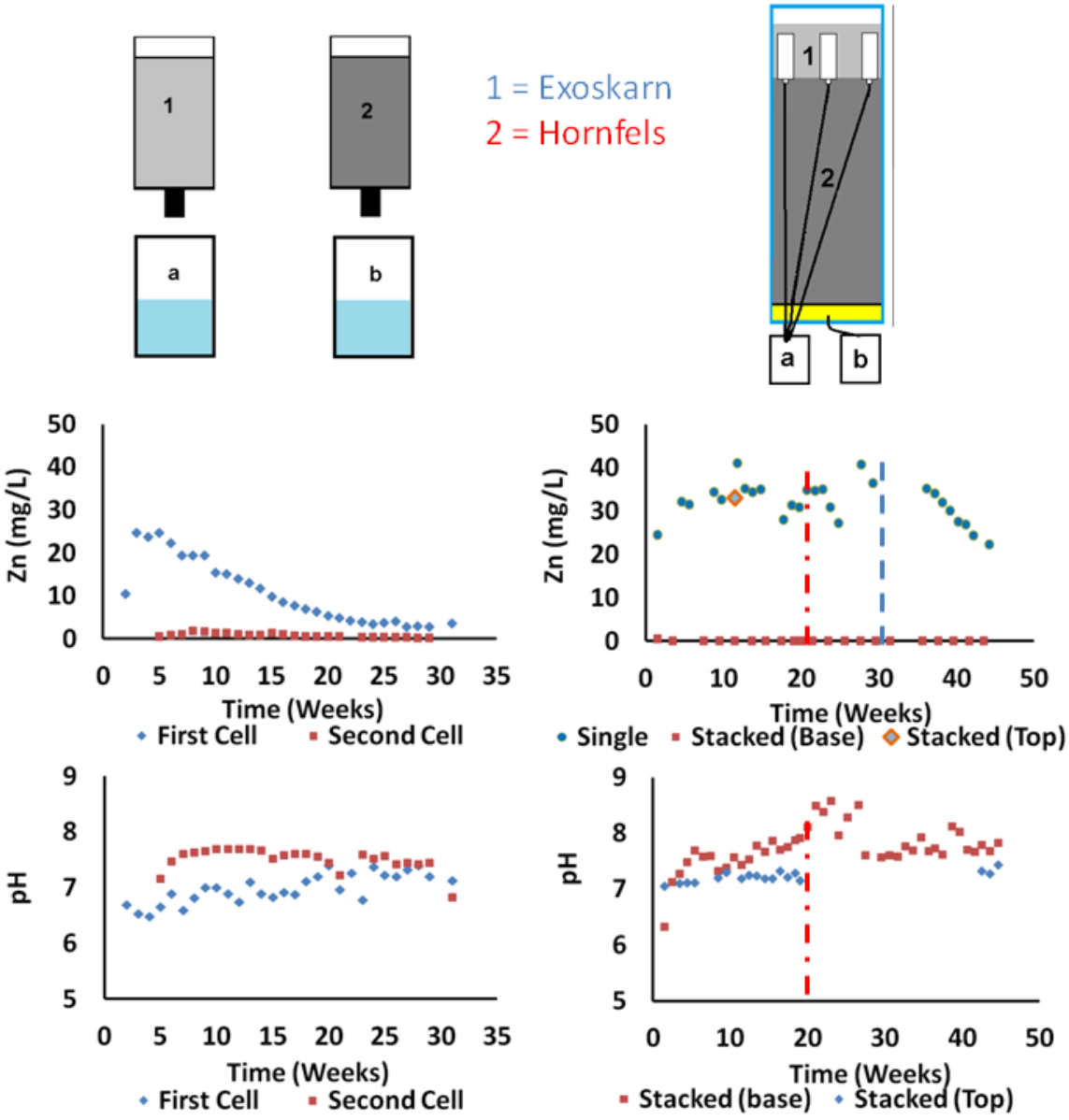

Figure 3.5 Mo-concentrations (middle) and leachate pH (bottom) as a function of time since the initiation of flow in stacked field cell FC-intrusive over black marble (right column) and corresponding humidity cells HC- intrusive over black marble (left column). The upper diagrams show the configuration of waste rock material in this stacked field cell and its corresponding humidity cells. The vertical red dashed line with an arrow on the field cell graphs indicates the position of the data gap at end of the first rainy season in the stacked field cell data, while the dashed blue line without the arrow indicates the end of the first rainy season on the single field cell series.

3.3.2 Geochemical modeling

No Zn- containing minerals were in equilibrium in the leachate from the base of FC-exoskarn over grey hornfels. The only Mo-bearing mineral in PHREEQC's MINTEQ.V4 database that

was supersaturated in leachate from the base of FC-intrusive over black marble (where Mo-releasing intrusive was placed on top of Pb-bearing black marble) was wulfenite, which had an SI greater than 0 in all samples were Pb was detected. Leachate from the base of UBC-Mo-T1L was also super-saturated with respect to wulfenite in the few samples that had detectable Pb. The same leachate was also consistently supersaturated with respect to Powellite ($CaMoO_4$), and Ca usually was present at concentrations greater than 100 mg/L. $ZnCO_3$:$1H_2O$ was close to saturation and in some cases supersaturated in samples from the single field cell containing Zn-bearing exoskarn.

Results from a simple reactive transport model of Mo attenuation in the base of stacked field cell FC-intrusive over black marble demonstrated that it is thermodynamic plausible that 4 mg/L of Mo could be attenuated in a solution in contact with oxidizing galena (PbS). Simulated Mo concentrations fell to below 0.0003 mg/L within 27 cm of initial contact with Pb-bearing black marble (Figure 3.6). The lowest Pb concentrations in the system, below 0.0001 mg/L coincided with the highest Mo concentrations and occurred in the first 18 cm below the contact between both material types. The decrease in leachate Mo concentrations in the first 18 cm below the contact with attenuating material coincided with wulfenite ($PbMoO_4$) precipitation. As expected, Pb was not very mobile in the simulated system, even in parts of the field cell where wulfenite was under saturated. Cerrusite ($PbCO_3$) sequestered the vast majority of the Pb that was released by Galena oxidation when Mo concentrations were below 0.0003 mg/L (Figure 3.6). Once 0.08 moles of wulfenite had precipitated the Mo source was ‘turned off’ to evaluate whether wulfenite precipitation could be counted on as a long-term attenuation mechanism. Although wulfenite dissolution occurred in this scenario, Mo concentrations in basal leachate did not exceed 0.003 mg/L.

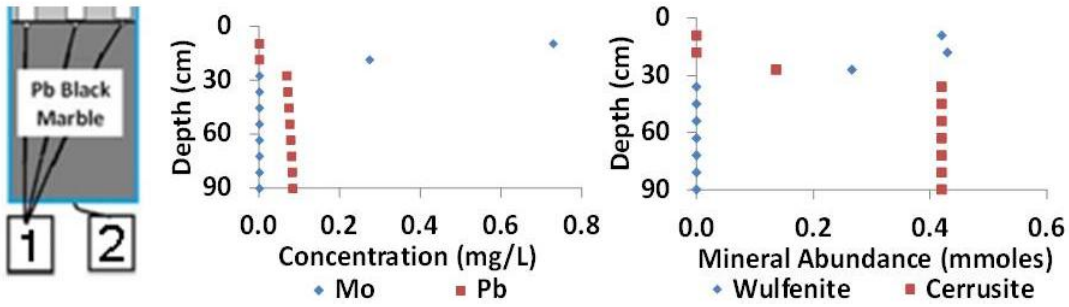

Figure 3.6 Plots of dissolved metal concentrations and solid phase mineral abundances (mmoles of each mineral in contact with 1 L of water) from a PHREEQC model of the attenuating (bottom) portion of FC-intrusive over black marble. The sketch to the left of the graphs shows the model domain. Note that depth refers to depth below the contact between the two rock types. These data were from a point in the study where 2.7 pore volumes of Mo-rich water had been flushed through the bottom field cell.

The depth to which molybdenum could penetrate the Pb-bearing material in the stacked field cell was controlled by a combination of the rate of Mo loading from the top of the field cell and the rate of Pb release from galena oxidation in the attenuating material. Sensitivity analysis demonstrated that the Mo loading rate, as determined either by flow rate or initial Mo concentration, influenced depth of the boundary between the wulfenite precipitation zone and the cerrusite precipitation zone in the field cell. Doubling the flow rate or the initial Mo concentration both had the effect of allowing Mo to penetrate twice as far into the Pb-bearing material before its concentration decreased to 0.0003 mg/L. Decreasing galena oxidation rate by a factor of 12, while not allowing powellite ($CaMoO_4$) to precipitate, led to a basal leachate Mo concentration of 2.7 mg/L because less Pb was available to remove Mo through wulfenite precipitation. To further explore the importance of Pb in controlling dissolved Mo concentrations, a simulation was run without galena dissolution, but allowing powellite to precipitate. Although a portion of the leachate Mo was removed through powellite precipitation, the Mo concentration of basal leachate, 0.5 mg/L, was higher in this scenario than when wulfenite was allowed to form.

The geochemical model designed to simulate Zn attenuation processes in the base of the FC-exoskarn over grey hornfels field cell suggested that mineral precipitation reactions (especially $ZnCO_3$:$1H_2O$) exerted some control on leachate Zn concentrations. Leachate contained 30 mg/L Zn when it first made contact with the modeled attenuating material;, however, this concentration was reduced to 11.3 mg/L by the time it exited from the field cell's base. A subsequent model run, which allowed for the adsorption of Zn onto iron oxides, resulted in a basal leachate Zn concentration of 0.14 mg/L. These results indicate that mineral precipitation alone could not account for all of the attenuation observed in the results from FC-exoskarn over grey hornfels.

3.3.3 XRD and SEM analysis

XRD analysis of un-weathered Zn-releasing skarn material revealed that its most abundant minerals were andradite, pyrite, sphalerite, diopside, and orthoclase, with possible occurrences of vesuvianite and biotite. The most abundant minerals detected in the Zn-attenuating grey hornfels material were calcite, quartz, anorthite, biotite, and clinochlore. A comparison of pre- and post-weathering X-ray diffractograms did not reveal any noticeable changes in the mineralogy in exoskarn or hornfels waste rock materials as a result of leaching during the humidity cell experiment. Furthermore, no mineralogical differences were observed between un-weathered hornfels material, and hornfels material that had been exposed to Zn-rich leachate during the humidity cell experiment.

In most cases EDX spectra revealed that Zn was not actually present in detectable quantities. In a few cases the presence of Zn was confirmed by EDX analysis, as evidenced by energy peaks at 1 and 8.6 KeV. The peak at 8.6 KeV on the EDX spectra was taken to be more diagnostic of the presence of Zn, given that the 1 KeV peak is also associated with sodium.

The distinctive x-ray dispersive spectrography (EDX) energy signature for Zn was encountered in some flaky or platy mineral grains in samples of grey hornfels (attenuating material) that had been exposed to zinc-rich leachate (Figure 3.7). The 8.6 KeV peak reached 1 to 3 CPS/KeV above the local baseline in mineral grains from the attenuating material in humidity cell HC-Zn-TL after the completion of the leaching experiment (Figure 3.8). These Zn peaks are associated predominantly with oxygen, magnesium, silicon, and aluminum, with less abundant calcium and iron. Zn was also encountered in a sample of the same Zn-attenuating grey hornfels material that had not been exposed to Zn-rich leachate, meaning that some Zn was present in the attenuating material before waste rock mixing occurred. In this case Zn occurred in a clearly defined mineral grain dominated by zinc and sulfur (Figure 3.9). More than 40 spot scans were performed in the attenuating material that had not been exposed to Zn; however, and none of these showed as strong an association between Zn and Si, Mg, Al, Ca and Fe as had been observed in samples that had been exposed to Zn-rich leachate.

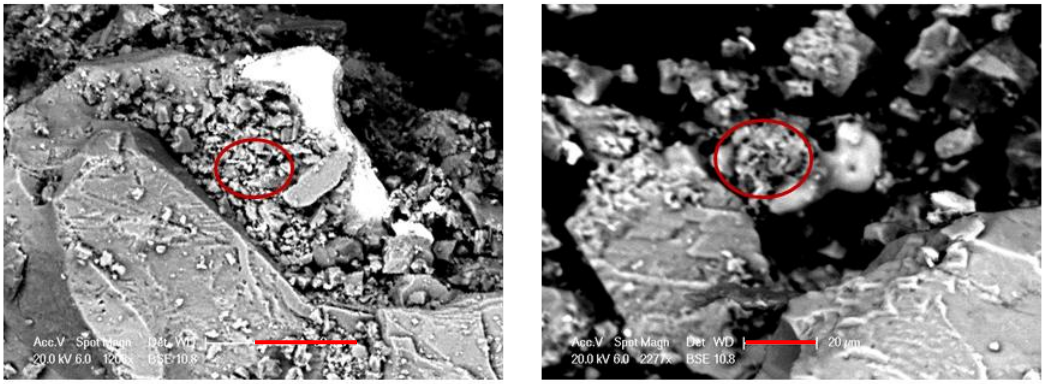

Figure 3.7 Two back-scattered SEM images of apparent Zn-bearing secondary minerals in hornfels waste rock material (Zn-attenuating) that had been exposed to Zn-rich leachate in humidity cell HC-exoskarn over grey hornfels. The red scale bar on the image to the left is 50 µm, whereas the red scale bar on the image to the right has a length of 20 µm.

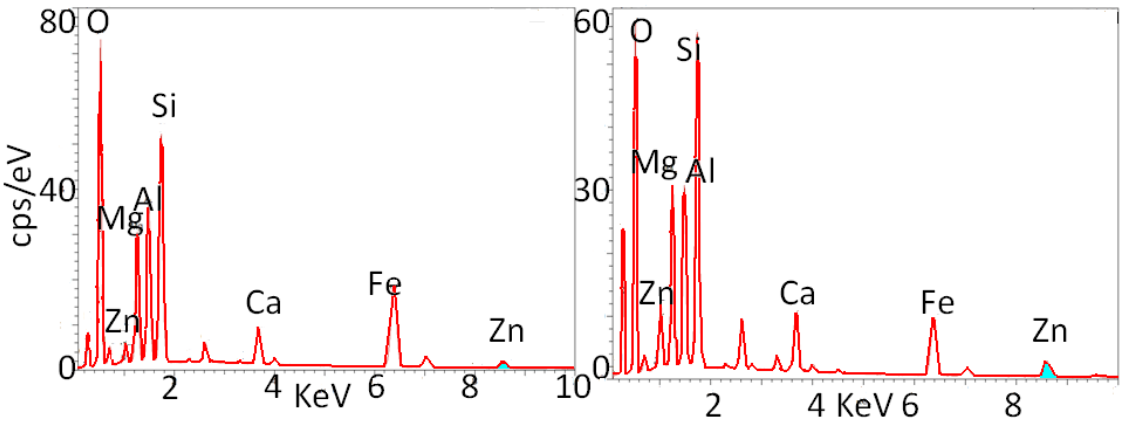

Figure 3.8 Energy dispersive x-ray micro-analysis (EDX) spectrographs from point scans taken in two distinct apparent Zn-rich secondary minerals in hornfels waste rock material that had been exposed to Zn-rich leachate in humidity cell HC-exoskarn over grey hornfels.

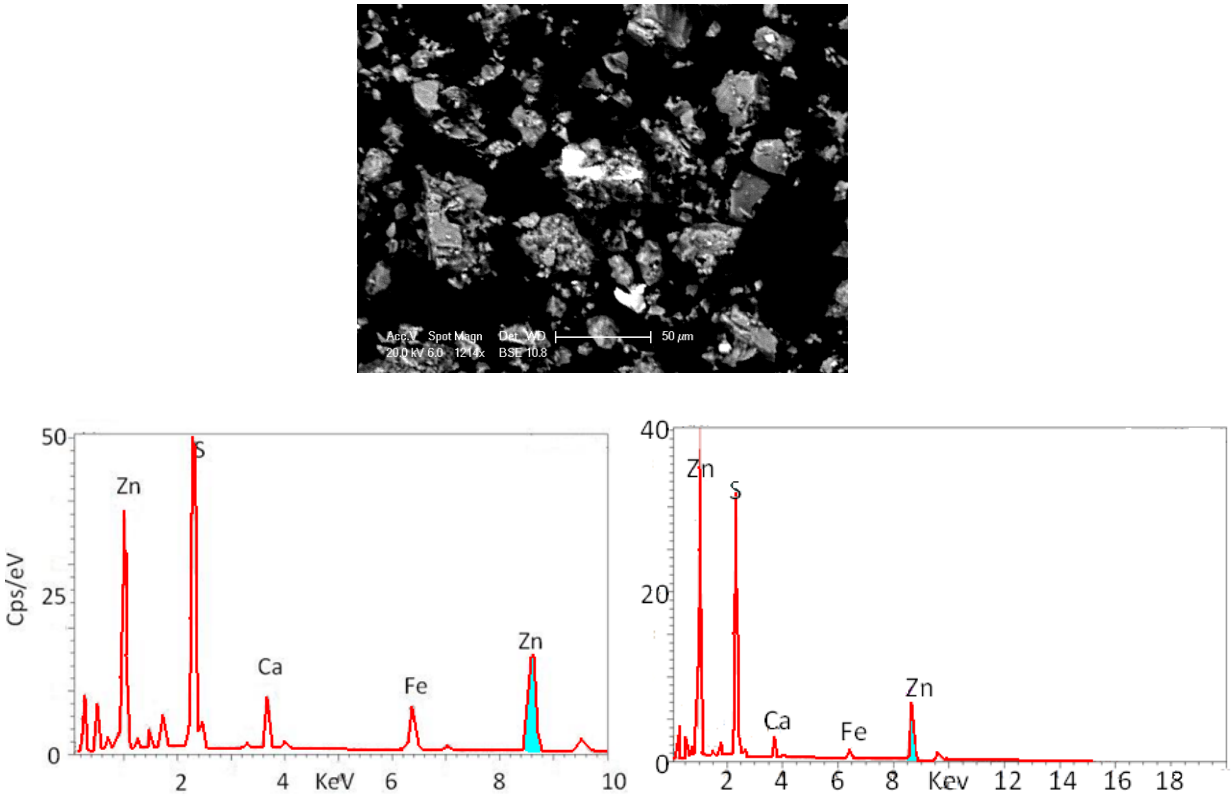

Figure 3.9 A back-scattered SEM image of a probable sphalerite grain (the lightest grey grain in the center of the image) in hornfels waste rock material (Top). The red scale bar on the image to the left is 50 µm. Two Energy dispersive x-ray micro-analysis (EDX) spectrographs from point scans on ZnS-dominated mineral grains in Zn-attenuating hornfels material (bottom – note that the one on the right is from the mineral grain pictured above).

3.4 Discussion

3.4.1 Molybdenum attenuation

Results from the first two rainy seasons after the installation of the stacked field cells demonstrated that Mo attenuation occurred in FC-intrusive over black marble, where Mo-rich intrusive waste rock was placed on top of Pb-rich black marble. Considering that typical Mo concentrations in leachate from the Mo-rich intrusive single field cell were between 1 and 4 mg/L in the first two years after its installation and the basal leachate from FC-intrusive over black marble was less than 0.03 mg/L, it appears that at least 97% of the Mo in the leachate from the intrusive rock was removed before it reaches the base of the stacked field cell. The Mo removal efficiency may have been as high as 99%, given that the single available leachate sample from the Mo-rich intrusive rock in the stacked field cells contained 6.7 mg/L Mo.

As was the case in the field cells, Mo was only removed from humidity cell leachate when direct contact occurred between the Mo bearing leachate and the Pb-rich attenuating material. Molybdenum concentrations were reduced to below the detection limit (0.09 mg/L) in all samples that had passed through Pb-rich black marble. Given that maximum Mo concentrations in leachate from the first cell in HC-instrusive over black marble were 6.9 mg/L at least 98.5% of Mo was removed after contact with Pb-rich black marble in the humidity cell experiment.

Although evidence from FC-intrusive over black marble and corresponding humidity cells demonstrated that reactions with Pb-rich black marble removed Mo from waste rock leachate, these attenuation reactions depended on the order in which the waste rock was placed. Mo concentrations in leachate from the base of FC-black marble over intrusive

generally ranged from 2 to 4 mg/L for most of the experiment, indicating that minimal, if any, attenuation took place in this stacked field cell. The lack of Mo attenuation when the Pb-rich black marble was placed on top of the Mo-rich intrusive rock could be explained by the low mobility of lead in this stacked field cell. Lead concentrations from the base of FC-intrusive over black marble and from the lysimeter in FC-black marble over intrusive were both less than 0.03 mg/L. This low concentration implies that virtually no lead from the top half of the FC-black marble over intrusive field cell had contact with the Mo-rich intrusive material at the base of the cell.

Modeling results showed that Mo may have been attenuated by powellite precipitation; however, that this process alone could not account for the low Mo concentrations observed at the base of FC-intrusive over black marble. Furthermore, Conlan et al.'s (2012) work showed that powellite formation was kinetically limited in Mo attenuation experiments carried out in neutral pH settings. The observation from this study that Mo is only attenuated when it makes direct contact with Pb-bearing rock provides strong evidence that wulfenite precipitation is the main mechanism for attenuating Mo in this system. Results from geochemical modeling suggested that Pb is highly immobile in this geochemical system due to cerrusite precipitation ($PbCO_3$). In the presence of Mo, however, modeling results suggested wulfenite precipitation to be a more thermodynamically favorable than cerrusite precipitation, allowing wulfenite to act as a sink for both Mo and Pb. These modeling results, along with Conlan et al.'s (2012) findings that wulfenite formed as a secondary mineral when Mo and Pb were co-mingled in both lab experiments suggest that when Mo came in direct contact with a zone of galena oxidation in FC-intrusive over black marble, wulfenite precipitation out competed cerrusite precipitation for the Pb released by the oxidation of

galena. On the other hand, modeling results suggest that the lack of Mo attenuation in FC-black marble over intrusive could be explained by cerrusite precipitation removing most of the Pb from leachate shortly after galena was oxidized, leaving insufficient aqueous Pb to be transported into the lower material in the stacked field cell and react with the Mo that was being released by molybdenite oxidation in the lower cell.

In addition to shedding further light on the Mo attenuation mechanism in this system, geochemical modeling results provided insight into the long-term fate of Mo sequestered by wulfenite precipitation. Results suggested that should the Mo source become exhausted prior to the Pb source, wulfenite dissolution would occur, remobilizing Mo into solution. The low solubility of wulfenite, however, would mean that a comparatively modest dissolved Mo concentration (0.003 mg/L) would result. This result implies that Mo attenuation through wulfenite precipitation will be long-lasting under these pH conditions.

3.4.2 Zn attenuation

Leachate from the exoskarn in UBC-3-2A, the material installed in the top of FC-exoskarn over grey hornfels contained between 20 and 42 mg/L of Zn (33 mg/L in the sample from the upper stacked field cell), while Zn concentrations in FC-exoskarn over grey hornfels's basal leachate were usually below 0.05 mg/L, implying that over 99% of the Zn in leachate was removed after contact with hornfels rock. Zn removal efficiency was not as high in the laboratory humidity cells as it was in the field cell portion of the study. The hornfels material in humidity cell HC-exoskarn over hornfels removed approximately 94% of Zn from leachate that passed through it. The lower removal efficiency of the humidity cell as compared to the equivalent stacked field cell could be related to the higher proportion of Zn attenuating material in the stacked field cell. The field cell contained 25% Zn releasing material and 75%

Zn attenuating material, whereas the humidity cell experiment contained an equal proportion of both materials.

Although Zn attenuation in the stacked field cell coincided with an increase in pH, geochemical modeling demonstrated that precipitation of zinc carbonate or hydroxide minerals could not account for all of the attenuation observed. When adsorption onto iron oxy hydroxides was included in the PHREEQC geochemical model, Zn was attenuated to much lower levels. This result is consistent with the assertions of several authors who have reported adsorption onto metal oxides can be an important mechanism for Zn attenuation (e.g. Trivedi and Axe 2000 and references therein).

The observation from this study's SEM-EDX analysis that attenuated Zn in the hornfels material co-existed with iron and oxygen, along with Ca, Mg, Al, and Si could be consistent with adsorption onto an iron oxide that had precipitated on the surface of a silicate mineral. In interpreting the co-occurrence of Zn and Fe, which would be expected if Zn were simply adsorbed onto an iron oxide mineral, along several other elements it is important to consider that the SEM electron beam excites atoms below the mineral surface. Exciting atoms below the mineral grain surface generates an EDX spectrum for a particular mineral grain that is representative of both its surface and its internal structure. It is therefore difficult to assess whether Fe and Zn are part of a surface coating, or incorporated in the crystal structure of the mineral itself on the basis of SEM/EDX analysis alone.

Although geochemical modeling at representative pH conditions suggests that adsorption onto iron oxy hydroxides may play an important role in attenuating Zn, three lines of evidence suggest that this is not the case. Firstly, the same hornfels material that attenuated Zn in this study also released As into solution. The mobility of As in the attenuating material

is surprising given that geochemical modeling predicted that As would be removed from solution by adsorption onto iron oxides in this geochemical system. Given that the adsorption of both As and Zn are thermodynamically favorable at typical pH values for this study, it is unclear why Zn would be adsorbed in this material but As would not. A second line of evidence suggesting that adsorption onto iron oxides is not responsible for Zn attenuation in the hornfels material is related to the abundance of pyrite in the Zn releasing material. The oxidation of this pyrite in neutral pH conditions would lead to the precipitation of iron oxide minerals, which would provide plentiful adsorption sites for Zn. It is unclear why Zn would be immobilized by adsorption onto iron oxides in the hornfels attenuating material, but not in the Zn-releasing exoskarn. The third line of evidence suggesting that adsorption onto iron oxides was not responsible for Zn attenuation was that several red, iron-containing, grains from the attenuating material that had been exposed to Zn-rich leachate in the humidity cell HC-Zn-TL were not found to be associated with Zn.

Another possible Zn attenuation mechanism in this system based on the work of Manceau et al. (2000) in neutral-pH soils and Dold and Fonboté (2001) in mine tailings is the integration of Zn into pre-existing aluminosilicate clay minerals through a form of cation exchange. XRD analysis identified clinochlore ($(Mg,Fe)_5Al(Si_3Al)O_{10}(OH)_8$) as one of the principle minerals in the hornfels material. Given the occurrence of Zn in platy grains containing Si, Al, Mg, and Fe, Zn attenuation could be explained by the substitution of Zn^{2+} for Mg^{2+} or Fe^{2+} in clinochlore. The relative abundance of clinochlore in the hornfels material compared to the Zn-releasing exoskarn helps explain why contact between leachate and a second waste rock material was necessary for Zn attenuation.

Further research is needed to test the hypothesis that cation exchange in clay minerals is responsible for Zn attenuation mechanisms in the hornfels material. A potential next step in the experiment would be to subject hornfels that has been exposed to Zn-rich leachate (possibly from the top of the hornfels attenuating material in stacked field cell FC-exoskarn over grey hornfels) to a sequential leaching procedure designed to target exchangeable Zn. Dold (2003) presented one such procedure for use in mine tailings that may be appropriate for this application. A comparison of the results from extractions performed on weathered hornfels material that had been exposed to Zn-rich leachate, and weathered hornfels material that had no contact with extra Zn could quantify the mass of Zn removed by cation exchange in clays.

3.4.3 Summary

The use of stacked field cells and humidity cells connected in series has provided insight into the mechanisms controlling the mobility of Zn and Mo in neutral mine systems. Between this work and the laboratory experiments by Conlan et al. (2012), we can state with some confidence that Mo is attenuated by wulfenite precipitation in this system. Its low solubility means that even if wulfenite were to become under saturated, Mo concentrations would remain much lower than they would otherwise be in non-attenuated leachate. The attenuation of Mo via wulfenite precipitation may be applicable in other mines that extract ore from skarn deposits, given that galena and molybdenite both tend to occur in these geologic settings (e.g. Chang and Meinert, 2008).

Zn is not attenuated by the same mechanism as Mo in this study. Evidence from geochemical modeling, has suggested that the precipitation of Zn secondary minerals cannot explain the degree of attenuation observed in this study. XRD and SEM/EDX analysis of the attenuating

hornfels material demonstrated that Zn may have been attenuated by becoming incorporated into clay minerals, however more research is needed to confirm this mechanism and predict whether Zn becomes re-mobilized again as geochemical conditions change with time. The results of this study suggest that layered deposition of the appropriate materials in waste rock dumps can control leachate Zn and Mo concentrations at Antamina and other mines that generate neutral mine drainage.

Chapter 4: Field cell hydrology, geochemistry, and directions for future research

4.1 Introduction

Chapters 2 and 3 of this thesis focused on the use of stacked field cells and humidity cells connected in series to explore As, Mo, and Zn attenuation; however, the research yielded several other results that can serve to deepen understanding of metal leaching and attenuation in neutral mine drainage. This chapter presents a collection of selected geochemistry and field cell results that offer further context to chapters 2 and 3, and provide direction for future research. The specific topics in this chapter include: cases where As and Mo were not attenuated by waste rock mixing, attenuation of Zn in FC-black marble over intrusive and FC-intrusive over black marble, the attenuation of other metals and metalloids (Ni, Cd, Cr, Cu, Sb, Sn, Se, Ni, Li, and Pb) by waste rock mixing, prospects for long-term leaching and attenuation in stacked field cells, along with field cell hydrology and implications for sulfate release rates.

Although the focus of this work has been on attenuation, cases where it did not occur in spite of waste rock mixing can also be useful in developing a holistic understanding of the geochechmical processes responsible for controlling metal concentrations in neutral mine drainage systems. To this end, the first results sub-section in this chapter explores the case where As was not attenuated in stacked field cell UBC-5A-T, and the case where Mo was not attenuated in stacked field cell UBC-5C-T. The pattern of Zn attenuation in FC-black marble over intrusive and FC-intrusive over black marble and associated humidity cells is discussed in the second results subsection, whereas the third results subsection assesses the attenuation of other metals and metalloids. Similar to the process used for studying Mo, As, and Zn, the attenuation of these elements was explored by comparing concentrations of each element in

leachate from the base of stacked field cells to leachate from their associated single field cells.

The results presented in chapters 2 and 3 of this thesis are based on the first two years of leaching from field cells at Antamina, and 30 week long humidity cell experiments. According to an estimate presented later in this chapter, the 30 week humidity cell experiment can be taken to approximate 120 weeks (less than 2.5 years) of leaching in the field cells. The application of the results from this study to mine closure planning would require that they be extrapolated many years into the future and scaled up from the laboratory scale to the full waste rock dump scale. The fourth results sub-section in this chapter explores the prospects of extrapolating the Zn, As, and Mo leaching and attenuation results into the future based on the solid phase elemental composition of the waste rocks studied.

Hydrology plays a critical role in determining the composition of leachate in waste rock systems both because the oxidation of sulfide minerals is kinetically limited, and thereby dependent on residence time, and because the degree of saturation strongly influences air flow through the system, thereby affecting oxidation rates (e.g. Fala et al., 2005). Kinetic limitations on sulfide oxidation imply that decreasing the flow rate, and in turn increasing contact time with oxidizing sulfide minerals, would likely increase the concentrations of sulfate and associated metals in the resultant leachate. The fifth sub-section of results presented in this chapter discusses a preliminary tracer test that was carried out on some of the field cells associated with the stacked field cells. The sixth and final sub-section of this chapter also deals with a leaching rate comparison – this time in the context of the single field cells and two different humidity cells methods used in this study.

4.2 Methods

4.2.1 Cases where Mo and As were not attenuated by waste rock mixing

The stacked and single field cells mentioned in this chapter were installed and sampled in the same way as those mentioned in chapter 2. This chapter focuses primarily on stacked field cells UBC-5A-T and UBC-5C-T (Table 4.1).

Table 4.1 Contents of the 5 field cells discussed in this chapter but not previously mentioned in chapters 2 and 3. UBC-4-5-5A, UBC-5-4A, and UBC-5-6A are single field cells.

Field Cell Code	Materials Used	Purpose
UBC-4-5-5A	Hornfels/marble waste rock, one of the materials used in UBC-5A-T and UBC-5C-T.	Determine composition of unmixed leachate from hornfels/marble.
UBC-5-4A	Hornfels waste rock – one of the material types used in UBC-5A-T.	Determine composition of unmixed leachate from hornfels material
UBC-5-6A	Instrusive waste rock used in UBC-5C-T.	Determine composition of unmixed leachate from intrusive material
UBC-5A-T	470 Kg of UBC-4-5-5A on top of 160 Kg of UBC-5-4A.	Simulate geochemical conditions above lysimeter 5A in UBC experimental waste rock pile.
UBC-5C-T	355 Kg of 5-6A on top of 280 kg of 4-5-5A	Simulate geochemical conditions above lysimeter 5C in UBC experimental waste rock pile.

4.2.2 Prospects for future As, Zn, and Mo leaching and attenuation stacked field cells

For each sampling session, the mass of Zn, As, or Mo released from the field cells was calculated by multiplying the concentration by the volume of water. The individual masses from each sampling event were used to calculate a cumulative running total mass, as well as

a total mass released through the first two rainy seasons. The total mass of each element available to leach in the field cell was calculated by multiplying the solid phase concentration of the element of interest by the mass of waste rock in the field cell in question. The solid phase composition of the waste rock was determined through acid digestion and ICP-MS analysis at ACME laboratories in Vancouver, BC.

4.2.3 Field cell hydrology and implications for sulfate leaching

A tracer test was initiated on January 24 and 25, 2010 by adding 7.12 L of 1 g/L Cl solution to the upper surface of selected field cells. The tracer (LiCl) solution was poured evenly onto the waste rock´s surface using a plastic camping shower consisting of a 10 L bag and a small shower head. Samples were collected as soon as water began to flow from the base of the field cells. During the first 48 hours after the tracer test´s initiation, samples were collected directly from the drainage spout at the base of the field cells (instantaneous samples), however, the rest of the test samples were collected on a weekly or bi-weekly basis from the field cells' sample collection buckets (composite samples). The instantaneous samples were analyzed for chloride with ion chromatography at UBC. The composite samples were analyzed by ALS laboratories in Lima, Peru.

Given that the application of tracer occurred at the height of the rainy season, and in some cases the tracer was applied during natural precipitation events, the results of this study represent an extreme precipitation event and faster than average flow conditions. Two challenges rendered it impossible to carry out quantitative analysis of the tracer test data: the loss of field notes and; imprecise water volume measurements, making it impossible to collect a reliable mass flux for chloride. In spite of these challenges, a qualitative interpretation of the tracer test data is presented in this chapter to provide a general

understanding of the field cells´ hydrologic behavior. For the purposes of comparing release rates between the single field cells and the two different humidity cell methods used in this study, mass loadings were calculated using Equation 1.

Equation 1: *Mass loadings (mg/kg/week) = VC/mt*

Where:

V = Volume of water in sample (L)

C = Concentration (mg/L)

m = mass of waste rock in field cell or humidity cell (kg)

t = time since last sample was collected (weeks)

4.3 Results and discussion

4.3.1 Cases where Mo and As were not attenuated by waste rock mixing

Data from UBC-5A-T provide an example of As-releasing material placed on top of another type of waste rock that was not capable of providing substantial attenuation. Arsenic concentrations in leachate from the single field cell corresponding to the As-releasing material ranged from 0.5 to 22 mg/L; however, they usually fell between 6 and 15 mg/L (Figure 4.1). The two data points available from the upper mini-lysimeters that sampled leachate from the top material type prior to mixing contained 10.2 mg/L in week 20 of the experiment and 10 mg/L As at week 35. Leachate from the base of the stacked field cell contained 5 mg/L to 18.6 mg/L of As, and its concentration generally declined as the experiment progressed. Leachate from the releasing material (UBC-4-5-5A) and the base of the stacked field cell had a similar range of As concentrations, suggesting that As was not attenuated by contact with the hornfels material (UBC-5-4A) at the base of UBC-5A-T.

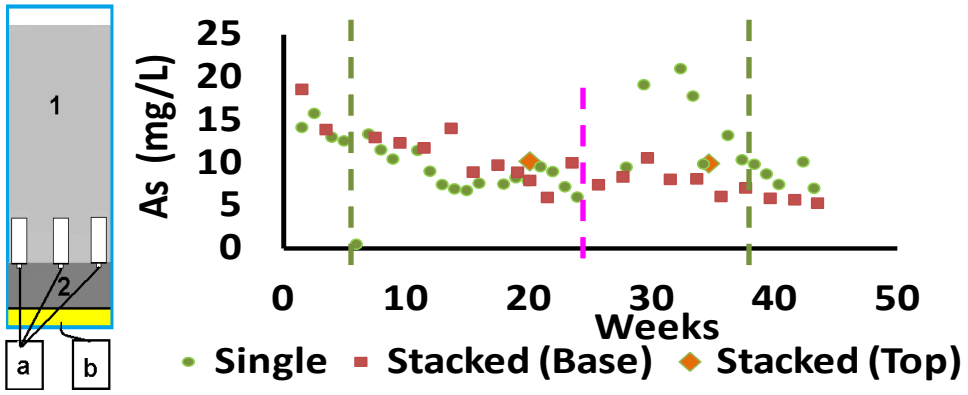

Figure 4.1 Dissolved As concentrations in leachate from stacked field cell UBC-5A-T (Right) demonstrating a lack of As attenuation due to contact with hornfels material, presented along side a schematic diagram of stacked field cell UBC-5A-T (Left). 'Stacked (Base)' series leachate that has come in contact with both material types in the field cell, whereas the 'Stacked (Top)' data points show As concentration in upper lysimeter samples, prior to contact with the bottom material in the stacked field cell. As concentrations from the single field cell of the As-releasing material are shown in the 'Single' data series. Since there was no flow from the field cells in the dry season, time is shown as weeks since the initiation of flow in each field cell. The pink vertical dashed line shows the timing of the end of the first rainy season in 'Stacked (Base)' data and the green dashed lines show the beginning of the second and third rainy seasons in the 'single' series. The schamtic diagram includes As-releasing hornfels/marble material (1), and basal hornfels material (2), along with the sample collection bucket for unmixed leachate from the top material (a), and leachate which has had contact with both material types (b).

The two data points from unmixed leachate from the top of the field cell averaged 10.1 mg/L As, whereas the average As concentration in leachate from the base of the UBC-5A-T was 7.4 mg/L. The lower As concentrations in the base of the stacked field cell suggest that some attenuation may have occurred; however, given the variabilty of As concentrations in the single field cell of the releasing material, more samples from the upper lysimeters would be needed to make this assessment. In any case, the removal effeciency of As is much lower in this stacked field cell than in FC-intrusive over black marble. Given that there were only 163 kg of UBC-5-4A at the base of the stacked field cell, it is possible that some attenuation did occur, but that the attenuating material's attenuation capacity was not sufficient to remove such high As concentrations from leachate.

Apart from FC-black marble over intrusive and FC-intrusive over black marble, another stacked field cell in this study provided an opportunity to gain insights into Mo attenuation in

waste rock: UBC-5C-T, where Mo-bearing intrusive material was installed on top of a hornfels/marble waste rock. Mo concentrations from a single field cell with the intrusive material varied widely, from 0.08 mg/L to more than 6.45 mg/L, however, concentrations were generally greater than 2 mg/L (Figure 4.2). The presence of Mo in leachate from the same material in the top of UBC-5C-T was confirmed by the single sample available from the upper lysimeters, which had a Mo concentration of 3.3 mg/L.

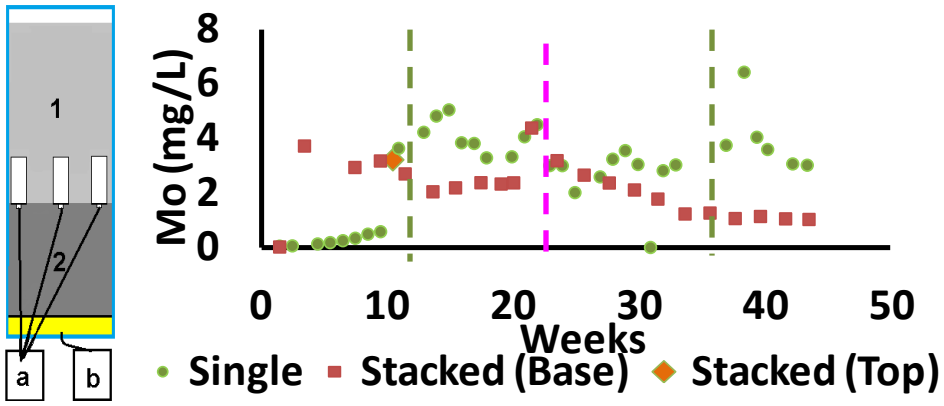

Figure 4.2 Dissolved Mo concentrations in leachate from stacked field cell UBC-5C-T (Right) demonstrating a lack of attenuation by contact with hornfels/marble material, along with a schematic diagram of the materials installed in UBC-5C-T (Left). The 'Stacked (Base)' series shows leachate that has come in contact with both material types in the field cell, whereas the Stacked (Top) data point shows the Mo concentration in upper lysimeter samples, prior to contact with the bottom material in the stacked field cell. Since there was no flow from the field cells in the dry season, time is shown as weeks since the initiation of flow in each field cell. The pink vertical dashed line shows the timing of the end of the first rainy season in 'Stacked (Base)' data and the green dashed lines show the beginning of the second and third rainy seasons in the 'single' series. The schamtic diagram includes Mo-releasing instrusive (1), and basal hornfels/marble material (2), along with the sample collection bucket for unmixed leachate from the top material (a), and leachate which has had contact with both material types (b).

Little to no Mo attenuation occurred in this stacked field cell, given that basal leachate Mo concentrations were generally higher than 1 mg/L, sometimes reaching as high as 4.4 mg/L. At first glance, this lack of attenuation is surprising, since co-precipitation with Pb is hypothesized to limit Mo concentrations, and the material in the base of UBC-5C-T (UBC-4-5-5A) contained 180 ppm of Pb (Table 4.2). A closer comparison between stacked field cells FC-intrusive over black marble and UBC-5C-T reveals that this lack of attenuation does not

necessarily contradict the hypothesis that wulfenite precipitation is an important Mo sink. Sensitivity testing carried out in PHREEQC in chapter 2 of this thesis suggested that increasing the Mo loading rate by a factor of 4 could overwhelm the black marble's capacity to attenuate Mo. The Mo loading rate into the attenuating material appears to have been similar in UBC-5C-T and FC-intrusive over black marble however, in comparison to the attenuating material in FC-intrusive over black marble, the total mass of Pb was only 1/6 of the Pb mass in basal material of UBC-5C-T. The lower mass of Pb in UBC-5C-T corresponds to a lower surface area of exposed galena, and therefore a slower release of Pb into solution, as compared to the attenuating material at the base of FC-intrusive over black marble. It is likely that wulfenite precipitation is occurring in this field cell, but that its rate is limited by low galena surface area for reaction, and therefore Mo concentrations are not markedly decreased.

There may be a connection between Mo attenuation and As attenuation given that the same Pb-bearing marble responsible for attenuating Mo in the FC-intrusive over black marble stacked field cell also attenuated arsenic. Data from stacked field cell UBC-5C-T connection between As attenuation and Mo attenuation, given that the material at the base of UBC-5-T, which failed to attenuate Mo, also released 3-15 mg/L of As. In chapters 2 and 3 it was hypothesized that both Mo and As could be attenuated through distinct co-precipitation reactions involving Pb. If co-precipitation with Pb were indeed responsible for the attenuation of both As and Mo, then it might be the case that the vast majority of the Pb in the base of UBC-5C-T was immobilized by reactions with As before it could form wulfenite.

Table 4.2 A comparison of the Mo and As leachate concentrations along with the Pb solid phase mass and concentration associated with field cells FC-instrusive over black marble and UBC-5C-T. The comparison is presented to help explain the lack of significant Mo attenuation through wulfenite precipitation in stacked field cell UBC-5C-T in spite of the presence of Pb in its attenuating waste rock. The averages shown in this table refer to average concentrations per sample over the first two rainy seasons that the field cells were installed at the Antamina mine.

Field cell	Mass of attenuating material (kg)	Solid phase Pb concentration (ppm)	Total mass of Pb (g)	Avg [Mo] (mg/L) from releasing material	Avg [As] (mg/L) from releasing material	Avg [As] (mg/L) from base
FC intrusive over black marble	349	867	302.6	1.75	0.27	0.004
UBC-5C-T	284	181	51.4	2.75	0.39	7.8

4.3.2 Zn attenuation in FC-black marble over intrusive and FC-intrusive over black marble and associated humidity cells connected in series

Stacked field cells FC-black marble over intrusive and FC-intrusive over black marble and their associated humidity cells connected in series provided the opportunity to study As attenuation (Chapter 2), Mo attenuation (Chapter 3), and Zn attenuation. As was discussed in chapters 2 and 3, both As and Mo were removed from leachate by contact with Pb-bearing black marble. Attenuation of As and Mo did not occur in FC-black marble over intrusive, where As and Mo releasing intrusive material was installed below the Pb-bearing black marble attenuating material. Zn, on the other hand, was released by the Pb-bearing black marble responsible for As and Mo attenuation. This Zn was attenuated by contact with Mo-releasing intrusive waste rock. Drainage from the Pb-bearing black marble single field cell showed Zn concentrations ranging from 1.4 to 14 mg/L (Figure 4.3). The single data point from the upper lysimeters of the stacked field cell FC-black marble over intrusive confirmed the presence of Zn (1.6 mg/L) in leachate. Leachate from the base of this stacked field cell; however, did not contain more than 0.5 mg/L Zn. After the 15th week of flow through the

field cell, Zn concentrations from the base of FC-black marble over intrusive did not exceed 0.1 mg/L.

Data from the HC-black marble over instrusive humidity cells also showed that contact with Mo-releasing intrusive rock reduced Zn concentrations in leachate, at least initially (Figure 4.3). Leachate from the first (Zn-releasing) humidity cell contained 1.3 mg/L during the first two samples sessions of the experiment, before its Zn concentration dropped to below 0.09 mg/L Zn in the 5th week of the experiment, and remained below detection for the rest of the experiment. The first leachate available from the second humidity cell (the Mo-containing and Zn-attenuating intrusive material) had a Zn concentration of 0.16 mg/L, later rising to a maximum concentration of 0.3 mg/L, before falling to around 0.09 mg/L. The intrusive material in the second cell continued to leach detectable zinc for the final 15 weeks of the experiment.

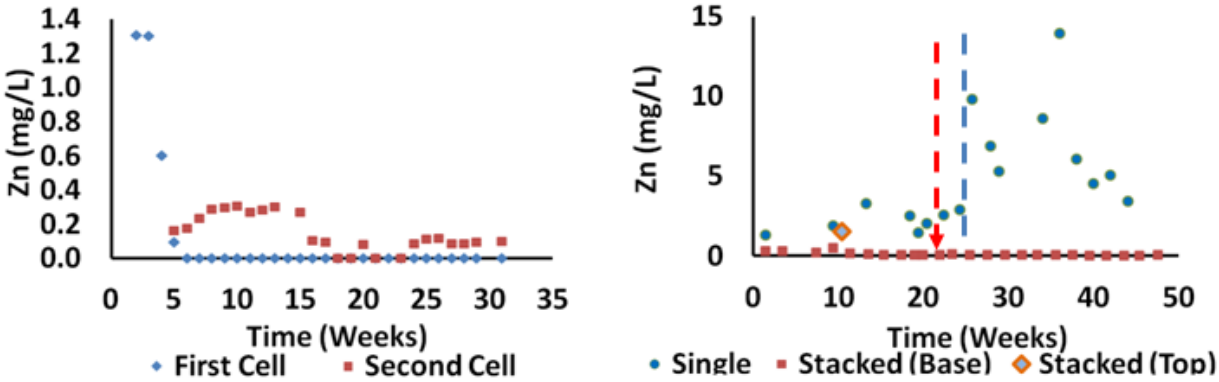

Figure 4.3 Dissolved Zn concentrations in leachate from stacked field cell FC-intrusive over black marble(right) and humidity cells HC-black marble over intrusive connected in series (left) demonstrating attenuation by contact with hornfels waste rock from the Antamina mine. The 'Stacked (Base)' series leachate that has come in contact with both material types in the field cell, whereas the Stacked (Top) data point shows the Zn concentration in upper lysimeter samples, prior to contact with the bottom material in the stacked field cell. Zn concentrations from the single field cell of the Pb-bearing black marble material are shown in the 'Single' data series. Since there was no flow from the field cells in the dry season, time is shown as weeks since the initiation of flow in each field cell. The red vertical dashed line shows the timing of the end of the first rainy season in 'Stacked (Base)' data and the blue dashed line shows the beginning of the second and third rainy seasons in the 'single' series. Data from the associated humidity cell experiment are also shown (left). The 'First Cell' series shows Zn concentrations in leachate prior to contact with the attenuating material, whereas the 'Second Cell' series shows Zn concentrations after contact with the attenuating material.

Stacked field cell FC-intrusive over black marble, where Zn-releasing Pb-bearing black marble was installed below Mo-releasing intrusive waste rock did not show evidence of Zn attenuation. Typical Zn concentrations in leachate from the single field cell of Mo-rich intrusive material installed in FC-intrusive over black marble ranged from 0.07 mg/L to 0.63 mg/L (Figure 4.4). The Zn concentration of leachate from the single sample available from the upper lysimeters fell within this range, at 0.19 mg/L. Leachate Zn concentrations were generally higher in leachate from the base of FC-intrusive over black marble, reaching a maximum value of 1.4 mg/L after 11 weeks of flow through the stacked field cell, before declining gradually to below 0.5 mg/L after 19 weeks of sampling. The minimum Zn concentration from the base of FC-intrusive over black marble was 0.12 mg/L.

The associated humidity cells connected in series, HC-intrusive over black marble, also demonstrated that Zn was not attenuated. The first (intrusive) cell released some Zn over the first six weeks of the experiment, with concentrations ranging from 0.09 to 0.029 mg/L (Figure 4.4). Zn concentrations increased markedly after the leachate from the Mo-releasing intrusives made contact with the Pb-bearing black marble material in HC-Mo-T2L. Leachate from HC-Mo-T2L contained a maximum of 1.6 mg/L Zn in the 6^{th} week of the experiment, thereafter Zn concentrations fell to 0.16 mg/L in the 15^{th} week and remained below 0.3 mg/L for the remaining leach cycles.

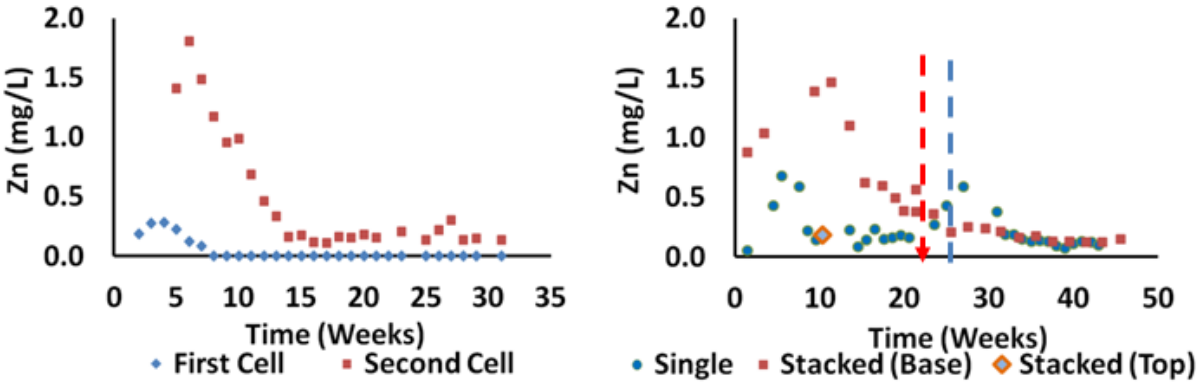

Figure 4.4 Dissolved Zn concentrations in leachate from stacked field cell FC-intrusive over black marble(right) and humidity cells HC-intrusive over black marble series (left) demonstrating attenuation by contact with hornfels waste rock from the Antamina mine. The 'Stacked (Base)' series leachate that has come in contact with both material types in the field cell, whereas the Stacked (Top) data point shows the Zn concentration in upper lysimeter samples, prior to contact with the bottom material in the stacked field cell. concentrations from the single field cell of the Zn-releasing material are shown in the 'Single' data series. Since there was no flow from the field cells in the dry season, time is shown as weeks since the initiation of flow in each field cell. The red vertical dashed line shows the timing of the end of the first rainy season in 'Stacked (Base)' data and the blue dashed line shows the beginning of the second and third rainy seasons in the 'single' series. Data from the associated humidity cell experiment are also shown (left). The 'First Cell' series shows Zn concentrations in leachate prior to contact with the attenuating material, whereas the 'Second Cell' series shows Zn concentrations after contact with the attenuating material. Note that the detection limit in the left hand graph is 0.09 mg/L, but since concentrations appeared to be well below detection the points were graphed as though the concentration were 0 mg/L.

Leachate from the black marble single field cell associated with FC-black marble over intrusive contained between 1 and 14 mg/L (1.6 mg/L in the sample from the upper stacked field cell), while FC-black marble over intrusive's basal leachate contained less than 0.1 mg/L, indicating a Zn removal efficiency of 94-99%. Similar to the Mo attenuation mechanism discussed in chapter 3, Zn attenuation occurred only when the Zn-rich leachate had direct contact with the attenuating material, and not when the attenuating material was placed above the Zn-releasing material. This observation suggests that attenuation depended on a surface reaction, or on co-precipitation with species that are immobile in this geochemical system.

About 88% of the Zn in leachate from black marble was initially removed by reactions with intrusive waste rock material in humidity cell HC-Mo-T1L. This humidity cell experiment provided a contrast to the equivalent stacked field cell because the Zn concentration in leachate from the releasing material dropped off sharply three weeks into the experiment. This decline in aqueous Zn concentration appeared to lead to a remobilization of Zn that had previously been attenuated. Although 0.6 mg of Zn was removed from Zn-bearing leachate by contact with intrusive material in the second (attenuating) cell of HC-exoskarn over horfnels in the first 4 weeks of the experiment, all of this Zn had been released from the attenuating material by the end of the experiment. The maximum Zn concentration in leachate from the Zn-attenuating material was 0.3 mg/L, much less than the 1.2 mg/L initially released from the Pb-bearing demonstrating that although the Zn attenuation reaction in this cell was reversible, it still served to reduce Zn concentrations to some extent.

4.3.3 Attenuation of other metals and metalloids by waste rock mixing

In most cases the concentrations of Ni, Cd, Cr, Cu, Sb, Sn, Se, Ni, Li, and Pb were below detection limit, indicating that they were either not released in the first place, or were attenuated prior to mixing with another waste rock material. In several other cases, one or more of these elements was detected in leachate from at least one of the constituent single field cells, but attenuation was not observed given that it occurred in similar concentrations in leachate from the base of the stacked field cell.

In some cases, the field cell study provided inconclusive evidence for attenuation. The clearest example of inconclusive evidence for attenuation occurred in stacked field cell FC-black marble over intrusive, where Pb and Cu concentrations in leachate from the base of the stacked field cell were much lower than they were in leachate from the UBC-1-3A (black

marble) single field cell. Data from the single leachate sample from the upper lysimeters in FC-black marble over intrusive did not support the occurrence of attenuation, however, since it also showed low Pb and Cu concentrations. This apparent discrepancy in leachate composition between the single field cell and the stacked field cell could indicate that Pb or Cu were not actually leached from the top material in FC-black marble over intrusive, and therefore that attenuation did not occur. More leachate from the upper lysimeters would need to be analyzed prior to determining whether or not attenuation occurred in this case.

Cadmium is the only metal or metalloid aside from Zn, As, and Mo that was verifiably attenuated in this study (Figure 4.5). In addition to leaching zinc, the single field cell of the same Zn-bearing exoskarn material leached between 0.04 and 0.15 mg/L of Cd. The single data point from the upper lysimeter in FC-exoskarn over grey hornfels confirmed that Cd also leached from the exoskarn installed in the stacked field cell, given that its leachate Cd concentration was 0.11 mg/L. The highest Cd concentration in basal leachate from FC-exoskarn over grey hornfels, 0.007 mg/L, occurred in the first available sample. For the rest of the experiment, Cd concentrations from basal leachate never exceeded 0.001 mg/L. These results suggest that as much as 99% of the Cd in leachate was removed by contact with the same hornfels material responsible for Zn attenuation in FC-exoskarn over grey hornfels. Data from the exoskarn over hornfels humidity cell also demonstrated evidence for attenuation. Eleven of the first 12 samples of leachate from the first field cell in the series (HC-Zn-T1U) had detectable Cd (above 0.09 mg/L), with a maximum concentration of 0.2 mg/L. After contact with the grey hornfels in HC-Zn-T1L, the Cd was consistently below detection (0.09 mg/L). Given that Cd is also a divalent cation, it is possible that it was

attenuated by a similar mechanism to that which removed Zn from solution when it made contact with the hornfels material 4-5-1A.

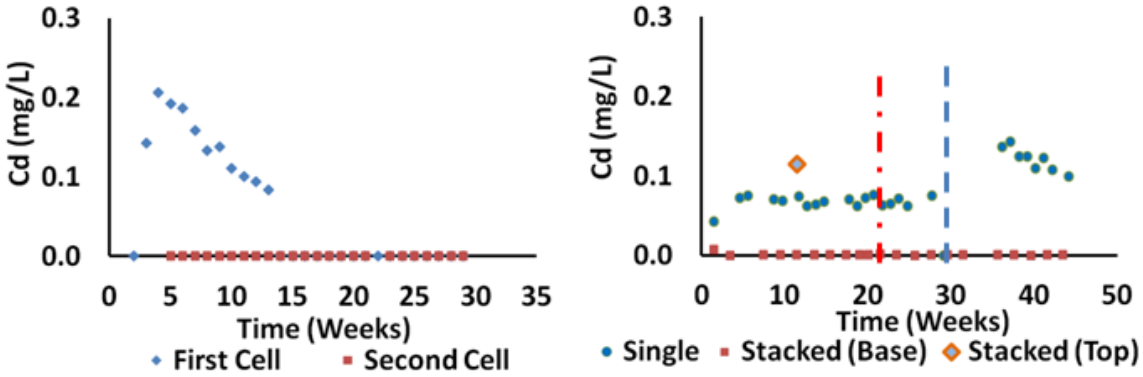

Figure 4.5 Dissolved Cd concentrations in leachate from stacked field cell FC-exoskarn over grey hornfels (right) and humidity cells HC-exoskarn very grey hornfels (left) demonstrating attenuation by contact with hornfels waste rock from the Antamina mine. The 'Stacked (Base)' series leachate that has come in contact with both material types in the field cell, whereas the Stacked (Top) data point shows the Cd concentration in upper lysimeter samples, prior to contact with the bottom material in the stacked field cell. Cd concentrations from the single field cell of the Zn-releasing material are shown in the 'Single' data series. Since there was no flow from the field cells in the dry season, time is shown as weeks since the initiation of flow in each field cell. The pink vertical dashed line shows the timing of the end of the first rainy season in 'Stacked (Base)' data and the green dashed lines show the beginning of the second and third rainy seasons in the 'single' series. Data from the associated humidity cell experiment are also shown (left). The 'First Cell' series shows Cd concentrations in leachate prior to contact with the attenuating material, whereas the 'Second Cell' series shows Cd concentrations after contact with the attenuating material. Note that the detection limit in the left hand graph is 0.09 mg/L, but since concentrations appeared to be well below detection the points were graphed as though the concentration were 0 mg/L.

4.3.4 Prospects for long-term As, Zn, and Mo leaching and attenuation stacked field cells.

The As release rate from the base of UBC-5A-T was fairly constant throughout the first two rainy seasons, averaging about 66 mg/week (Figure 4.6). After two rainy seasons a total of less than 4 g of As had been released from the stacked field cell, amounting to just over 5% of the total mass of As present in UBC-5A-T's As-releasing material. The constant release rate during the rainy seasons was also observed in for Mo and As in stacked field cell FC-black marble over intrusive and Zn in single field cell FC-exoskarn over grey hornfels.

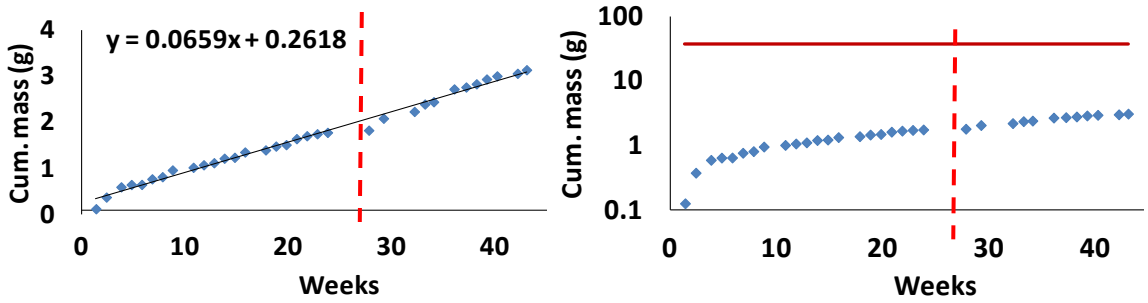

Figure 4.6 The cumulative mass of As relased from waste rock from the UBC-5A-T stacked field cell over the course of the first two two rainy seasons after its installation at the Antamina mine. The same data are presented with a linear y-axis (left) and a logarithmic y-axis (right). The horizontal red line on the diagram to the right shows the total As mass in the stacked field cell's As-releasing hornfels/marble waste rock. Since there was no flow from the field cells in the dry season, time is shown as weeks since the initiation of flow in the field cell. The dashed red lines show the timing of the end of the first rainy season.

Less than 2% of the total Mo in FC-black marble over intrusive had been released from the base of the FC-black marble over intrusive by the end of the second rainy season (Table 4.3). Less than 0.2% of the available Zn was released from FC-exoskarn over grey hornfels and from FC-intrusive over black marble in the first two rainy seasons. A similarly low percentage of the total As had been released from the base of FC-black marble over intrusive. In all of the above-listed cases, the small percentage of the total Mo, As, or Zn mass that had been released from the field cells suggest that leaching could continue for several decades to centuries without exhausting the source of Mo, As, or Zn.

Table 4.3 A summary of the total amount of As, Zn, and Mo available to leach from various field cells installed at Antamina, presented alongside the mass that was released through leaching during the first two rainy seasons after the field cells were installed. The '% Released' column shows the percentage of total solid phase As, Zn, or Mo that was leached through the duration of the first two rainy seasons. All of the data presented, except those from UBC-3-2A are from stacked field cells.

Field cell	Element	Total Mass (g)	Mass released (g)	% Released
UBC-5A-TU	As	66.2	3.6	5.4
UBC-3-2A	Zn	>3332	7.5	<0.2
FC-black marble over intrusive	Mo	106	1.7	1.6
UBC-Mo-T1L	As	53.9	0.05	0.09
UBC-Mo-T2L	Zn	524	0.25	0.05

The elemental composition and total mass of waste rock, together with an understanding of the attenuation stoichiometry can be used to make a first order prediction of a system's attenuation capacity. Assuming that Mo is indeed attenuated by wulfenite precipitation in FC-intrusive over black marble, then such a prediction is possible, given that each mole of wulfenite precipitated removes a mole of Mo and a mole of Pb from solution (Conlan et al., 2012). According to the available data on solid phase composition, there are 0.93 moles (89 g) of Mo in the releasing material and 1.5 moles (303 g) of Pb the attenuating material in this stacked field cell. The surplus of Pb suggests that the black marble in this field cell has adequate capacity to attenuate the Mo that may be released in stacked field cell FC-intrusive over black marble. Unfortunately, similar calculations will not be possible for FC-exoskarn over grey hornfels until the Zn attenuation mechanism is better understood.

Although useful as a first order approximation, the simplistic calculation discussed in the previous paragraph cannot be relied upon for developing a waste rock mixing strategy to attenuate Mo. A more realistic estimate of the attenuation capacity would need to consider kinetics and take into account the fact that much of the Pb released during galena oxidation would likely re-precipitate as cerrusite before it comes in contact with Mo, possibly making it unavailable for reaction with Mo (Chapter 3). Armoring of galena and molybdenite, a process where secondary minerals accumulate on their surfaces, rendering them less reactive, would also need to be accounted for in predicting the long-term behavior of a waste rock system (Holtzen and Smith, 1998).

4.3.5 Field cell hydrology and implications for sulfate leaching

Within only a few hours of tracer application, Cl was already detected at full concentration in instantaneous samples from the UBC-4-5-5A and UBC-5-4A single field cells (Figure 4.7).

In the case of UBC-5-4A the Cl concentration increased from baseline 1 mg/L at the time of the first sample after tracer application to 1,000 mg/L in only 40 minutes. Within a few hours of reaching full tracer concentration (1,000 mg/L), the concentrations of the 2nd and 3rd instantaneous samples dropped to below 300 mg/L in both field cells. The first composite sample, taken a few days after the tracer experiment, fell within the same concentration range. Within 40 days of the initiation of the tracer experiment, concentrations in both field cells had fallen to near baseline levels.

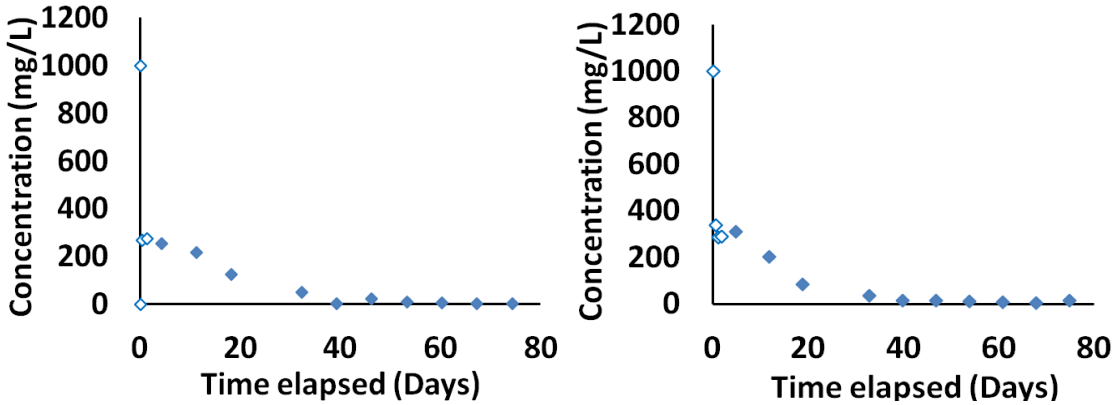

Figure 4.7 Evidence for preferential flow in breakthrough curves showing chloride concentrations in basal leachate vs. time after the application of a LiCl tracer solution to single field cells at the Antamina mine. The data are from field cells UBC-5-4A (left) and UBC-4-5-5A (right). The empty shapes show data from instantaneous samples, whereas the solid shapes show data from composite samples (See section 4.2 for an explanation of those terms).

Field cells UBC-4-4B, UBC-2-0A, UBC-3-2A, and UBC-1-3A showed similar trends, with maximum tracer concentrations occurring only a few hours after the initiation of the test, and several weeks to months passing before additional chloride was flushed from the field cells and Cl concentrations returned to normal levels (Table 4.4). The breakthrough curves demonstrated in the single field cells, with very early, high-concentration peaks, and long tails are indicative of preferential flow, where some tracer passes very quickly through macro-pores in the waste rock and ends up immobilized in low permeability parts of the material and slowly diffuses out (Eriksson et al., 1997). The implication of these preferential flow paths is that residence time in the field cells is highly variable, depending on the flow

path that water takes through the cell. It is probable that during high precipitation events, a significant portion of precipitation may pass through preferential flow paths and have very little time to react with waste rock.

Table 4.4 A summary of key results for the tracer tests carried out in field cells at the Antamina mine in Peru. All concentrations (conc.) mentioned are in mg/L. The time is measured in days since the initiation of the tracer test. The * symbol indicates that the time includes a 150 day dry season where very little flow occurred in the field cell. UBC-5A-TL indicates data from the basal leachate of stacked field cell UBC-5A-T, and UBC-5A-TU shows data from its upper lysimeters.

Field Cell Code	Highest Cl conc.	Last inst. Conc.	Last Jan. 2010 Composite Cl Conc.	Days before Cl drops below 50 mg/L	Days until Cl flushed
UBC-1-3A	1000	268	n/a	17	275*
UBC-2-0A	1000	192	219	24	110
UBC-3-2A	1000	209	174	71	67
UBC-4-4B	1000	232	176	78	274*
UBC-4-5-5A	1000	291	310	33	59
UBC-5-4A	1000	278	257	64	59
UBC-5A-TL	43	43	269	35	47
UBC-5A-TU	242	242	n/a	n/a	n/a

Although instantaneaous samples were not available for the Li that was added to the field cells during the tracer test, it appears to have followed a similar pattern to that of Cl, showing the same signs of preferential flow (Figure 4.8). An important difference between Cl and Li in this tracer test is that Li took much longer to flush out of the system. In all field cells Li concentrations were below 1 mg/L, but still well above pre-tracer test baseline levels at the end of the 2010/2011 rainy season, more than a year after the test was conducted. The fact that Li takes much longer to flush from the field cells than Cl, indicates that Li is retarded by adsorption onto waste rock surfaces.

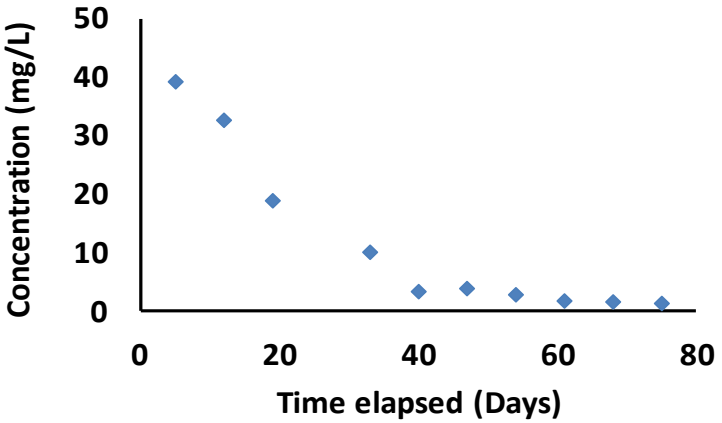

Figure 4.8 Evidence for preferential flow in a typical breakthrough curve showing lithium concentrations in basal leachate vs. time after the application of a LiCl tracer solution to a single field cells at the Antamina mine. The data are from field cell UBC-4-5-5A, but are representative of all other single field cells in the tracer test, and all data points are from composite samples (See section 4.2 for an explanation of those terms).

Only one of the stacked field cells, UBC-5A-T, was included in the tracer test. It was included together with its associated single field cells UBC-5-4A and UBC-4-5-5A, since both of these rock types are included in the stacked field cell. UBC-5A-T was compared with its associated single field cells to explore any differences in flow between stacked and single field cells containing the same materials. Tracer was sampled from both the upper lysimeters and the stacked field cell base, generating two distinct curves. Unlike the single field cells, none of the instantaneous samples taken from the stacked field cell within the first 48 hours after the tracer was applied reached maximum tracer concentrations (Figure 4.9). The higher concentrations in samples from the upper lysimeters in the hours after the tracer was applied suggest that tracer plumes center of mass had not yet reached the base of the field cell 48 hours after it was applied to the field cell's top surface. By the time the first composite sample was taken a few days later, the concentration at the base of the stacked field cell was similar to those observed in the single field cells at the same time. Another similarity with the tracer test results from the single field cells, was that Cl concentrations had decreased to near pre-tracer test levels within 40 days of tracer application. The results from the stacked field

cell still show characteristic signs of preferential flow, with high early time tracer concentrations, and along trail off before all the tracer is flushed out, however, preferential flow appears to be less dominant in stacked field cells than it is in single field cells.

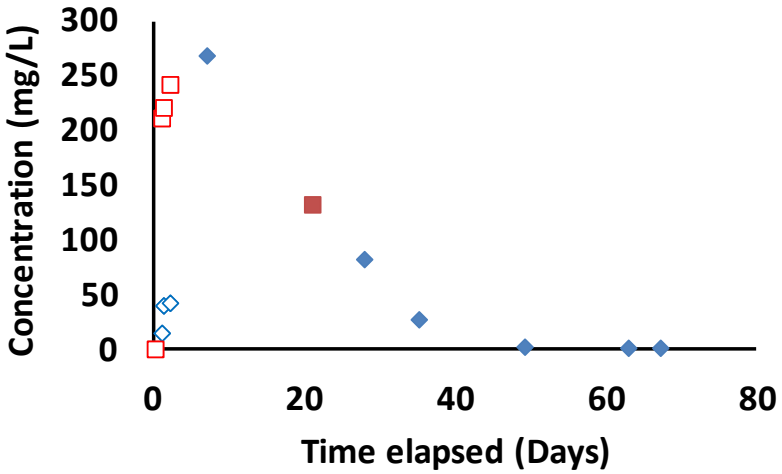

Figure 4.9 Evidence for preferential flow in a composite breakthrough curve showing chloride concentrations in basal and upper lysimeter leachate vs. time after the application of a LiCl tracer solution to stacked field cell UBC-5A-T at the Antamina mine. The red series shows data from the upper lysimeters installed at the contact between waste rock types and the blue series shows data from basal leachate. The empty shapes show data from instantaneous samples, whereas the solid shapes show data from composite samples.

The data from the tracer tests carried out in UBC-5A-T and its companion field cells give the impression that preferential flow is less dominant in the stacked field cells than in single field cells. The amount of sulfate released per kg of waste rock material was compared in four different stacked field cells and their constituent single field cells in order to evaluate the effects of distinct flow regimes on the chemical composition of leachate. Given that the waste rock material in both the stacked and single field cells had been well-mixed it was expected that the amount of sulfate leached per kg of waste rock material in the single field cells would be comparable to that of the associated stacked field cells. All single field cells and stacked field cells leached between 0.15 and 0.95 g of sulfate per kg of waste rock during the course of the first two rainy seasons (Table 4.5). UBC-5A-T released only half the sulfate per kg of material as single field cell UBC-4-5-5A, even though the material from UBC-4-5-

5A composed well over half of the waste rock in the stacked field cell. The difference between stacked field cells and associated single field cells was even more substantial in FC-black marble over intrusive and FC-intrusive over black marble, although in this case the stacked field cell released much more sulfate than the associated single field cells. The stacked field cell FC-exoskarn over grey hornfels released a similar amount of sulfate to UBC-3-2A (exoskarn), even though the material from UBC-3-2A made up only 24% of the mass in the stacked field cell. Based on the results presented in this section, it is very difficult to predict the sulfate release rate of a stacked field cell based on that of its companion single field cells. Some of the difference in sulfate release between stacked field cells and their associated single field cells is likely related to the difference in hydrologic behaviour discussed in this section. These differences in hydrologic behavior and sulfide leaching raise some doubts as to the effectiveness of chemistry data from a single field cell as a surrogate for the composition of unmixed leachate from the upper material in a stacked field cell.

Table 4.5 The mass of sulfate released during the first two rainy seasons after installation per kg of waste rock in four selected field cells and their associated single field cells. UBC-5A-T, FC-black marble over intrusive, FC-intrusive over black marble, and FC-exoskarn over grey hornfels are stacked field cells. Single field cells are shaded the same color as their associated stacked field cells.

Field cell code	Sulfate Released (g/kg)
UBC-4-5-5A	0.29
UBC-5-4A	0.21
UBC-5A-T	0.15
UBC-2-0A	0.33
UBC-1-3A	0.14
FC-black marble over intrusive	0.45
FC-intrusive over black marble	0.51
UBC-3-2A	0.95
UBC-4-5-1A	0.15
FC-exoskarn over grey hornfels	0.85

4.3.6 Comparison of leaching rates from different approaches used in this study

The current study employed three different leaching regimes: the standard ASTM humidity cell leaching method, a modified ASTM method that was used in the humidity cells connected in series to study attenuation, and field cells leached under ambient temperature and precipitation conditions at Antamina. Release rates of As, Mo, and sulfate from intrusive rock under each of these distinct leaching regimes were compared to understand how differences in temperature, water to rock ratio and grain size distribution affected experimental results (Figure 4.10). Mo release rates were highest during the first few weeks of the experiment in both ASTM and non-ASTM humidity cells, starting at 2 mg/kg/week in the second week of the experiment, before stabilizing at close to 0.3 mg/kg/week for the final twenty-two weeks of leaching. The non-ASTM humidity cell tended to release Mo at a marginally higher rate than the ASTM humidity cell in this experiment. The equivalent field cell released Mo at a much lower rate, generally ranging from 0.05 to 0.15 mg/kg/week

during the first two rainy seasons after it was installed. The As leaching rate from the ASTM humidity cell increased steadily during the first 10 weeks of the experiment before levelling off near 0.3 mg/L. The non-ASTM humidity cell released As at a lower rate than its ASTM equivalent, averaging about 0.1 mg/kg/week for most of the experiment. Arsenic leaching occurred at the lowest rate in the field cell, where it ranged from 0.01 to 0.03 mg/kg/week during the first two rainy seasons after it was installed. The highest sulfate release rate, a surrogate for sulfide mineral oxidation in mine drainage systems, occurred in the non-ASTM humidity cell for most of the experiment. Near the beginning of the experiment the non-ASTM intrusive material humidity cell leached sulfate at more than 600 mg/kg/week. The release rate dropped over several weeks before stabilizing for most of the experimental duration at around 20 mg/kg/week. Release rates from the ASTM humidity cell showed a similar pattern to those of the non-ASTM humidity cell, although they were generally lower for the past 20 weeks, averaging about 10 mg/kg/week. The sulfate release rate from the field cell during the first two rainy seasons was highly variable, but like the ASTM humidity cell it generally leached close to 10 mg/kg/week.

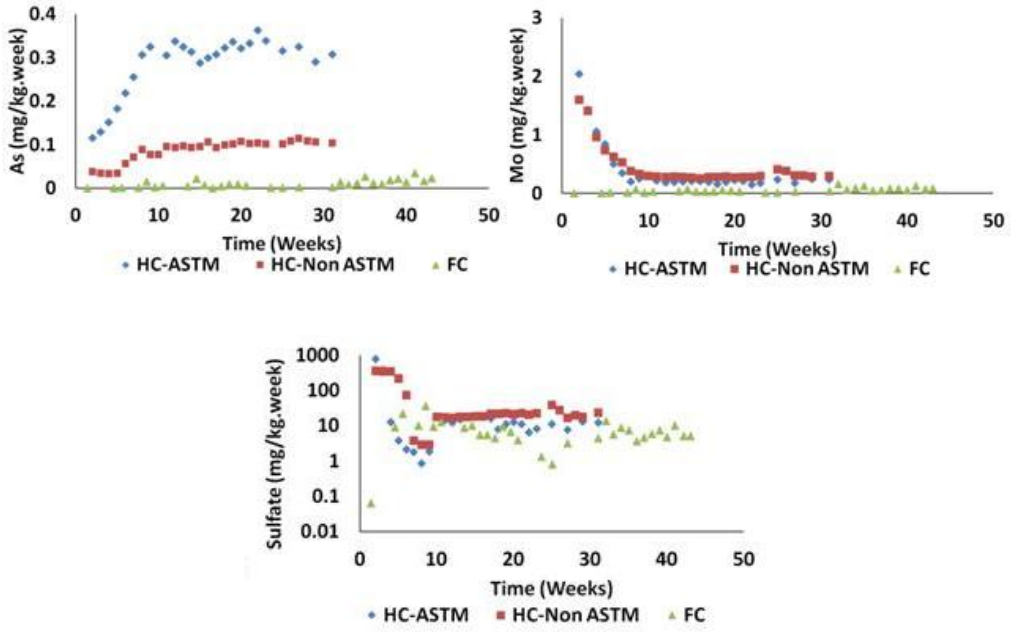

Figure 4.10 A comparison of As (top left), Mo (top right) and sulfate (bottom) release rates from an intrusive Mo-bearing material installed in humidity cells with a standard ASTM leaching procedure (HC-ASTM series), a modified humidity cell leaching procedure (HC-Non ASTM series) and a field cell installed at Antamina mine in Peru (FC series) plotted against time since installation. The vertical axis in the sulfate graph has a logarithmic scale. The field cell data series has had its dry seasons removed to facilitate comparison with the more continuous humidity cell data.

The release rates of Mo, As, and sulfate per unit mass of waste rock material were higher from the humidity cells than they were from the field cells used in this study. The higher release rates from humidity cells was not unexpected given that their small grain size allowed for more mineral surface area for oxidation reactions and the higher temperatures in the laboratory setting likely hastened the rate of kinetic reactions. The non-ASTM cell leached Mo, and sulfate at an even higher rate than the ASTM humidity cell, perhaps because its lower water to waste rock ratio facilitated the aeration of material in the cell, thereby enhancing sulfide oxidation. It is unclear why As was released more rapidly from the ASTM humidity cell in this experiment.

Although figure 5 demonstrates that the intrusive material releases sulfate twice as rapidly (per kg of material) than the field cells, this is likely an underestimate, given that the field

cells only have substantial water flow for about twenty weeks a year. Taking this into account, a week of leaching in the non-ASTM humidity cell is equivalent to at least 4 weeks of leaching in field cells under ambient conditions.

4.3.7 Summary and future research

While the data presented and discussed in this chapter provide some further insight into the processes controlling metal release and attenuation in the field cells, they also highlight some areas where further research is required. The following points highlight the key findings presented in the chapter:

- As was not strongly attenuated by contact with fornfels UBC-5-4A.
- Mo was not strongly attenuated by contact with UBC-4-5-5A (marble/hornfels) even though UBC-4-5-5A contained Pb. Given relatively small amount of Pb in the attenuating material it is possible that its attenuation capacity was overwhelmed.
- Zn is attenuated by contact with intrusive material in the FC-black marble over intrusive field cell and associated humidity cells. The lack of attenuation in the FC-intrusive over black marble field cell suggests that a surface reaction is responsible for removing Zn from solution.
- Aside from As, Mo, and Zn, Cd is the only element for which conclusive evidence for attenuation was found, like Zn it was removed by contact with hornfels material in FC-exoskarn over grey hornfels.
- It appears that Mo, Zn, and As will continue to be released from field cells for many years, based on the small percentage of their overall mass that has been released from field cells so far.

- FC-black marble over intrusive seems to contain enough Pb to attenuate the Mo that may leach from its Mo-releasing material.
- Preferential flow occurs in both stacked and single field cells, however it appears to be a more dominant mechanism in single field cells.
- The slower release of Li, relative to Cl, after the tracer test suggests that Li may be retarded to some extent by adsorption.
- Differences in flow characteristics between stacked field cells and their associated single field cells may help explain the difficulty in predicting stacked field cell sulfate release rates based on single field cell sulfate release rates.
- The differences in flow and sulfate loading between stacked field cells and associated single field cells highlight a downside of relying on data from single field cells as a surrogate for pre-mixing leachate composition. The challenges associated with using single field cell leachate as a surrogate for unmixed single field cell leachate highlight the importance of data from upper lysimeters for determining unmixed leachate composition in stacked field cells.
- The FC humidity cell leaching procedure yields higher chemical release rates than the ASTM humidity cell leaching procedure, which in turn leads to faster leaching than the field cells.

The following key areas of uncertainty were identified and may require further research:

- Little information is currently available on hornfels UBC-5-4A's solid phase composition, so it is unclear why so little As attenuation occurred due to contact with this material.

- The lack of data on the chemical and mineralogical composition of UBC-4-5-5A may provide further insight as to whether the lack of Mo attenuation by this material is related to its low Pb content, or wulfenite ($PbMoO_4$) precipitation is limited by some other factor.
- If whole rock composition is to be used to predict the attenuation potential of a given material, it will be important to account for the effects of armoring by secondary minerals that form on sulfides or other mineral surfaces.
- Future tracer tests should focus on FC-exoskarn over grey hornfels, FC-black marble over intrusive, FC-intrusive over black marble and their associated single field cells since these stacked field cells are the most interesting in terms of geochemical attenuation, and their hydrologic behavior is not yet well understood.
- The lack of quality flow volume data complicates quantitative analysis of tracer test data and makes it difficult to estimate residence time in the field cells.

Chapter 5: Conclusion

This chapter will review the key findings presented in the thesis, highlight their potential implications for Antamina and for the mitigation of neutral mine drainage in general, and highlight uncertainties and areas where further research is still required.

5.1 Summary of key findings

As outlined in the introduction, the principal objectives of this research were:

- To evaluate the effectiveness of stacked field cells and humidity cells connected in series for the study of metal attenuation by waste rock mixing
- To test the hypothesis that Pb could limit aqueous Mo concentrations through the precipitation of wulfenite ($PbMoO_4$) under field conditions at neutral pH
- To assess the degree to which Zn could be attenuated by contact with non-reactive hornfels or limestone material in neutral pH conditions
- To identify the mechanism(s) responsible for Zn attenuation

This section of the conclusion chapter will review the key findings related to each of the four principal research objectives.

5.1.1 Effectiveness of stacked field cells and humidity cells connected in series

This thesis has presented the results of two hitherto untested methods for the study of metal attenuation by waste rock mixing. Both experimental methods were proven capable of detecting attenuation reactions by allowing the comparison of pre-mixing and post-mixing chemical compositions of leachate from waste rock. Furthermore results from both experiments were generally consistent. Data from the stacked field cells demonstrated five distinct attenuation reactions: Zn and Cd were both attenuated by contact with calcite rich hornfels waste rock in FC-exoskarn over grey hornfels, Zn was attenuated by contact with

Mo-releasing intrusive material in FC-black marble over intrusive, and both Mo and As were attenuated by contact with Pb-bearing black marble waste rock in FC-intrusive over black marble. The same metals were attenuated by the same materials in the associated humidity cells. Both stacked field cells and humidity cells connected in series also demonstrated that Zn, Mo, and As were not attenuated when the releasing material was installed below (down flow from) the attenuating material – demonstrating further consistency between the distinct experimental approaches. The largest difference between the experimental approaches was observed with respect to Zn attenuation, given that a higher percentage of Zn was removed from leachate in the stacked field cell experiments than in the associated humidity cell experiments. Overall, in spite of the difference in grain size distribution, experimental scale, and climate between the stacked field cells and humidity cells operated in series, the smaller-scale and more cost-effective humidity cell version of the experiment appears to be a reasonable method for identifying attenuation reactions that may occur in waste rock dumps. The inadequate data from the upper lysimeters in the stacked field cells were supplemented by relying on single field cells as surrogates, however this approach had limitations. Generally the single field cell surrogate approach worked quite well, however, in some cases (e.g. Pb and Cu leaching from black marble in UBC-3-2A, but not leaching from identical material in FC-black marble over intrusive and FC-intrusive over black marble) the same waste rock material leached metals in the single field cell that it appeared not to leach in the associated stacked field cell. It seems likely that this sort of discrepancy was caused by heterogeneities in the waste rock material, however it may also be related to the different flow behavior between stacked field cells and single field cells, as mentioned in chapter 4.

One possible flaw in the upper lysimeter design is that they were not tall enough, and that the formation of a perched water table at the lysimeters' bases caused unfavorable hydraulic gradients, leading flow to bypass them (Figure 5.1, Ayres et al., 2003). The second factor was eventually addressed by sending 30 mL samples to Canada for chemical analysis instead of relying on ALS laboratories in Lima. This change in sampling procedure yielded samples from the upper lysimeters in the third rainy season, although these samples were not yet analyzed at the time of publication.

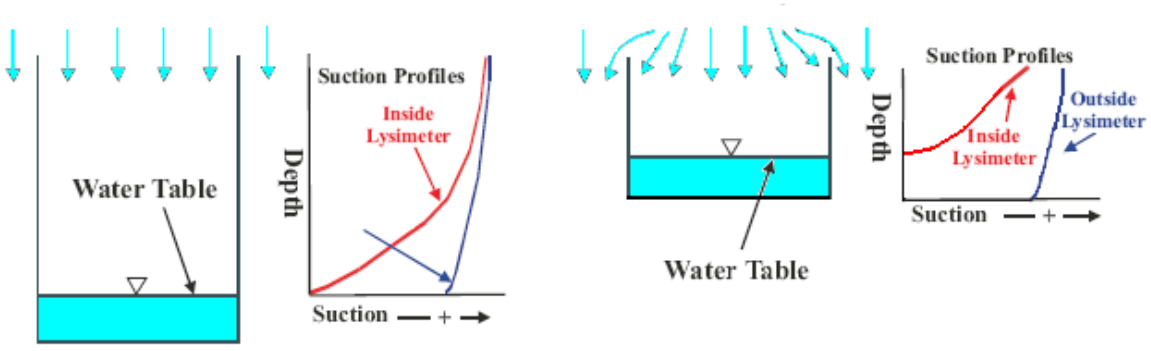

Figure 5.1 A schematic diagram demonstrating how inadequate lysimeter depth can cause water flow (represented by blue arrows) to bypass lysimeters in unsaturated conditions by leading to a situation where suction along the outside of the lysimeter is much stronger than inside it (modified from Ayres et al., 2003).

5.1.2 Attenuation of Mo through wulfenite precipitation

Conlan et al. (2012) laid the groundwork for this portion of the thesis by establishing that wulfenite precipitation could play an important role in controlling Mo concentrations in geochemical conditions similar to those found in Antamina waste rock. This study's principal contribution was to demonstrate that Pb can play an important role in attenuating Mo in actual waste rock from the mine and under field conditions rather than under more carefully controlled laboratory experiments. Results from stacked field cell FC-intrusive over black marble and associated humidity cells connected in series proved that Pb-bearing marble waste rock from Antamina was capable of removing aqueous Mo from leachate. Based on

the work of Conlan et al. (2012), and the observation that attenuation only occurred when Mo leachate had direct contact with Pb-bearing waste rock, and geochemical modeling, it appears that wulfenite precipitation was responsible for the removal of Mo from solution. Given that galena is the most likely source of Pb in the waste rock, the degree of Mo attenuation is limited by a kinetically controlled oxidation reaction (Figure 5.2). In spite of Pb's low mobility at typical pH values for Antamina waste rock, geochemical modeling suggests that wulfenite precipitation out occurs more readily than cerrusite precipitation when Mo makes close contact with an oxidizing galena mineral grain.

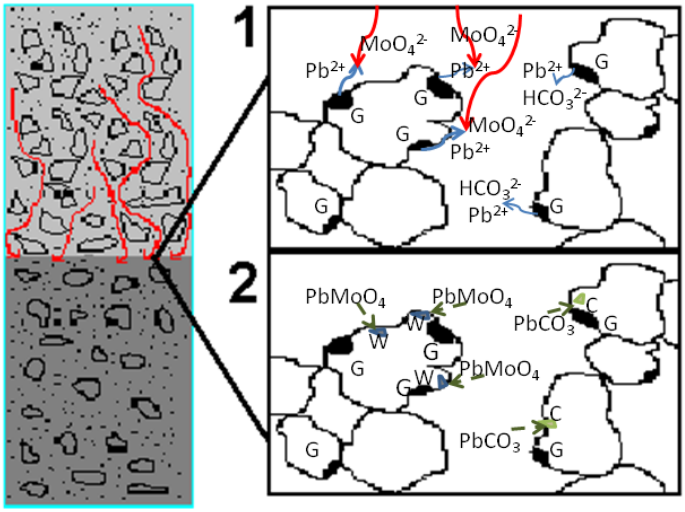

Figure 5.2 Diagram of Mo from molibdenite dissolution (red arrows) being attenuated near the top of the Pb-bearing black marble layer in FC-intrusive over black marble (left). Panel 1 on the right shows the attenuation at the scale of a single pore, where MoO_4^{2-} is intercepted by Pb^{2+} (blue arrows) from galena (G) oxidation. Pb^{2+} that does not come in contact with MoO_4^{2-} reacts with HCO_3^- in solution. In panel 2 $PbMoO_4$ precipitates as wulfenite and $PbCO_3$ precipitates as cerrusite on the surfaces of nearby grains of waste rock material

The results presented in chapters 3 and 4 also demonstrate that merely mixing Pb-bearing waste rock with Mo-releasing material is not sufficient to guarantee precipitation. Layering Pb-bearing waste rock on top of Mo-releasing waste rock does not appear to have any significant attenuating affect, likely because Pb is immobilized by cerrusite precipitation before it can react with Mo to form wulfenite.

Even if Pb-bearing material is placed below (downstream of) Mo-releasing waste rock, as was the case in field cell UBC-5C-T, Mo attenuation will not necessarily occur. Given the lower concentration of Pb in UBC-5C-T as compared to FC-intrusive over black marble, and by extension lower galena surface area in the attenuating material, it is likely that the Mo loading rate exceeded the field cell's capacity to release Pb for wulfenite precipitation.

Conlan et al. (2012) identified powellite as another potential sink for Mo in neutral drainage conditions, however, noted that its formation was kinetically limited. SI calculations performed on leachate from the field cells in this study supported this hypothesis, given that powellite was supersaturated in leachate from Mo-releasing field cells (UBC-2-0A, and FC-black marble over intrusive). This result suggests that kinetic limitations on powellite precipitation prevent it from playing an important role in controlling Mo concentrations in Antamina waste rock, at least at the time scale of the stacked field cell experiments.

It was hoped that Mo attenuation mechanism could be confirmed by solid phase analysis of the attenuating waste rock material after several months of exposure to Mo-bearing leachate. Unfortunately, this was not possible in the humidity cells because the miniscule mass of Mo that was attenuated led to an insufficient solid phase concentration of these metals in the attenuating material. Given that the aqueous concentration of Mo was higher in the field cells than in the humidity cells, an attempt was made to sample waste rock from the upper boundary of the attenuating material in stacked field cells FC-intrusive over black marble. This attempt at sampling was unsuccessful, however, because miscommunication with field staff at the Antamina mine led to the retrieval of samples from the base of the attenuating material, where solid phase concentrations of Mo would have been at their lowest, and no Mo was found.

5.1.3 An assessment of Zn attenuation by contact with non-reactive hornfels

Field cell experiments revealed that more than 99% of Zn was removed from leachate that passed through calcite rich hornfels material. A lower percentage of Zn was attenuated by contact with the same material in the humidity cell version of the experiment. This lower removal percentage may have been related to a relative lack of reaction sites or a lower residence time (if the reaction were kinetically limited) in the humidity cell in comparison with the stacked field cell.

5.1.4 The mechanism responsible for Zn attenuation in hornfels

A review of the scientific literature (summarized in Chapter 3) suggested that there are 3 principal mechanisms by which Zn could have been attenuated in this system: 1) precipitation as a Zn-carbonate or Zn-hydroxide mineral; 2) adsorption on to oxide mineral surfaces; 3) or incorporation into the inter-layer of a phyllosilicate clay mineral. Geochemical modeling cast doubt on the importance of Zn-carbonate or Zn-hydroxide precipitation for attenuating Zn, as none of the modeled Zn-bearing phases in the MINTEQ.V4 database were insoluble enough to account for the degree of attenuation observed in the study. The likelihood that adsorption onto iron or aluminum oxide minerals could have been responsible for Zn attenuation was low, since iron oxide minerals are a product of pyrite oxidation and would be present in both the releasing and the attenuated material. Furthermore, SEM analysis did not find evidence of Zn associated with iron oxide surfaces in the hornfels Zn-attenuating material from the humidity cell experiment, despite its having been exposed to Zn-bearing leachate for 30 weeks.

On the other hand, several lines of evidence from SEM and XRD analyses of attenuating material from the humidity cells connected in series suggested that phyllosilicate clays played an important role in attenuating Zn. SEM /EDX analysis consistently showed an association between Zn and fine-grained, platy, clay-like minerals that were rich in Al, Mg, Si, O, and Fe. XRD analysis demonstrated that clinochlore, a phyllosilicate clay mineral composed of Al, Mg, Si, O, and Fe, was quite abundant in the Zn-attenuating material, but not in the Zn-releasing material. The abundance of clinchlore in the Zn-attenuating material relative to the Zn-releasing material provides a likely explanation as to why waste rock mixing was necessary to facilitate Zn attenuation in this case – the releasing material did not contain enough clinochlore clay to provide sufficient exchanges sites to remove Zn from solution. Based on the evidence presented in chapter 3, it is hypothesized that Zn^{2+} is attenuated by replacing Mg^{2+} or Fe^{2+} in the interlayer of clinochlore clays (Figure 5.3). Another divalent cation, Cd^{2+}, was also attenuated by contact with the same hornfels material, suggesting that it may have been subject to a similar attenuation mechanism.

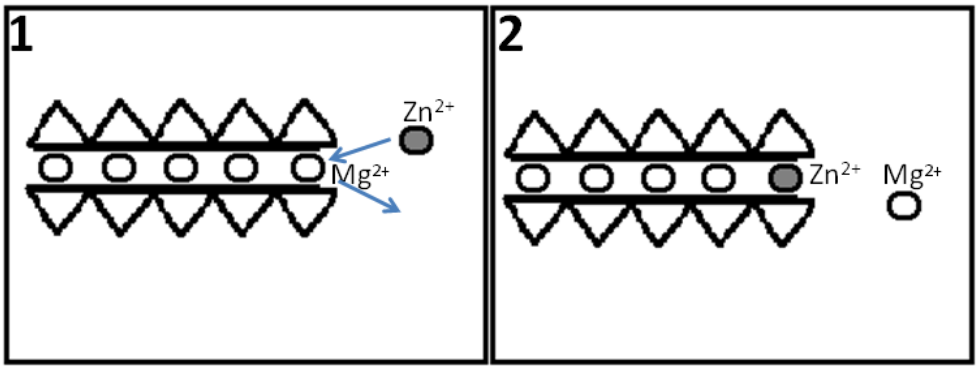

Figure 5.3 A schematic diagram showing the Zn^{2+} replacing an Mg^{2+} ion in the interlayer of a clay mineral. The triangles are alumino-silicate tetrahedral. Figure modified from Dold and Fonboté, 2001.

It should be noted that some Zn was detected by SEM/EDX in a similar mineral phase in weathered attenuating material that had not been exposed to Zn-rich leachate. This is not entirely unexpected, given that some Zn-bearing sphalerite is also present in the attenuating

material and Zn from the weathering of this sphalerite would probably be attenuated by the same mechanism. A sample from the attenuating material in FC-exoskarn over grey hornfels was taken for solid phase analysis in the hopes that the higher aqueous Zn concentrations in the field cells would yield higher solid phase Zn concentrations and facilitate the identification of Zn-bearing secondary phases. As was the case for samples from FC-intrusive over black marble, field staff at Antamina took the sample from the base of the stacked field cell rather than the upper boundary of the attenuating material, resulting in very low solid phase Zn concentrations.

5.1.5 Summary of metal attenuation reactions presented in this study

Five distinct metal attenuation reactions have been identified in this study. In each case an attenuation mechanism has been postulated, however the degree of confidence in the mechanism varies widely (Table 5.1). Mo attenuation is the best understood of the four metals that were attenuated in this research, due to Conlan's (2009) previous investigation on the topic. The work in this thesis has led to the development of a hypothesis as to the fate of attenuated Zn, however, more work is needed to confirm the proposed mechanism and predict Zn's long-term fate. The mechanisms behind As and Cd attenuation are still less well understood than the Zn attenuation mechanism, and much more research would be needed to confirm them. The degree of certainty in the attenuation mechanism must be considered when applying the findings of this research to the prediction of drainage quality or the strategic layering of waste in waste rock dumps.

Table 5.1 A summary of the 5 different attenuation reactions observed in the stacked field cells installed at the Antamina mine site. The 'references from the literature' column refers to papers or theses where the proposed mechanism is described.

Stacked field cell	Metal attenuated	Proposed mechanism	Evidence from this study	References from literature	Degree of certainty
FC-intrusive over black marble	Mo	Wulfenite precipitation	Association with Pb bearing waste rock in field cells and humidity cells, geochemical modeling	Conlan et al., 2012; Lindsay and Vlek, 1977	High
FC-exoskarn over grey hornfels	Zn	Incorporation into clay minerals	SEM/EDX work, geochemical modeling	Manceau et al., 2000; Dold 2003	Medium-high
FC-black marble over intrusive	As	Co-precipitation with Pb	Association with Pb bearing waste rock in field cells and humidity cells	Villalobos et al., 2010	Medium-low
FC-exoskarn over grey hornfels	Cd	Incorporation into clay minerals	Also divalent cation, attenuated in same material as Zn	Barbier et al., 2000	Medium-low
FC-black marble over intrusive	Zn	Co-precipitation with Mo	Attenuation in Mo-releasing material	Conlan, 2009	Low

5.2 Research implications

This section of chapter 5 will highlight and discuss the importance and potential applications of the research to the Antamina mine and to the mining industry in general.

5.2.1 Implications for the Antamina mine

As is the case with UBC's entire Antamina waste rock project, this research was initiated to assist the Antamina mine in understanding hydrological and geochemical processes that occur in their waste rock to aid in the development of their plans for waste rock disposal and mine closure. Specifically, this research sought to confirm that Mo could be attenuated by wulfenite attenuation due to contact with Pb under conditions representative of the mine's waste rock dumps. The observed attenuation of Mo by contact with Pb-bearing waste rock

suggests that wulfenite precipitation could be included in models of sections of the East Dump where Mo- and Pb-bearing waste rock is intermingled. It also may help explain the low Mo concentration in leachate from the East Dump in spite of the high Mo concentrations leached from some waste rock materials that are deposited there. Another factor likely contributes to Mo attenuation in leachate from the East Dump, is that some parts of the leachate have turned acidic, allowing Mo to be removed by sorption.

The stacked field cell experiment was designed to determine whether there are any mechanisms by which non-reactive waste rock material could attenuate Zn. At the time of study design this issue was particularly relevant given that some moderately reactive Zn-releasing materials were being disposed of in the class C dominated Tucush Dump at Antamina. Results from this study provide strong evidence that the attenuation of Zn by non-reactive waste rock at Antamina is possible. The hypothesized Zn attenuation mechanism may be useful in predicting the degree to which Zn attenuation will occur in the Tucush dump once it has been confirmed. Given the possibility that adsorption or cation exchange is responsible for Zn attenuation, it is possible that the capacity of the attenuating material will run out before the Zn-leaching ceases.

The attenuation of Mo, Zn, Cd, and As observed in this study points to reactions that should be taken into account for understanding and modeling the behavior the full scale waste rock dumps. These reactions, however, occurred in stacked field cells that were designed to answer specific research questions related to Antamina's full scale piles and not UBC's experimental piles. On the other hand, stacked field cells UBC-5C-T, UBC-4B-T, and UBC-4C-T were designed to mimic the geochemical conditions directly overlying specific small sub-lysimeters (5C, 4B, and 4C, respectively) in UBC's experimental piles 4 and 5. The lack

observed attenuation of Mo, Zn, As, Ni, Cd, Cr, Cu, Sb, Sn, Se, Ni, Li, or Pb in these field cells suggests that attenuation reactions do not play an important role in these sections of UBC's experimental waste rock piles.

5.2.2 Implications for waste rock management

The study presented in this thesis has provided evidence that strategically mixing waste rock, especially placing attenuating material beneath metal releasing material, can attenuate Mo, Zn, and other metals of concern in neutral mine drainage. Even in cases where strategically layering waste rock is not feasible, the attenuation mechanisms explored in this study will aid in predicting drainage chemistry in mines where Mo and Zn cause concern. The stacked field cell and humidity cells connected in series approaches to the study of attenuation by waste rock mixing are relatively low-cost options and can be useful in the design of waste rock layering schemes, or prediction of contaminant behavior in waste rock dumps at other mines.

5.3 Directions for future research

The work presented in this thesis touches on three related topics in the study of the hydrologic and geochemical behavior of waste rock: the detection of metal attenuation by waste rock mixing, the mechanisms behind metal attenuation in waste rock, and the effects of experimental scale in comparing results from humidity cells, field cells, and experimental waste rock piles. This section of Chapter 5 will present potential future research topics in each of these 3 topics.

5.3.1 Detection of metal attenuation reactions by waste rock mixing

Overall, this aspect of the study was very successful, given that five different attenuation reactions were confirmed or identified. Section 4.3.2 describes an exception to this success: the case of unconfirmed Cu and Pb attenuation in stacked field cell FC-black marble over

intrusive. The following steps are recommended to better understand the behavior of Cu and Pb in FC-black marble over intrusive and research other attenuation reactions in the future:

- Submit samples from humidity cells HC-black marble over intrusive for ICP-MS analysis to determine whether or not Cu and Pb was leached from 1-3A and attenuated in the humidity cells connected in series
- Results of a detailed solid phase analysis of the UBC-1-3A material from the stacked field cell could be compared to those already performed on UBC-1-3A to determine if there is a mineralogical explanation for the apparent lack of Pb and Cu leaching in stacked field cells FC-black marble over intrusive and FC-intrusive over black marble
- Other suspected attenuation reactions should be confirmed using humidity cells connected in series or stacked field cells as they are identified.

The following suggestions may improve the performance of stacked field cells in future applications:

- Future stacked field cells should have taller upper lysimeters to avoid the sample by-pass problem described in section 5.1.1.
- Arrangements for chemical analysis from upper lysimeters should be made beforehand to account for the low sample volume that will be collected form these samples.

5.3.2 Identification of metal attenuation mechanisms

Five distinct metal attenuation stories were described in this thesis. In each of the five cases, some uncertainty exists with regards to the exact mechanism of metal attenuation. The following courses of action are recommended to improve understanding of attenuation mechanisms in neutral drainage:

- Samples of waste rock should be taken from the top of the attenuating materials in field cells FC-exoskarn over grey hornfels, FC-black marble over intrusive and FC-intrusive over black marble where aqueous Zn and Mo attenuations are highest.
- Samples from the top of the attenuating material in the field cells should be subjected to SEM/EDX, MLA, or other solid phase analysis to identify Mo or Zn bearing secondary mineral phases attenuating materials.
- Mineralogical analysis of UBC-4-5-5A should be carried out to better understand why Mo is not strongly attenuated by this material even though it contains Pb. As discussed in chapter 4, the current hypothesis is that Pb is simply not abundant enough, or released into solution quickly enough to attenuate Mo in field cell UBC-5C-T.
- The hypothesis the Zn is attenuated by incorporation into phyllosilicate clay minerals may be tested by carrying out a sequential leaching procedure such as that described by Dold (2003) on a hornfels material that has been exposed to Zn-bearing leachate.
- In the case of Cd and As, given the low aqueous concentrations in field cell leachate it may be necessary to expose sediments to artificially high As or Cd concentrations in laboratory experiments in order to produce enough secondary As or Cd phases to allow solid phase analysis.

5.3.3 Scale effects

An understanding of the effects of different experimental scales is essential for applying results from this experiment to the full scale waste rock dumps at Antamina. In spite of differences in grain size, residence time, temperature and sulfate release rates, stacked field cells and humidity cells connected in series have identified the same attenuation reactions in this study. Stacked field cells UBC-5C-T, UBC-4B-T, and UBC-4C-T provide an opportunity to make comparisons between the stacked field cell and experimental pile scales. To facilitate the comparison of results across different experimental scales, however, a more detailed understanding of flow and residence times in the stacked field cells is required. The following courses of action may improve understanding of attenuation across different scales:

- A tracer test should be carried out on stacked field cells UBC-5C-T, FC-black marble over intrusive, FC-intrusive over black marble, UBC-Zn-T and their associated single field cells to develop a better understanding of how water flows through waste rock in the field cells. Special care should be taken to accurately measure water volumes in this case, so as to calculate mean residence times in each field cell
- Chemistry results from UBC-5C-T, UBC-4B-T and UBC-4C-T and their associated single field cells should be compared with those of corresponding sub-lysimeters in experimental waste rock piles 4 and 5 to determine if any attenuation reactions occur in the piles that have not been captured in the field cell experiment. Special attention should be paid to Mo in lysimeter C of pile 5 and its comparison with data from UBC-5C-T.

References

Andrina, J., Wilson, G.W., Miller, S., Neale, A. 2006. Performance of the acid rock drainage mitigation waste rock trial dump at Grasberg Mine. In, Proceedings of the 7th International Conference on Acid Rock Drainage (ICARD), March 26-30, 2006, St. Louis, United States of America. R.I. Barnhisel (ed.)

Andrina, J., Wilson, G.W., Miller, S., Neale, A. 2003. The design, construction, instrumentation and performance of a full-scale overburden stockpile trial for mitigation of acid rock drainage, Grasberg Mine, Papua province, Indonesia. In, Proceedings from the 5th International Conference on Acid Rock Drainage (ICARD), Cairns, Aulstralia, July 12 - 18.

Antamina. 2011. Who we are. Viewed on November 6th, 2011, http://www.antamina.com/en/content.php?331/quienes_somos/our_company.html

Alloway, B. 1973. Copper and molybdenum in swayback pastures. Journal of Agricultural Science, 80: 521–524.

Aranda, C., Klein, B., Beckie, R., Mayer, U. 2009. Assessment of waste rock weathering characteristics at the Antamina mine based on field cell experiments. In, proceedings of Securing the Future and 8th ICARD, Skellefteå, Sweden, June 23-26, 2009.

Aranda, C. 2009. Assessment of waste rock weathering characteristics at the Antamina mine based on field cells experiment. M.A.Sc. thesis, University of British Columbia, Vancouver, Canada.

ASTM. 1996. Standard Test Methods for Accelerated Weathering of Solid Materials Using a Modified Humidity Cell. ASTM Standards Designation: D5744-96.

Ayres, B., Diram, G., Christensen, D., Januszewski, S., O'Kane, M. 2003. Performance of cover system field trials for waste rock at Myra Falls Operations. In, Proceedings from the 5th International Conference on Acid Rock Drainage (ICARD), Cairns, Aulstralia, July 12 - 18.

Barbier, F., Duc, G. Petit-Ramel, M. 2000. Adsorption of lead and cadmium ions from aqueous solution to the montmorillonite/water interface. Colloids and Surfaces A: Physicochemical and Engineering Aspects, 166: 153-159.

Bay, D., Peterson, H., Singurindy, O., Aranda, C., Dockrey, J., Sifuentes Vargas, F., Mayer, U., Smith, L., Klein, B., Beckie, R., 2009. Assessment of neutral pH drainage from three experimental waste-rock piles at the Antamina Mine, Peru. Paper presented at Securing the Future and 8th International Conference on Acid Rock Drainage, Skellefteå, Sweden. June 23-26.

Benner, S., Blowes, D., Gould, W., Herbert, R., Ptacek, C. 1999. Geochemistry of a permeable reactive barrier for metals and acid mine drainage. Environmental Science and Technology 33: 2793-2799.

Benzaazoua, M., Bussière, B., Dagenais, A.-M., Archambault, M. 2004. Kinetic tests comparison and interpretation for prediction of the Joutel tailings acid generation potential. Environmental Geology 46: 1101-1086.

Bertocchi, A., Ghiani, M., Peretti, R., Zucca, A., 2006. Red mud and fly ash for the remediation of mine sites contaminated with As, Cd, Cu, Pb, and Zn. Journal of Hazardous Materials B134: 112-119.

Blowes, D., Smith, L., Sego, D., Smith , L., Neuner, M., Gupton , M. , Moncur, M. , Moore, M., Klassen, R., Deans, T., Ptacek, C., Garvie, A., Reinson., J. 2007. Prediction of

effluent water quality from waste rock piles in a continuous permafrost region. IMWA Symposium 2007: Water in Mining Environments, R. Cidu & F. Frau (Eds), 27th - 31st May 2007, Cagliari, Italy.

Borden, R. 2003. Environmental geochemistry of the Bingham Canyon porphyry copper deposit, Utah. Environmental Geology 43: 752-758.

Carpenter, J., Odum, W., Mills, A. 1983. Leaf litter decomposition in a reservoir affected by acid mine drainage. Oikos 41: 165-172.

CCME. 2007. Canadian Water Quality Guidelines for the Protection of Aquatic Life, 13 pp. Viewed on November 6th, 2011, http://st-ts.ccme.ca/.

Chang, Z., Meinert, L. 2008. The Empire Cu-Zn Mine, Idaho: Exploration implications of unusual skarn features related to high fluorine activity. Economic Geology 103: 909-938.

Colmer, A., Hinkle, M. 1947. The role of microorganisms in acid mine drainage: Preliminary Report. Science 106: 253-256.

Conlan, M., Mayer, U., Blaskovich, R., Beckie, R. 2012. Solubility controls for Mo in neutral rock drainage. Geochemistry: Exploration, Environment, Analysis 12: 21-32.

Conlan, M. 2009. Attenuation mechanisms for molybdenum in neutral rock drainage. M.A.Sc. thesis, University of British Columbia, Vancouver, Canada.

Dixit, S., Hering, J. 2003. Comparison of Arsenic(V) and Arsenic(III) Sorption onto Iron Oxide Minerals: Implications for Arsenic Mobility. Environmental Science & Technology 37: 4182-4189.

Dold, B., Fontboté, L., 2001. Element cycling and secondary mineralogy in porphyry copper tailings as a function of climate, primary mineralogy and mineral processing. Special

Issue: geochemical studies of mining and the environment. Journal of Geochemical Exploration 74: 3-55.

Dold, B., 2003. Speciation of the most soluble phases in a sequential extraction procedure adapted for geochemical studies of copper sulfide mine waste. Journal of Geochemical Exploration 80: 55-68.

Evans, D., Letient, H., Aley, T. (2005). Aquifer vulnerability mapping in karstic terrain Antamina mine, Peru. In, proceedings of the 2005 SME Annual Meeting, Salt Lake City, United States of America, February 26- March 2.

Eriksson, N., Gupta, A., Destouni, G. 1997. Comparative analysis of laboratory and field tracer tests for investigating preferencial flow and transport in mining waste rock. Journal of Hydrology 194, 143-163.

Fala, O., Molson, J., Aubertin, M., and Bussiere, B. 2005. Numerical modeling of flow and capillary barrier effects in unsaturated waste rock piles. Mine Water, and the Environment 24, 172-185.

Frostad, S., Klein, B., and Lawrence, R. 2002. Evaluation of laboratory kinetic test methods for measuring rates of weathering. Mine water and the environment, Volume 21, 183-192.

Fukushi, K., Sasaki, M., Sato, T., Yanase, N., Amano, H., Ikeda, H. 2003. A natural attenuation of arsenic in drainage from an abandoned arsenic mine dump. Applied Geochemistry, Volume 18: 1267-1278.

Fyson, A., Kalin, M., Smith, M. 1995. Reduction of acidity in effluent from pyritic waste rock using natural phosphate rock. In: Proceedings of the 27th Annual Meeting of Canadian Mineral Processors, Ottawa, Ontario, 17–19 January, pp. 270–277.

Goldberg, S., Forster, H., Godfrey, C. 1996. Molybdenum Adsorption on oxides, clay minerals, and soils. Soil Science Society of America Journal, 60: 425–432.

Golder Associates Ltd. (2010). Waste Rock and Tailings Geochemistry, Field Cell Monitoring December 2002 to May 2009. Report number 09-1427-0482C/089-415109P. 125 pp.

Gupta, S., Elshout, V. and Abrol, I. 1987. Effect of pH on zinc adsorption-precipitation reactions in alkali soil. Soil Science 143: 198–204.

Gustafsson, J. 2003. Modeling molybdate and tungstate adsorption to ferrihydrite. Chemical Geology 200: 105-115.

Hakkou, R., Benzaazoua, M., Bussiere, B. 2009. Laboratory evaluation of the use of alkaline phosphate wastes for the control of acid mine drainage. Mine Water Environment 28: 206-218.

Holtzen, M., Smith, D. 1998. Minerals and Mine Drainage. Water Environment Research 70: 652-658.

Heikkinen, P., Räisänen, M., Johnson, R. 2009. Geochemical Characterisation of Seepage and Drainage Water Quality from Two Sulphide Mine Tailings Impoundments: Acid Mine Drainage versus Neutral Mine Drainage. Mine Water and the Environment: 30-49.

Johnson, D., Hallberg, K. 2005. Acid mine drainage remediation options: a review. Science of the Total Environment 2005: 3-14.

Johnson, D. 2003 Chemical and microbiological characteristics of mineral spoils and drainage waters at abandoned coal and metal mines. Water Air Soil Pollution: Focus 3:47– 66.

Kalin, M. 2004. Passive mine water treatment: the correct approach? Ecological Engineering 22: 299-304.

Kalin, M., Harris, B. 2005. Chemical precipitation within pyritic waste rock. Hydrometallurgy 78: 209-225.

Kwong, J. 2003. Comprehensive environmental ore deposit models as an aid for sustainable development. Exploration Mining Geology, Vol. 12, pp. 31-36.

Klohn Crippen Berger Ltd. 2010. Modificación EIA del Proyecto Minero Antamina por Incremento de Reservas y Optimización del Plan de Minado. Volumen II. 2096 pp.

Langmuir, D., 1997. Aqueous Environmental Geochemistry, Prentice Hall, Englewood Cliffs N.J.

Lapakko, K., White, W. 2000. Modification of the ASTM 5744-96 Kinetic Test. In, Proceedings of the 5th International Conference on Acid Rock Drainage (ICARD) Volume I, Denver, Colorado May 21-24.

Love, D., Clark, A., Glover, J. 2004. The lithologic, stratigraphic, and structural setting of the giant Antamina copper-zinc skarn deposit, Ancash, Peru. Economic Geology and the Bulletin of the Society of Economic Geologists 99: 887–916.

Lupankwa, K., Love, D., Mapani, B., Mseka, S., Meck, M. 2006. Influence of the Trojan Nickel Mine on surface water quality, Mazowe valley, Zimbabwe: Runoff chemistry and acid generation potential of waste rock. Physics and Chemistry of the Earth 31: 789–796.

Manceau, A., Lanson, B., Schlegel, M. Harge, J., Musso, M., Eybert-Berard, L., Hazemann, J., Chateigner, D., and Lamble, G.. 2000. Quantitative Zn speciation in smelter-contaminated soils by EXAFS spectroscopy. American Journal of Science, 300: 289-343.

Mehling Environmental Management. 1998. Blending and layering waste rock to delay, mitigate or prevent acid rock drainage and metal leaching: A case study review. Canadian MEND Program Report 2.37.1. 242 pp.

Miller S. D, Smart, R., Andrina, J., and Richards, D. 2003. Evaluation of limestone covers and blends for long term ARD control at the Grasberg Mine, Papua Province, Indonesia: Proceedings of Sixth International Conference on Acid Rock Drainage (Cairns, QLD, Australia, July 14-17, 2003), The Australasian Institute of Mining and Metallurgy, Australia.

Morin, K., Hutt, N., 2000. Discrete-zone mixing of net-acid-neutralizing and net-acid-generating rock: Avoiding the argument over appropriate ratios. IN: Proceedings from the Fifth International Conference on Acid Rock Drainage, May 20-26, Denver, USA, Volume II, p. 797-803. Society for Mining, Metallurgy, and Exploration, Inc., Littleton, CO, USA. Pages 797-803.

Muyssen B., De Schamphelaere K., Janssen, C. 2006. Mechanisms of chronic waterborne Zn toxicity in Daphnia magna. Aquatic Toxicology, 77: 393-401.

O'Connor, G. Brobst, R., Chaney, R. Kincaidd, R., McDowell, L., Pierzynskie, G., Rubinc, A., Van Riper, G. 2001. A modified risk assessment to establish molybdenum standards for land application of biosolids. Journal of Environmental Quality, 30: 1490–1507.

Odor, L., Wanty, R., Horvath, I., Fugedi, U., 1999. Mobilization and attenuation of metals downstream from a base-metal mining site in the Matra Mountains, northeastern Hungary. Journal of Geochemical Exploration, 65: 47-60.

Plante, B. Benzaazoua, M., Bussiere, B. 2011a. Predicting Geochemical Behaviour of Waste Rock with Low Acid Generating Potential Using Laboratory Kinetic Tests. Mine Water Environment 30: 2–21.

Plante, B. Benzaazoua, M., Bussiere, B. 2011b. Kinetic Testing and Sorption Studies by Modified Weathering Cells to Characterize the Potential to Generate Contaminated Neutral Drainage. Mine Water Environment 30: 22–37.

Redwood, R. 1999. The geology of the Antamina copper-zinc skarn deposit, Peru. The Gangue, 60: 1-7.

Robinson-Lora, M., Brennan, R. 2009. Efficient metal removal and neutralization of acid mine drainage by crab shell chitin under batch and continuous-flow conditions. Bioresource Technology, 1000: 5063-5071.

Rusdinar, Y. 2006. Long-term acid rock drainage (ARD) management at PT Freeport Indonesia. In, Proceedings of the 7th International Conference on Acid Rock Drainage (ICARD), March 26-30, 2006, St. Louis, United States of America. R.I. Barnhisel (ed.).

Sapsford, D., Bowell, D. Dey, M., Williams, K. 2009. Humidity cell tests for the prediction of acid rock drainage. Minerals Engineering 22: 25-36.

Smart, R., Millar, S., Stewart, W., Rusdinar, Y., Schumann, R., Kawashima, N., Li, J. 2010. In situ calcite formation in limestone-saturated water leaching of acid rock waste. Science of the Total Environment 408: 3392-3402.

Smedley, P., Kinniburgh, D. 2002. A review of the source, behaviour and distribution of arsenic in natural waters. Applied Geochemistry 17: 517-568.

Sullivan, P., Yelton, J., Reddy, K. 1988. Solubility relationships of aluminum and iron minerals associated with acid mine drainage. Environmental Geological Water Science 11: 283-287.

Strömberg, B., Banwart, S. 1999. Experimental study of acidity-consuming processes in mining waste rock: some influences of mineralogy and particle size. Applied Geochemistry 14: 1–16.

Trivedi, P., Axe, L. 2000. Modeling Cd and Zn Sorption to Hydrous Metal Oxides. Environmental Science & Technology 34: 2215-2223.

Villalobos, M., García-Payne, D., López-Zepeda, J., Ceniceros-Gómez, A., Gutiérrez-Ruiz, M. 2010. Natural Arsenic Attenuation via Metal Arsenate Precipitation in Soils Contaminated with Metallurgical Wastes: I. Wet Chemical and Thermodynamic Evidences. Aquatic Geochemistry 16: 225-250.

Vlek, P., Lindsay, W. 1977. Thermodynamic stability and solubility of molybdenum minerals in soils. Soil Science Society of America Journal, 41: 42–46.

Webster, J., Swedlund, P., Webster, K. 1998. Trace metal adsorption onto an acid mine drainage iron(III) oxy hydroxy sulfate. Environmental Science & Technology, 32: 1361-1368

Appendices

Appendix A Detailed stacked field cell construction and installation procedure

A.1 Support structure construction

The field cell study of metal attenuation at Antamina required the installation of stacked field cells, with a total height of about 1.8 m. A wooden frame was constructed to hold these field cells in place to prevent them from toppling during the course of the experiment. Eucalyptus wood was chosen for the frame, given its local availability and the frame was coated in a preservative to in order to enhance its durability. Construction of the frame was carried out by a Peruvian company called MECOMA over the last two weeks of May 2009.

The first step in the construction process was to dig eight 50 cm deep and 80 cm long trenches, which served as the structure's foundations. Sixteen 2.95 m long pieces of 4" x 4" wooden posts, and eight 0.8 m long pieces of 6" x 6" wooden posts were then installed in the foundational trenches and cemented in place and concrete pad was poured at the base of the structure, filling the foundational trenches and creating a concrete pad to maximize stability (Figure A1 shows the process of digging and filling the structure's foundation). Next, eight 68cm long 4" x 4" wooden posts were used as horizontal cross-beams to connect the 2.95 m long vertical 4" x 4" wooden posts near their base. Later on, four 5.56 m long 2" x 4" wooden planks were set on their side and hammered into the 6" x 6" wooden pieces. All parts of the base were fastened together using 4" long metal bolts which had been custom made out of rebar in a welding shop in Huaraz, Peru. Several 2" x 4" pieces of wood were then added to the structure to create a crib for each of the seven stacked field cells that were to be installed, as well as a platform with safety railings, which could serve to assist in the process of filling the field cells, as well as for easy inspection of the waste rock materials' upper

surface (Figures A2 and A3 show a detailed design of the structure). Wooden planks (2” x 12”) were used for the structure’s stairs and platform.

Figure A1: A MECOMA working stabilizing the field cell support structure prior to pouring the concrete in the structure’s foundation (left), and the process of pouring concrete to fill the foundation (right). Note that the structure was composed of 8 identical vertical wooden frames, which were connected together by horizontal planks.

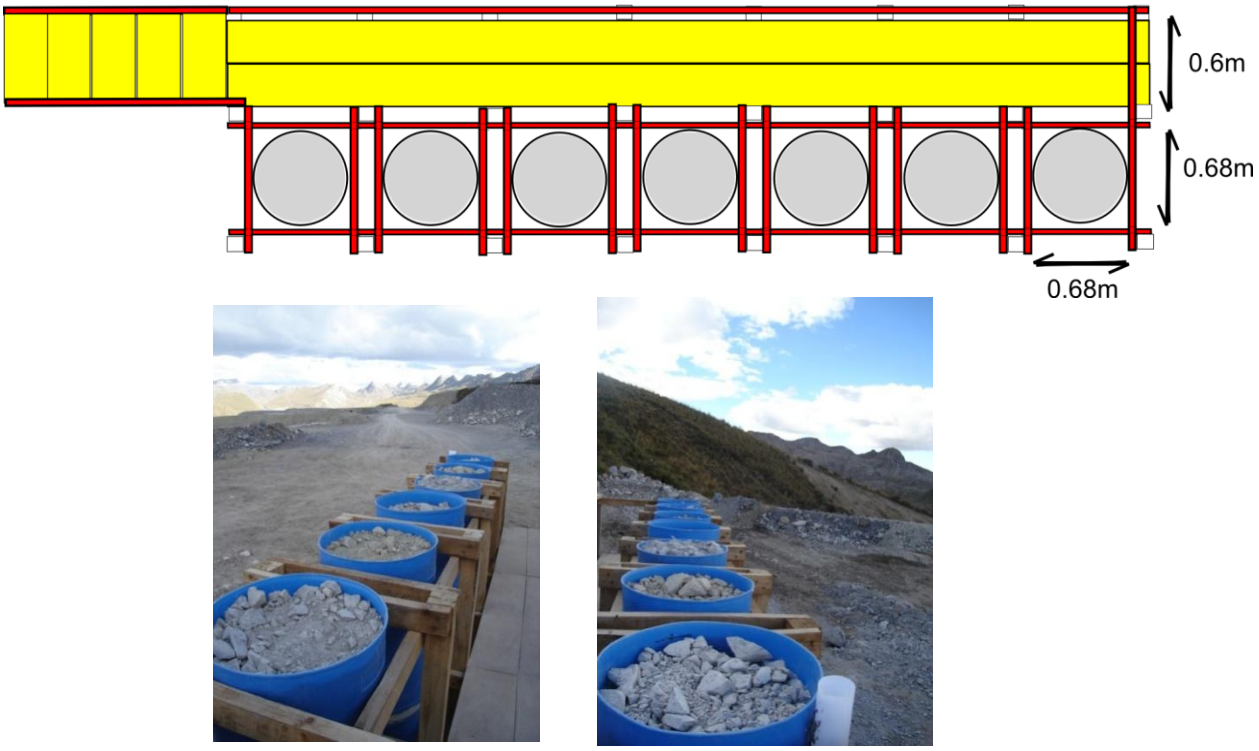

Figure A2: Schematic diagram showing the stacked field cell support structure from above (top) along with two photographs showing the structure from above after the field cells had been installed (bottom). The red rectangles in the diagram are planks of 2”x 4” wood, whereas the yellow rectangles are planks of 2” x 12” wood.

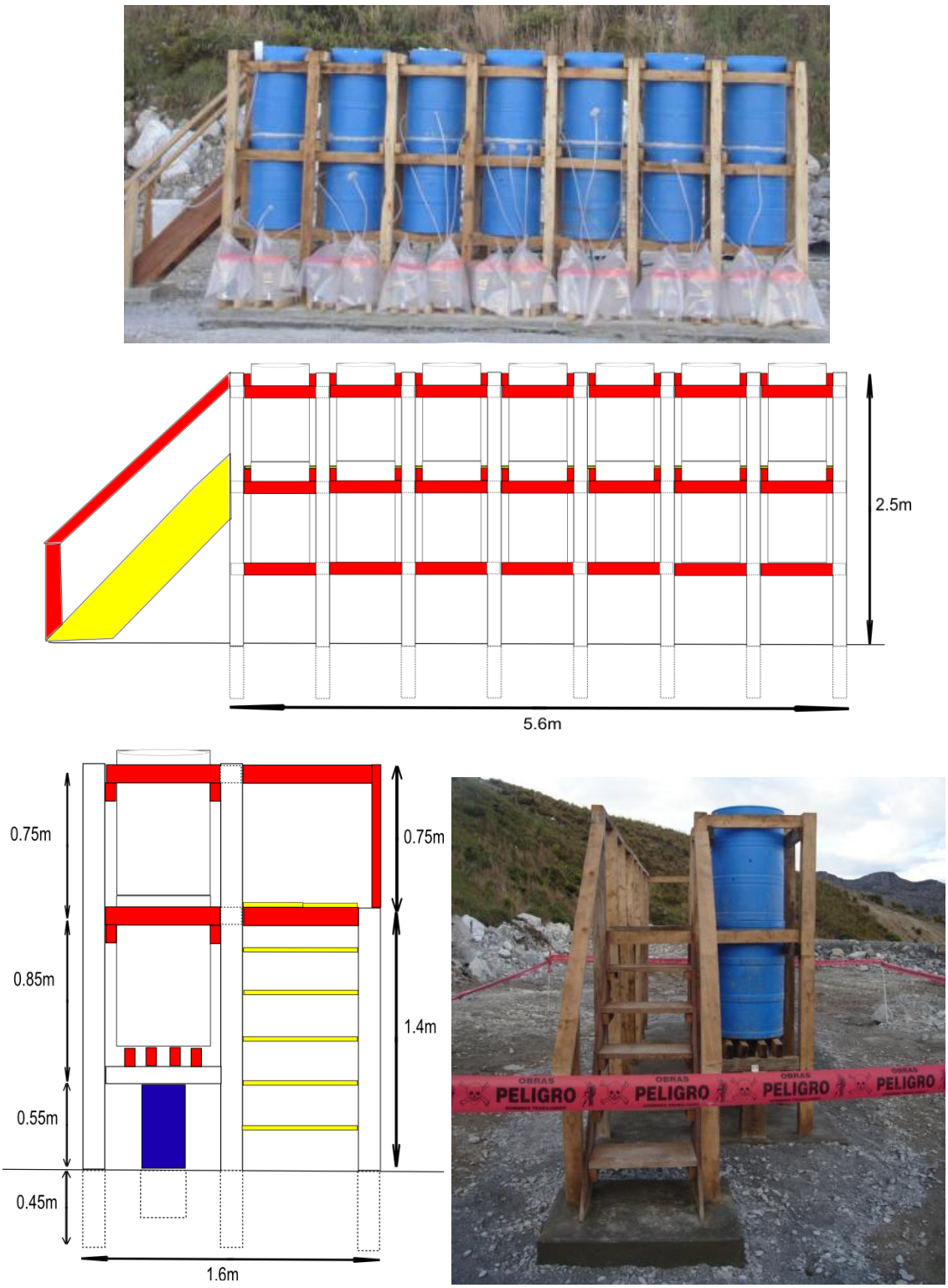

Figure A3: Schematic diagrams showing the stacked field cell support structure from the front (top row) and side view (bottom left) along with two photographs showing the structure from the front (middle row) and side (bottom right – note that this diagram also shows the depth of the wooden posts). The red rectangles in the diagram represent planks of 2"x 4" wood, the yellow rectangles represent planks of 2" x 12" wood, white rectangles represent 4" x 4" posts, and blue rectangles represent 6" x 6" posts.

A.2 Stacked field cell construction and installation

The methods section of Chapter 2 described the materials used for the stacked field cell construction. The purpose of this appendix is to provide more detail as to how the stacked field cells and their upper lysimeters were installed. Unlike the single field cells described by Aranda (2009), the drainage apparatus in the stacked field cells was installed at its base, in an effort to reduce the amount of standing water at the bottom of the stacked field cell (Figure A4). The drainage apparatus itself consisted of a hose connecter held in place by a reducing bushing (With the exception of the plastic barrels themselves, and the sample bottles used for the lysimeters, all of the hoses, hose connectors, and buckets mentioned in this section were purchased at SODIMAC home and garden stores in Lima, Peru). As in the single material field cell, geotextile was used to cover the hose connector inside the field cell. A layer 5cm of sand was placed on top of the geotextile, followed by another layer of geotextile. The stacked field cells were installed with finer sand in this layer (#60 mesh) than were the single material field cells at Antamina (#30 mesh). Apart from the position of the drainage aparatus in the field cell, and the grain size of the sand, the stacked field cell was identical to that described by Aranda (2009) for the single material field cells.

Figure A4: A photograph of the drainage apparatus installed in the base of the stacked field cell (left), with a diagram of the interior of the field cell (right) showing the depth of standing water during field cell operation.

The stacked field cells were designed to hold twice as much material as a single material field cell. As described in chapter 2, two stacked field cells were cut and stuck together such that they effectively formed a single, 180 cm tall field cell. The plastic barrels used for the field cells came with a built in base and top. The top half of the stacked field cell was formed by opening both ends of the barrel with a saw, whereas only the top of the bottom barrel was removed. Both top and bottom barrels were cut such that a ledge was left at the interface between the two barrels (Figure A5). This ledge was coated in silicone and left to dry to seal the two barrels together.

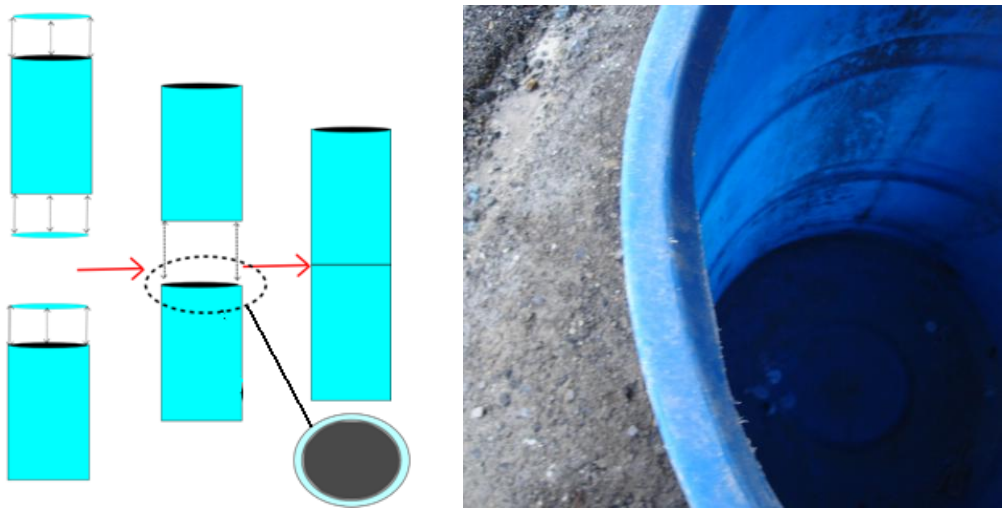

Figure A5: A schematic diagram of the process of preparing the stacked field cell (left) and a close up photograph of the ledge that is used to seal the two plastic barrels together. Note that on the figure to the left, the black circle with a blue edge is a view of the bottom barrel from above.

As chapter 2 described, three simple lysimeters were fabricated from 1 L plastic bottles. They consisted of a hose connector inserted into the opening of the sampling bottle. The base of the bottle was cut off with a saw in order to collect leachate solution from the top material in the field cell. Each upper lysimeter contained a circular piece of geotextile to prevent its drainage hose from clogging. This was covered by a 2 cm thick layer of sand, followed by a second layer of geotextile (Figure A6). The hose connector was attached to the bottle using PVC cement.

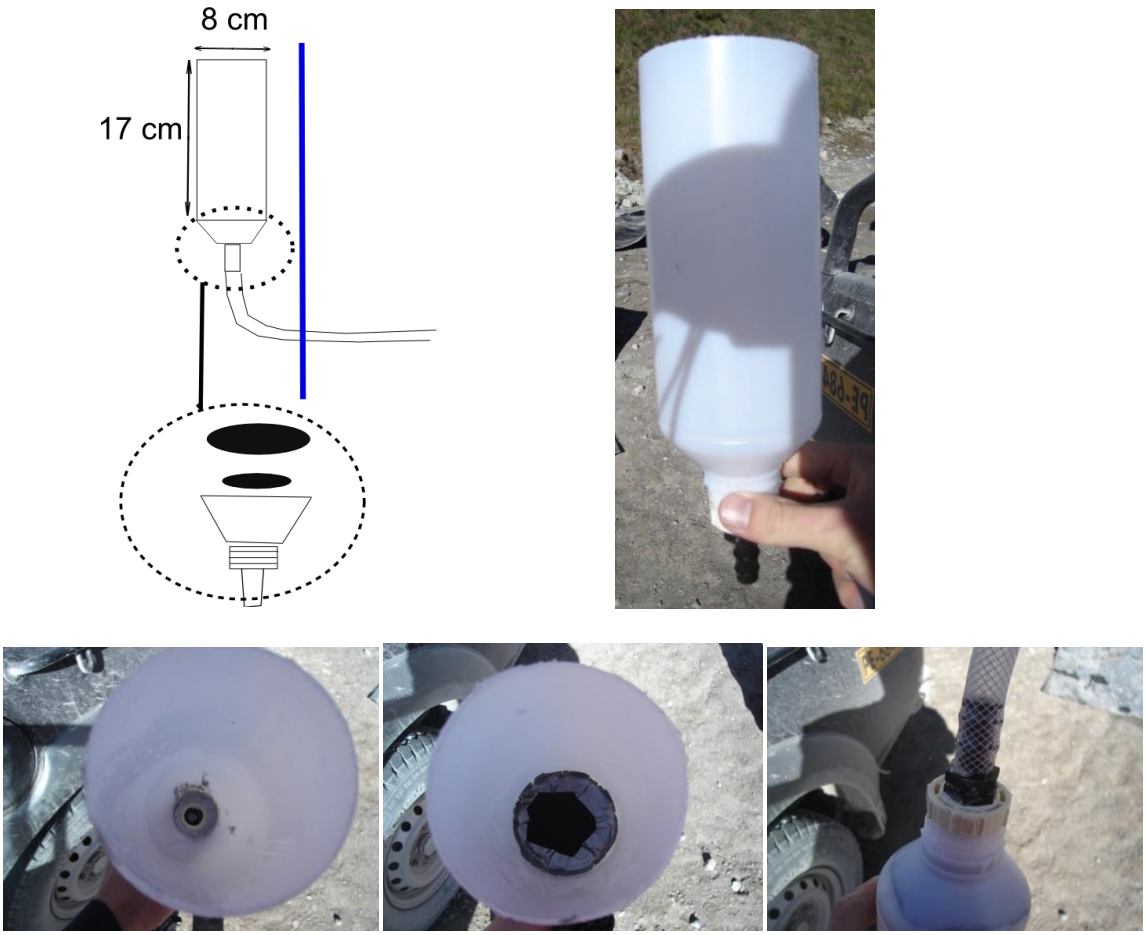

Figure A6: A schematic diagram of an upper lysimeter (top left) and a series of 4 photos showing various stages of its assembly (top right, bottom row). The black circles in the diagram and in the photos are the layers of geotextile. The vertical blue line in the diagram represents the side of the field cell barrel.

A total of seven stacked field cells were installed for this study. Results from five stacked field cells were discussed in the body of the thesis, however, two stacked field cells did not contribute significantly to developing a better understanding of attenuation reactions. Each stacked field cell was designed to investigate the attenuation of a particular metal, or to simulate the geochemical conditions above a specific sub-lysimeter in one of UBC's experimental waste rock piles (Table A1).

Table A1: Contents of the 7 stacked field cells. Note that direct contact exists between each material type. Waste rock masses are corrected for their moisture content.

Stacked Field Cell Code	Materials Used	Purpose
UBC-5A-T	Class C hornfels and marble (471.4 kg of UBC-4-5-5A on top of 161.5 kg of class C hornfels UBC-5-4A)	Intended to simulate sub-lysimeter A in pile 5, but 5-4A was erroneously installed
UBC-5C-T	342.3 kg of Class A (UBC-5-6A - intrusive) on top of 280.6 kg of Class C (UBC-4-5-5A – hornfels and marble)	Mimic geochemical conditions above sub-lysimeter C in Pile 5
UBC-4C-T	157.3 kg of Class B (UBC-4-4B – black and white marble) on top of 511.5 kg class C (330.5 kg of UBC-4-3A – black and white marble and 175.9 kg of UBC-4-5-5A – grey/brown hornfels)	Mimic geochemical conditions above sub-lysimeter C in Pile 4
UBC-4B-T	274.3 kg of Class B (UBC-4-2A – grey/brown hornfels) on top of 331.9 kg of Class C (174 kg of UBC-4-3A and 162.8 kg of UBC- 4-1A, both are grey/brown hornfels)	Mimic geochemical conditions above sub-lysimeter B in Pile 4
UBC-Zn-T	Zn-rich Class A (161.2 kg of UBC-3-2A – exoskarn class A) on top of Class C (511.8 kg of 4-5-1A – grey hornfels)	Investigate possible Zn attenuation by class C material
UBC-Mo-T1	Pb-rich Class B material (385.3 kg of UBC-1-3A – black marble) on top of Mo-rich class A material (299.2 kg of UBC-2-0A - intrusive)	Investigate possible Mo attenuation by co-precipitation with Pb
UBC-Mo-T2	Mo-rich Class A material (321.7 kg of UBC-2-0A - intrusive) on top of Pb-rich Class B material (UBC-1-3A 345.7 kg – black marble)	Investigate possible Mo attenuation by co-precipitation with Pb

The names of the field cells and humidity cells were modified in this thesis in order to improve the clarity of the text. The following table (Table A3) presents a summary of the names that were used at the mine site and the names that were used in this thesis and related publications.

Table A2: The names of the stacked field cells and humidity cells in series used in the thesis with those used in the lab notes or field cell labels. FC indicates stacked field cells and HC indicates humidity cells in series.

Field cell or humidty cell code used at Antamina or in lab notes	Name used in thesis
UBC-5A-T	FC-hornfels/marble over hornfels
UBC-5C-T	FC-intrusive over hornfels/marble
UBC-Zn-T	FC-exoskarn over grey hornfels
UBC-Mo-T1	FC-black marble over intrusive
UBC-Mo-T2	FC-instrusive over black marble
HC-Mo-T1U/HC-Mo-T1L	HC-black marble over intrusive
HC-Mo-T2U/HC-Mo-T2L	HC-intrusive over black marble
HC-Zn-TU/HC-Zn-TL	HC-exoskarn over hornfels

Prior to being loaded into the stacked field cells, the waste rock material was stored in sealed plastic bags at Antamina. Each of these bags weighed 20-30 kg. Once the barrels were in place, with their drainage apparatuses installed, the bags of waste rock were dumped into the barrels (Figure A7). The bags were weighed with a balance immediately prior to dumping them into the stacked field cells, and a tally was recorded to measure the total mass of each material in each stacked field cell. The upper lysimeters were held in place and sealed with duct tape while the first waste rock type was installed in the stacked field cells. After the installation of the first rock type, the tape was removed so that the second (top) rock type could be placed inside the upper lysimeters. Care was taken to fill the upper lysimeters with finer than average particles, in an effort to prevent capillary breaks.

Figure A7: Photos of the process of weighing (top left) and loading waste rock into the stacked field cells installed at the Antamina mine.

Two handfuls of waste rock were taken from each bag that was loaded into the stacked field cells to measure the material's humidity content. The samples placed on trays, weighed, put in an oven in Antamina's metallurgical laboratories at 45^{o}C for 24 hours, and then weighed again. The humidity content of each waste rock type was usually less than 4% (Table A3).

Table A3: The humidity content of each of the samples used in the stacked field cells.

Sample	Initial (humid) weight (g)	Dry Weight (g) includes tray	Mass lost (g)	Humidity (%)
1-3A	8193.3	9386.1	76.9	0.94
3-2A	6122.3	7228	124.3	2.03
2-0A	5751.7	6824.2	155.0	2.69
5-4A	6585.8	7736.8	82.0	1.25
4-3A	4264.2	5454.3	38.7	0.91
5-6A	5852.7	6869.1	217.8	3.72
4-5-5A	10887.9	11982.1	128.6	1.18
4-2A	5361	6555.3	32.7	0.61
4-3B	5110	6250.3	81.9	1.60
4-4B	8826.7	9712.9	333.4	3.78
4-5-1A	8035.6	9245.5	11.0	0.14

The five stacked field cells that were discussed in this study contained a total of seven different rock types. The elemental composition of 5 of the seven rock types was analyzed at ACME laboratories in Vancouver. A summary of some of the elements of interest for each of the 5 samples is presented below (Table A4).

Table A4: The elemental composition of the materials used in the 5 stacked field cells that formed the focus of this study, and their associated humidity cells. Samples that are marked with asterisks were not originally important in this study and were not analyzed for elemental composition prior to publication.

Field cell and Position	Material code	Lithology	As (ppm)	Pb (ppm)	Mo (ppm)	Zn (ppm)	Cu (ppm)	Cd (ppm)	S (%)
UBC-5A-T, Base	UBC-5-4A*	Hornfels	N/A	N/A	N/A	N/A	N/A	N/A	N/A
UBC-5A-T, Top; UBC-5C-T, Base	UBC-4-5-5A	Hornfels and Marble	185	181	3	227	103	1	0.4
UBC-5-6A, Top	UBC-5-6A*	Intrusive	N/A	N/A	N/A	N/A	N/A	N/A	N/A
UBC-Zn-T (FC-Exoskarn over Grey Hornfels), base	UBC-4-5-1A	Grey Hornfels	168	82	5	173	51	1	0.5
UBC-Zn-T (FC-Exoskarn over Grey Hornfels), Top	UBC-3-2A	Exoskarn	51	242	45	>10000	9919	103	8.5
UBC-Mo-T1/T2 (FC Black Marble over Intrusive/ Intrusive over Black Marble), Top/Bottom	UBC-1-3A	Black Marble	32	869	71	1516	763	4	1.3
UBC-Mo-T1/T2 (FC Black Marble over Intrusive/ Intrusive over Black Marble) Bottom/Top	UBC-2-0A	Intrusive	140	34	275	189	3484	<0.1	0.6

A.3 Materials needed to make a similar apparatus

This list of materials is given per field cell with the associated support structure.

- Duct tap
- Markers
- Balance
- Waste rock (at least 2 types)
- 0.9 m tall x 0.5 m diameter barrels (2)
- Hack saw
- Measuring tape
- Drill
- 1” drill bits
- Geotextile
- Grey silicone
- PVC cement
- 1/4” hose connectors (3)
- ½” hose connector (1)
- 20 L bucket with lid
- ½” ID garden hose (2m)
- Wood
- Nails
- Gravel
- Sand
- Cement
- Zip ties
- Hammers
- Saws

Appendix B Assembly, installation, and sampling for humidity cells connected in series

B.1 Apparatus design and assembly

The humidity cell apparatus used in this study was modified slightly from apparatus that were designed and assembled by four Applied Science undergraduate students as a part of their honors theses (Edgar, 2009; Moug 2009; Joiya 2009; Yu 2009). Given that their theses are not widely available, the following modified excerpt taken from the methods section and appendices of Joiya (2009) will serve to explain the assembly, leaching, and sampling, and analysis procedures in more detail than the methods section of Chapter 2.

18 Nalgene bottles (1L) served as the humidity cell containers in this experiment. The bottoms of 18 1 L Nalgene bottles were machine cut and the top caps were removed. Another 18 Nalgene bottles (500 mL) were used to collect leachate samples. PVC pipe holding cells provided support to the humidity cells, and prevented them from toppling. These PVC pipe holding cells were secured onto the acrylic plastic base using zap straps (Figure B1).

Figure B1: the PVC pipe holding cells for the humidity cell experiment attached to their base (left), and holding a humidity cell (right). The humidity cell to the right is held in place by a piece of steel wire, however they rested directly on top of the leachate sample bottle during the experiment.

The humidity cells (1 L Nalgene bottles with their base removed) were stored with the open end facing upwards. Rubber stoppers, which were fitted to polyethylene tubing were used to prevent waste rock from falling out of the mouth of the Nalgene bottles. These stoppers helped form the drainage apparatus. Nylon mesh, with a 37 micron mesh size, (ordered from

Smallparts.com – part number B000FMWTL0610) was used to prevent particles from washing out of the field cell with leachate. In practice, some small particles still washed out of the humidity cells, therefore a finer mesh, or filter membrane is recommended for future experiments. Opposite the nylon mesh, on the other side of the rubber stopper, the remainder of the drainage apparatus consisted of a Luer lock (Ordered from Cole-Parmer, part number: R-45510-05) attached to a stopcock (Ordered from Cole-Parmer, Part number: R-30600-00). This drainage apparatus was designed to easily stop the flow of water from the 1L humidity cell into the 500 mL leachate container when necessary (Figure B2). All components of the apparatus that had contact with waste rock or leachate samples were submerged in a 10% HNO_3 acid bath, for at least 1-2 hours, then soaked and rinsed with distilled & de-ionized water.

Figure B2: Rubber stopper showing draining apparatus and mesh (left). The same drainage apparati are shown at the base of the Nalgene bottles that were later used to hold the waste rock samples in the humidity cells.

The humidity cells were stored in Rubbermaid containers with sealed lids to provide dark conditions and minimize exposure to contamination (Figure B3). The containers were filled with 8 L of water, which served as a source of passive humidification.

Figure B3: The Rubbermaid containers in which the humidity cells were stored during the experiment, showing all 17 humidity cells after installation.

B.2 Waste rock sample selection and humidity cell installation

The material installed in the humidity cells was derived from bags of waste rock that had been stored in the field cell area at the Antamina mine in Peru. This material was left over after the installation of the field cells and had been coned and quartered to ensure that it was well-homogenized. In August 2010 portions of materials UBC-1-3A, UBC-2-0A, UBC-3-2A, and UBC-4-5-1A were quartered and sieved through a ¼" mesh until a few kg of -1/4" material had been collected. Once at UBC, this material was coned and quartered again, then loaded into the humidity cells (Figure B4).

Figure B4: waste rock material being coned and quartered in the lab prior to humidity cell installation.

The waste rock material was not dried prior to humidity cell installation and was transported in sealed plastic bags. The decision to not dry the waste rock was made in an effort to not unduly affect its natural microbial community, which would have been harmed by

desiccation. Its moisture content was likely similar to the moisture content of the materials that were installed in the stacked field cells (see appendix A), albeit higher because the finer grains tended to retain moisture more than the larger grains. The four waste rock materials from stacked field cells UBC-Mo-T1, UBC-Mo-T2, and UBC-Zn-T, were used in the humidity cell version of the experiment. The specific waste rocks used where Pb-bearing black marble (UBC-1-3A), Mo-leaching intrusive (UBC-2-0A), Zn-leaching exoskarn (UBC-3-2A), and Zn-attenuating hornfels (UBC-4-5-1A) (Table B1). A table spoon was used to scoop the waste rock material into a beaker for weighing. A tally was made of each beaker's weight to determine the mass of waste rock in each humidity cell. After weighing, each beaker was dumped into the humidity cell.

B.3 Detailed leaching and sampling procedure

From the installation of the humidity cells, to the collection of the last samples, this experiment lasted a total of 32 weeks. The experiment was initiated in late September, 2010 and concluded in late April 2011. Many details of the sampling procedure, including the distinction between ASTM and Field Cell leaching methods are included in chapter 2. The humidity cells were leached by gently pouring distilled and de-ionized water (prepared in the UBC hydrogroup lab - with a resistivity of at least 17.6 MΩ/cm) onto the waste rock's surface with a 500 mL graduated cylinder. The leaching procedure for the ASTM humidity cells (UBC-32-T1, UBC-20-T1, UBC-13-T1, UBC-451-T1, UBC-32-T2, UBC-20-T2, UBC-13-T2, UBC-451-T2) was straightforward. An empty humidity cell (installed the same way as the others, but with no waste rock material) was leached and sampled in the same way as the ASTM cells to detect contamination from the apparatus. With the stopcock closed on the training apparatus, 500 mL was added each to each cell on a weekly basis. After 1 hour, the

stop cock was opened so that the leachate could drain from the humidity cell. Approximately 80 mL of leachate from these cells was set aside for chemical sampling and analysis, whereas the rest was discarded.

Table B1: The contents, leaching regime, and purpose of each of the humidity cells in the experiment. The number in the humidity cell code corresponds to the waste rock material used in the humidity cell (HC-13-T1 contains UBC-1-3A material, etc.). The three to four digit number in brackets in the humidity cell code column corresponds to mass of waste rock in the cell (including water content).

Humidity Cell Code	Purpose	Leaching Regime	Other comments
HC-13-T1 (961), HC-20-T1 (1005), HC-451-T1 (1177), HC-32-T1 (1071)	Determine composition of leachate under ASTM leaching protocol	ASTM	N/A
HC-13-T2 (1054), HC-20-T2 (957), HC-451-T2 (1097), HC-32-T2 (1052)	Duplicates to assess heterogeneity	ASTM	N/A
HC-Mo-T1U (UBC-1-3A, 1067) HC-Mo-T1L (UBC-2-0A, 1070)	HC version of field cell UBC-Mo-T1	Field Cell	These were connected in series such that leachate from HC-Mo-T1U was poured through HC-Mo-T1L
HC-Mo-T2U (UBC-2-0A, 1034) HC-Mo-T2L (UBC-1-3A, 1042)	HC version of field cell UBC-Mo-T2	Field Cell	These were connected in series such that leachate from HC-Mo-T2U was poured through HC-Mo-T2L
HC-Zn-TU (UBC-3-2A, 1071), HC-Zn-TL (UBC-4-5-1A, 1121)	HC version of field cell UBC-Zn-T	Field Cell	These were connected in series such that leachate from UBC-Zn-TU was poured through UBC-Zn-TL
HC-Zn-TU (UBC-3-2A, 1078), HC-Zn-TL (UBC-4-5-1A, 932)	Assess the effects of a ´dry season´ on Zn release and attenuation	Field Cell	These were connected in series, as described above, but in this case the leach cycles ceased for 3 months, and then returned to normal in order to simulate a dry season
HC-451-T3 (1106)	Determine composition of leachate under Field cell leaching protocol	Field Cell	N/A

Humidity cells HC-Mo-T1U, HC-Mo-T2U, HC-Zn-TU, HC-ZnD-TU and HC-451-T3 were all leached according to the field cell leaching procedure. In the field cell leaching procedure, 230 mL of distilled de-ionized water was applied to each humidity cell on a weekly basis. The stop-cock in these humidity cells was left shut for 1 hour, and then the humidity cell was allowed to drain. 80 mL of leachate from the above-listed humidity cells was taken for pH, alkalinity, and chemistry samples. In all but HC-451-T3, the remaining leachate was then applied to the second humidity cell in series.

HC-Mo-T1L, HC-Mo-T2L, HC-Zn-TL, and HC-ZnD-TL were the 'bottom' humidity cells connected in series and were rinsed on a weekly basis with 150 mL of leachate from the 'top' humidity cells connected in series: HC-Mo-T1U, HC-Mo-T2U, HC-Zn-TU, HC-ZnD-TU, respectively. Instead of allowing 1 hour for reaction between leachate and the humidity cell material, the stop-cocks on the four 'bottom' humidity cells connected in series were left closed for 24 hours prior to allowing them to drain. After drainage their leachate was analyzed for the same parameters as leachate from all of the other humidity cells in the experiment. It should be noted that very little leachate drained from the 'upper' humidity cells in the first leach cycle, meaning that the 'bottom' humidity cells were not rinsed until the second leach cycle, and did not drain enough leachate to allow for sampling until the fourth leach cycle.

The same sampling technique was used for each sample from each humidity cell. A 60 mL Luer lock graduated plastic disposable syringe (Henke-Sass-Wolf) was used in conjunction with a Millipore Millex® 0.45 µm syringe filter membrane to filter 25 mL of leachate into a glass graduated cylinder. The leachate's electrical conductivity was then measured in the graduated cylinder using an Oakton Con 6 Acorn Series hand held conductivity meter.

Leachate was then poured into a graduated cylinder for an alkalinity titration, using an Oakton pH 11 series pH/mV/^{o}C hand held meter. A new 60 mL sample of leachate was then filtered into two 30 mL polyethylene sample bottles for posterior chemical analysis. The cation samples were acidified to below pH 3 using nitric acid. The sample bottles were new and were triple rinsed with sample prior to filling them. All surfaces and instruments that came in contact with multiple samples were triple rinsed with distilled, de-ionized water prior to making contact with the next leachate sample.

The exact amount of time between leaching sessions varied somewhat throughout the experiment. Leaching took place each Thursday, however, depending on the week, the leach time varied by up to 12 hours in the first 20 weeks of the experiment. After 20 weeks, the ASTM humidity cells were leached every week, but were only sampled every two weeks. During the second last week of sampling, the 'bottom' humidity cells were only allowed 1 hour of contact time with waste rock prior to drainage. Leach cycles 29 and 30 were each 10 days long.

B.4 Chemical analysis

Alkalinity was determined at the time of leachate sampling by titrating leachate with a 0.019 N H_2SO_4 solution. Acid was added to the leachate sample with an Eppendorf pipette, and the pH was recorded for each volume added. The pH and volume data was used to generate Gran plots in order to determine the equivalence point of the titration (the X intercept on the Gran plots). The Gran Plot represents the Gran Function (Y-axis) with respect to the volume of acid added (X-axis). The Gran Function is determined by the following equation:

Gran Function = (Volume of Sample + Volume of Acid Added) x 10^{-pH}

A trend line was fit to the linear portion of the graph and the line's equation was used to solve for 0. This solution referred to the amount of acid required to reach the equivalence point. The x-intercept was then used to find alkalinity.

Alkalinity = (Normality of Acid x Vequivelnce)/Volume of Sample

Humidity cell leachate samples were poured into 10 mL acid washed test tubes and analyzed for cations and Sulfur using the Varian ES-725 ICP-OES in the department of Earth and Ocean Sciences at UBC (Figure B5). The ICP-OES was equipped with ICP Expert II software to assist in calibrating the instrument and processing the data. The ICP analysis required a set of chemical standards for calibration purposes. A PlasmaCal Multi-Element Standard (including B, Be, Co, Cd, K, V, Ti, Mo, Ag, Pb, Ti, Sb, Cu, Mo, Zn, Cr, As, Ba, Ni, S, Se, Al, Ca, Mg, Mn, Na, Si) was used for total metals along with a Single-Element Calcium and Sulfur standards (Table B2). Standards were mixed with nitric acid to ensure that they had the same matrix as the samples and diluted to desired concentrations with the same distilled de-ionized water that was used to leach the humidity cells.

Table B2: A summary of the standards used for the ICP-OES analysis. n/a means that the element was not included in the standard. K was 10x more concentrated than the other elements in the standard.

Standard #	Concentration (mg/L)
Blank	
Total Metals Standard 1	0.09
Total Metals Standard 2	0.19
Total Metals Standard 3	4.9
Total Metals Standard 4	19.9
Total Metals Standard 5	99.3
Ca-S Standard 6	S: 196.6 Ca: n/a
Ca-S Standard 7	S: 298 Ca: 301.8
Ca-S Standard 8	S: 500 Ca: 402.4
Ca-S Standard 9	S: 983.33 Ca: n/a
Ca-S Standard 10	S: n/a Ca: 989.2

Given the large range of concentrations used in the standards, some calibration curves fit much better at low concentrations than at high concentrations or vice versa. To achieve the best results for the typical concentration range each element, the calibration curves were re-calculated in Microsoft Excel (ICP Expert II calibration equations were not used to determine the elemental concentrations presented in this study). It should also be noted that the ICP-OES detected several wavelengths of light associated with each element. The best wavelength for each element was chosen and used throughout the experiment based on having a low detection limit and a high R^2 on the calibration curve's line of best fit.

Figure B5: The Varian ICP-OES used to analyze the chemistry samples in this study with its autosampler in the foreground.

B.5 QA/QC

The following steps were taken to ensure that data from the humidity cell experiment were accurate and representative:

- pH probes were calibrated with pH 4, 7, and 10 buffers prior to each sampling session
- The calibration of EC probes was checked before each session in order to ensure that no drift occurred
- Lab blanks were taken and analyzed
- Equipment blanks were analyzed
- Standards with known concentrations were re-analyzed several times to check for precision
- Duplicate chemistry samples were analyze

The full results of QA/QC can be found in the supporting information on the compact disc that accompanies this thesis. Data from duplicate samples of As, Zn, and Mo are presented to provide a brief assessment of data quality (Table B3). Although some duplicates varied by as much as 30% the average difference between duplicates was less than 15%. As discussed in chapters 2 and 3, attenuation reactions normally remove more than 90% of the metals of interest. The relatively small degree of variation between duplicate samples supports the fact that attenuation is actually occurring in the field cells, and that differences between pre- and post-attenuation leachate composition are not artifacts of analytical error.

Table B3: A summary of duplicate samples for elements of interest in humidity cells from the Antamina study.

Humidity cell	Week	Element	Conc. (mg/L)	% Difference
HC-20-T1	5	Mo	0.99	0.3
HC-20-T1	5	Mo	1.00	
HC-20-T1	12	Mo	0.31	32.3
HC-20-T1	12	Mo	0.46	
HC-20-T2	7	Mo	3.94	2.6
HC-20-T2	7	Mo	3.84	
HC-20-T2	8	Mo	4.00	0.4
HC-20-T2	8	Mo	3.98	
HC-20-T2	14	Mo	0.42	11.6
HC-20-T2	14	Mo	0.47	
HC-20-T2	15	Mo	0.46	7.9
HC-20-T2	15	Mo	0.50	
HC-20-T2	16	Mo	0.56	4.0
HC-20-T2	16	Mo	0.58	
HC-20-T2	17	Mo	0.50	22.0
HC-20-T2	17	Mo	0.39	
HC-20-T2	19	Mo	0.54	6.4
HC-20-T2	19	Mo	0.51	
HC-20-T2	20	Mo	0.48	25.0
HC-20-T2	20	Mo	0.39	
HC-20-T1	12	As	0.65	1.6
HC-20-T1	12	As	0.64	
HC-20-T2	7	As	0.50	10.4
HC-20-T2	7	As	0.56	
HC-20-T2	8	As	0.61	6.6
HC-20-T2	8	As	0.57	
HC-20-T2	14	As	0.61	7
HC-20-T2	14	As	0.57	

Table B3: Continued

Humidity cell	Week	Element	Conc. (mg/L)	% Difference
HC-20-T2	15	As	0.56	7.8
HC-20-T2	15	As	0.61	
HC-20-T2	16	As	0.56	4.1
HC-20-T2	16	As	0.53	
HC-20-T2	17	As	0.61	11
HC-20-T2	17	As	0.68	
HC-20-T2	19	As	0.58	5.3
HC-20-T2	19	As	0.56	
HC-20-T2	20	As	0.59	11.9
HC-20-T2	20	As	0.66	
HC-20-T2	21	As	0.57	7.5
HC-20-T2	21	As	0.61	
HC-20-T2	23	As	0.59	3.1
HC-20-T2	23	As	0.57	
HC-32-T1	3	Zn	10.89	2.7
HC-32-T1	3	Zn	11.20	
HC-32-T1	4	Zn	10.61	1.15
HC-32-T1	4	Zn	10.49	
HC-32-T1	9	Zn	5.72	31.4
HC-32-T1	9	Zn	8.34	
HC-32-T2	8	Zn	6.17	0.26
HC-32-T2	8	Zn	6.19	
HC-32-T2	11	Zn	3.13	24.4
HC-32-T2	11	Zn	2.37	
HC-32-T2	12	Zn	2.12	12.5
HC-32-T2	12	Zn	1.85	
HC-451-T1	6	Zn	0.09	22.1
HC-451-T1	6	Zn	0.12	

B.6 List of materials used

- 1L Nalgene Bottle (18)
- 500ml Nalgene Bottle (18)
- #6 Rubber Stopper (18)
- Low density polyethylene tubing - 1/4 inch OD 0.17 inch ID
- Tygon tubing
- Nylon mesh
- Zap Straps – Marr Multipurpose Ties 1/16" – ¾" diameter.
- Stop cocks (18)
- Luer locks (18)
- PVC pipes – 10-4" ID, 10- 3 ¼" ID
- Acrylic Plastic
- 2 Rubbermaid containers
- Utility knife
- Measuring Tape
- Sharpie Pen
- Syringe
- Syringe filters
- ICP Varian 725-ES
- Various Beaker sizes
- Graduated Cylinders (500 mL and 50 mL)
- pH meter
- EC meter

Appendix C Field cell tracer test

An overview of the methods employed in the field cell tracer test is given in chapter 4 of the thesis. The purpose of this appendix is to provide more detailed information regarding the methodology and some of the problems that prevented an in-depth analysis of the tracer results. The field cell tracer test was carried out by Antamina technicians and contractors under the direct supervision of Dr. Roger Beckie. Tracer solution was prepared by adding 8.6 g of LiCl to each 7.125 L of water (to simulate a 3 cm rain event). A plastic bag camp shower (purchased at Canadian Tire in Vancouver, Canada) was used to sprinkle tracer evenly over the top surface of each of the field cells that was involved in the test (Figure C1).

Figure C1: The plastic camp shower used to sprinkle tracer onto the field cells (left) and an Antamina contractor initiating the tracer test on stacked field cell UBC-4A-T.

The instantaneous samples mentioned in chapter two were collected directly from the drainage hose at the base of the field cells (i.e. before the water touched the inside of the sample bucket) in opaque 30 mL polyethelene sample containers. These samples were collected in next 48 hours or so after tracer application. Composite tracer samples were taken by Antamina staff for their regular chemical analysis of field cell leachate. These samples represented a composite Cl concentration over a 1 week period (Figure C2). In the confusion of moving researchers and samples from Antamina back to UBC, the notebook that contained

the field notes for the study was lost at the mine site. Although the sample bottles' labels identified the field cell from which they had been sampled and the time at which the samples were taken, it was unclear when the tracer test was initiated at each field cell. A short post-sampling video noted that flow from UBC-3-2A was 10 mL/minute several hours after the initiation of the tracer test. Dr. Beckie also mentioned that since the tests were carried out at the height of the 2009/2010 rainy season and the waste rock was already near field capacity, meaning that drainage from the field cells' bases began shortly after tracer application.

Figure C2: The sample bucket (foreground) of field cell UBC-4-5-5A, from which composite samples were taken.

A second barrier to the collection of high quality data from this tracer test was that the staff responsible for sampling from the field cells' sample buckets did not consistently record the volume of water in the buckets at the time of sampling. In some cases water volumes were not recorded on dates when chemistry samples were available, meaning that the flow through the field cells is likely under-estimated.